A STUDY ON THE *IN VITRO* STABILITY AND METABOLISM OF CURCUMIN DIETHYL DISUCCINATE IN PLASMA

Mr. Pahweenvaj Ratnatilaka Na Bhuket

A Thesis Submitted in Partial Fulfillment of the Requirements
for the Degree of Master of Science in Biomedicinal Chemistry
Department of Biochemistry and Microbiology
Faculty of Pharmaceutical Sciences
Chulalongkorn University
Academic Year 2018

การศึกษาความคงตัวและเมแทบอลิซึมในหลอดทดลองของเคอร์คิวมินไดเอทิลไดซัคซิเนตในพลาสมา

นายปวีณวัชร์ รัตนดิลก ณ ภูเก็ต

วิทยานิพนธ์นี้เป็นส่วนหนึ่งของการศึกษาตามหลักสูตรปริญญาวิทยาศาสตรมหาบัณฑิต
สาขาวิชาชีวเวชเคมี ภาควิชาชีวเคมีและจุลชีววิทยา
คณะเภสัชศาสตร์ จุฬาลงกรณ์มหาวิทยาลัย
ปีการศึกษา 2561

Thesis Title	A STUDY ON THE *IN VITRO* STABILITY AND METABOLISM OF CURCUMIN DIETHYL DISUCCINATE IN PLASMA
By	Mr. Pahweenvaj Ratnatilaka Na Bhuket
Field of Study	Biomedicinal Chemistry
Thesis Advisor	Associate Professor Pornchai Rojsitthisak, Ph.D.
Thesis Co Advisor	Assistant Professor Boonsri Ongpipattanakul, Ph.D.

Accepted by the Faculty of Pharmaceutical Sciences, Chulalongkorn University in Partial Fulfillment of the Requirement for the Master of Science

..... Dean of the Faculty of Pharmaceutical Sciences

(Assistant Professor Rungpetch Sakulbumrungsil, Ph.D.)

THESIS COMMITTEE

..... Chairman

(Associate Professor Maneewan Suksomtip, Ph.D.)

..... Thesis Advisor

(Associate Professor Pornchai Rojsitthisak, Ph.D.)

..... Thesis Co-Advisor

(Assistant Professor Boonsri Ongpipattanakul, Ph.D.)

..... Examiner

(Wanatchaporn Arunmanee, Ph.D.)

..... External Examiner

(Professor Leena Suntornsuk, Ph.D.)

ปวีณวัชร์ รัตนดิลก ณ ภูเก็ต : การศึกษาความคงตัวและเมแทบอลิซึมในหลอดทดลองของเคอร์คิวมินไดเอทิลไดซัคซิเนตในพลาสมา. (
A STUDY ON THE *IN VITRO* STABILITY AND METABOLISM OF CURCUMIN DIE THYL DISUCCINATE IN PLASMA) อ.ที่ปรึกษาหลัก : รศ. ภก. ดร.พรชัย โรจน์สิทธิศักดิ์, อ.ที่ปรึกษาร่วม : ผศ. ภญ. ดร.บุญศรี องค์พิพัฒนกุล

ความคงตัวของสารที่มีศักยภาพในการเป็นยาในตัวกลางที่มีน้ำเป็นองค์ประกอบหลัก เช่น บัฟเฟอร์และพลาสมาเป็นหนึ่งในคุณสมบัติสำคัญสำหรับกระบวนการพัฒนายา เคอร์คิวมินไดเอทิลไดซัคซิเนต (CDD) เป็นโปรดรักของเคอร์คิวมินที่ถูกพัฒนาขึ้นเพื่อเพิ่มความคงตัวทางเคมี ในการศึกษานี้ ได้ทำทำการศึกษาความคงตัวของ CDD ในสารละลายบัฟเฟอร์กรดไฮโดรคลอริก (pH 1.2) บัฟเฟอร์แอซิเตต (pH 4.5) บัฟเฟอร์ฟอสเฟต (pH 6.8, 7.4 และ 8.0) และการเกิดเมแทบอลิซึมในพลาสมาของหนูแรท สุนัข และมนุษย์ที่อุณหภูมิ 4, 25 และ 37 °C จากการวิเคราะห์ด้วยไฮเปอร์ฟอร์แมนซ์ลิควิดโครมาโตกราฟีและการวิเคราะห์ถดถอยแบบไม่เป็นเส้นตรงพบว่าการสลายตัวของ CDD ในสารละลายบัฟเฟอร์ขึ้นกับอุณหภูมิและเป็นไปตามจลนศาสตร์อันดับหนึ่งเทียม ในทุกอุณหภูมิที่ทำการศึกษา CDD มีความคงตัวน้อยที่สุดในบัฟเฟอร์แอซิเตต การเกิดเมแทบอลิซึมของ CDD ในพลาสมาขึ้นกับอุณหภูมิแต่ปฏิกิริยาการเสื่อมสลายนี้เป็นไปตามจลนศาสตร์อันดับหนึ่งเทียมแบบต่อเนื่อง การเกิดไฮโดรลิซิสของ CDD ในพลาสมาถูกเร่งโดยเอนไซม์เอสเทอเรส โดยการสลายตัวของ CDD ในพลาสมาหนูแรทจะสูงกว่าในมนุษย์และสุนัขตามลำดับ จากการวิเคราะห์ด้วยลิควิดโครมาโตกราฟีแทนเดมแมสสเปคโตรเมตรีแสดงให้เห็นว่าการเกิดไฮโดรลิซิสของ CDD เกิดที่พันธะเอสเทอร์ของหมู่ฟีนอลิก จึงเกิดเมแทบอไลต์มัธยันตร์เพียงหนึ่งชนิดคือโมโนเอทิลซัคซินิลเคอร์คิวมิน การใช้ตัวยับยั้งเอนไซม์เอสเทอเรสชนิดต่างๆบ่งชี้ว่าเอนไซม์คาร์บอกซิลเอสเทอเรสเกี่ยวข้องกับการเกิดไฮโดรลิซิสของ CDD ในพลาสมาหนูแรทขณะที่เอนไซม์หลายชนิดมีบทบาทในการเกิดไฮโดรลิซิสของ CDD ในพลาสมาสุนัขและมนุษย์ ผลจากการศึกษานี้ ให้ข้อมูลที่สำคัญต่อการศึกษาในสัตว์ทดลองและการพัฒนา CDD ให้เป็นยาในอนาคต

สาขาวิชา ชีวเวชเคมี
ปีการศึกษา 2561

ลายมือชื่อนิสิต .....
ลายมือชื่อ อ.ที่ปรึกษาหลัก .....
ลายมือชื่อ อ.ที่ปรึกษาร่วม .....

5876116933 : MAJOR BIOMEDICINAL CHEMISTRY

KEYWORD: Curcumin diethyl disuccinate, Curcumin, Stability, Plasma metabolism, Hydrolysis

Pahweenvaj Ratnatilaka Na Bhuket :

A STUDY ON THE *IN VITRO* STABILITY AND METABOLISM OF CURCUMIN DIE THYL DISUCCINATE IN PLASMA. Advisor: Assoc. Prof. Pornchai Rojsitthisak, Ph.D. Co-advisor: Asst. Prof. Boonsri Ongpipattanakul, Ph.D.

Stability in aqueous media such as buffers and plasma are the one of important properties of drug candidates. Curcumin diethyl disuccinate (CDD), an ester prodrug of curcumin, has been developed to improve the chemical stability of curcumin. In this study, the *in vitro* stability of CDD in HCl buffer (pH 1.2), acetate buffer (pH 4.5), phosphate buffer (pH 6.8, 7.4 and 8.0) and *in vitro* metabolism of CDD in rat, dog and human plasma were investigated at 4, 25 and 37 °C. HPLC and nonlinear regression analyses showed that the degradation of CDD in buffers was temperature-dependent and followed pseudo-1st order kinetics. CDD was least stable in acetate buffer at all tested temperatures. The plasma metabolism of CDD was temperature-dependent and the reaction followed consecutive pseudo-1st order kinetics. The CDD hydrolysis in plasma was accelerated by plasma esterases in the following order: rat >> human > dog. LC-MS/MS analysis showed that the cleavage of ester bonds of CDD was preferential at the phenolic ester, producing monoethylsuccinyl curcumin as the intermediate metabolite. The use of various esterase inhibitors indicated that carboxylesterase was the enzyme involving CDD hydrolysis in rat plasma while multiple enzymes played a role in dog and human. This study provides useful information for future *in vivo* studies and further development of CDD as a therapeutic agent.

Field of Study:	Biomedicinal Chemistry	Student's Signature .....
Academic Year:	2018	Advisor's Signature .....
		Co-advisor's Signature .....

ACKNOWLEDGEMENTS

I would like to show my deep gratitude to my thesis advisor, Associate Professor Dr. Pornchai Rojsitthisak for his valuable advice, motivation and encouragement throughout my graduate study. I would like to show appreciation to my co-advisor, Assistant Professor Dr. Boonsri Ongpipattanakul, for her useful suggestion and support for the experimental work at the Chulalongkorn University Drug and Health Products Innovation & Promotion Center (CU-D-HIP). Also, I would like to thanks thesis committee for their invaluable comments on this thesis.

I am very grateful to the Research Instrument Center of Faculty of Pharmaceutical Sciences, Chulalongkorn University, Pharma Nueva Co., Ltd and Research and Development Institute of the Government Pharmaceutical Organization for providing research facilities. I also thanks to the committee of Biomedicinal Chemistry Program for giving me opportunity to pursue my Master's degree study.

I would like to express my deepest appreciation to my beloved family for their continual support, encouragement and understanding. Also, I would like to express my gratefulness to my colleagues and friends whose names are not mentioned here for everything over the past years of my graduate life.

This research was supported by the scholarship from the Graduate School, Chulalongkorn University to Commemorate the 72nd Anniversary of His Majesty King Bhumibala Aduladeja, the 90th Anniversary Chulalongkorn University Fund (Ratchadaphiseksomphot Endowment Fund, Grant No. GCUGR1125602053M), the Overseas Research Experience Scholarship from the Graduate School and Faculty of Pharmaceutical sciences, Chulalongkorn University, and Ratchadaphiseksomphot Endowment Fund of Chulalongkorn University (Grant No. CU-GR_60_07_33_01).

Pahweenvaj Ratnatilaka Na Bhuket

TABLE OF CONTENTS

Page

LIST OF TABLES

Page

LIST OF FIGURES

Page

LIST OF ABBREVIATION

AChE	Acetylcholinesterase
ArE	Arylesterase
BNPP	Bis-*p*-nitrophenyl phosphate
BChE	Butyrylcholinesterase
BW284C51	1,5-Bis(4-allyldimethylammoniumphenyl) pentan-3-one dibromide
CES	Carboxylesterase
CDD	Curcumin diethyl disuccinate
CUR	Curcumin
ºC	Degree Celcius
DMAP	4-(*N*,*N*-dimethylamino)pyridine
DMC	Dimethylcurcumin
DTNB	5,5′-Dithiobis-2-nitrobenzoic acid
EDTA	Ethylenediamine tetraacetic acid
EGTA	Ethyleneglycol-bis(2-aminoethylether)-tetraacetic acid
g	Gram
GI	Gastrointestinal
h	Hour
IC_{50}	Half maximal inhibitory concentration
HPLC	High-performance liquid chromatography
i.v.	Intravenous
kg	Kilogram
LC-MS/MS	Liquid chromatography-tandem mass spectrometry
m/z	Mass-to-charge ratio
MW	Molecular weight
µg	Microgram

µL	Microliter
µM	Micromolar
mg	Milligram
mL	Milliliter
mm	Millimeter
mM	Millimolar
mmol	Millimol
min	Minute
MSCUR	Monoethylsuccinyl curcumin
nm	Nanometer
N	Normal
p-NPA	*p*-Nitrophenyl acetate
PAR	Peak area ratio
PON	Paraoxonase
rpm	Revolutions per minute
sec	Second
Iso-OMPA	Tetra isopropyl pyrophosphoramide
TLCK	*N*-α-tosyl-l-lysine chloromethylketone hydrochloride
PMSF	Phenylmethylsulfonyl floride
v/v	Volume-by-volume

CHAPTER I

INTRODUCTION

1.1 Background and rationale

Curcumin (CUR; **Figure 1**) is a bioactive compound found in turmeric (*Curcuma longa* L.) with the high safety profile (1). It has been documented to possess vast biological activities including antioxidant (2, 3), anti-inflammatory (4, 5) and anticancer properties (6-8). It also has been demonstrated its benefits to Alzheimer's disease (9-11), cardiovascular status (12) and arthritis (13). CUR up to 8 g per day is well-tolerated in patients with advanced pancreatic cancer, demonstrating the safety of CUR (14). Because of its prominent bioactivities and safety, CUR therefore has been considered as a potential phytochemical for treatment and prevention of a variety of diseases.

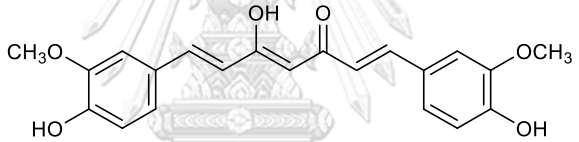

Figure 1 Structure of curcumin

Although CUR has a variety of pharmacological activities, its poor bioavailability, extensive metabolism and instability in neutral and basic solutions limit itself to be developed as a therapeutic agent (15, 16). To overcome these limitations, a prodrug of CUR, curcumin diethyl disuccinate (CDD; **Figure 2**), was developed by esterifying both phenolic hydroxyl groups of curcumin with ethyl succinyl chloride. CDD was found to be more stable in phosphate buffer at pH 7.4 than CUR. It can be converted to the active metabolite CUR in human plasma, which is the desired property of a prodrug. CDD is taken up by human epithelial colorectal adenocarcinoma cells (Caco-2 cells) and has greater cytotoxicity than CUR (17, 18). Furthermore, it exhibited antinociceptive effects in mice in both central and peripheral nociception models (19). This evidence demonstrates the potential of CDD to be developed as a prodrug of CUR.

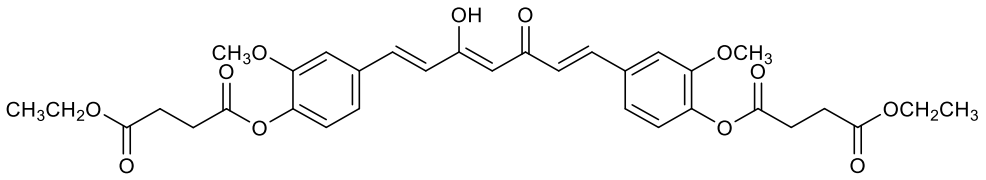

Figure 2 Structure of curcumin diethyl disuccinate

Preclinical pharmacokinetic evaluation is an important part in drug discovery and development because the information obtained from preclinical pharmacokinetic studies of a new drug candidate is used for making "go/no-go" decision. Additionally, the data from pharmacokinetic studies in preclinical species is used for calculating drug doses for further clinical studies. Previously, a pharmacokinetic study of CDD was investigated in rat (20). Unfortunately, pharmacokinetic parameters of CDD could not be calculated because negligible amounts of CDD were present in the study samples. Previously, Ratnatilaka Na Bhuket and colleagues have used 10 mM BNPP, a carboxylesterase inhibitor, to prevent *ex vivo* degradation of CDD in rat plasma (21). The use of BNPP enabled the quantification of CDD in rat plasma collected from rats after intravenous administration and pharmacokinetic parameters could be calculated. This study suggests that blood may play an important role in the metabolism CDD *in vivo*.

Stability in solutions relevant to physiological pH is one of important properties of drug candidates that has been implemented in the early phase in drug discovery and development. Stable compounds usually have more chance to be successfully developed as therapeutic agents. Also, the plasma metabolism of drug candidates, especially ester prodrugs, is an important part of *in vitro* ADME assay (22). Parallel screening of *in vitro* and *in vivo* pharmacokinetic profiles of drug candidates during the early phase would help and accelerate the go/no go decision. Because pharmacokinetic properties of a drug candidate are usually studied in different animal species, understanding the interspecies differences in plasma stability would be beneficial for the design of experiments. Therefore, the aims of this study are to investigate the stability of CDD in non-enzymatic solutions, which mimic the pH conditions of several biological fluids, as well as the *in vitro* stability of CDD in enzymatic conditions of plasma. Metabolites formed during plasma metabolism of

CDD were elucidated by LC-MS/MS. Plasma esterases involved in the metabolism of CDD in plasma were also deduced using esterase inhibitors.

1.2 Objectives

1. To investigate the stability of CDD in buffer solutions and rat, dog and human plasma.
2. To explore the involvement and type of plasma esterases involving the *in vitro* metabolism of CDD.

1.3 Hypothesis

1. CDD has the good stability in buffer solutions.
2. The hydrolysis of CDD in plasma is due to the presence of plasma esterases in plasma.
3. The plasma metabolism of CDD in terms of hydrolysis rate and esterases involved in the hydrolysis is different among the tested species.

CHAPTER II
LITERATURE REVIEW

2.1 Pharmacological activities and limitations of CUR

CUR is a bioactive polyphenolic compound found in turmeric (*Curcuma longa* L.) with a number of biological activities including antioxidant (2, 3), anti-inflammatory (4, 5) and anticancer properties (6-8). It also shows the benefits to Alzheimer's disease (9-11), cardiovascular status (12) and arthritis (13). Curcumin has been proved for its safety as shown in clinical trials even at high doses. For instance, a phase II clinical trial of curcumin in patients with advanced pancreatic cancer indicated that taking curcumin 8 g/day is well tolerated (14). Therefore, CUR has been considered as a potential phytochemical for treatment and prevention of a variety of diseases because of its prominent pharmacological activities and safety.

Despite CUR exhibits interesting pharmacological efficacy and safety, a limitation that hinders it from having been approved as a therapeutic agent is its relatively low oral bioavailability. This limitation can be attributed to its inherent physicochemical properties. CUR has very low water solubility (0.068 μg/mL) at 25 ºC (23). It is decomposed dramatically in buffer solutions at neutral and basic pH. This may be due to the removal of a phenolic proton leading to hydrolytic degradation (15). At basic pH, CUR also undergoes the auto-oxidative transformation to a bicyclopentadione derivative, 2-[4′-hydroxy-3′-methoxy)-phenoxy]-4-(4″-hydroxy-3″-methoxyphenyl)-8-hydroxy-6-oxo-3-oxabicyclo[3.3.0]-7-octene (24). On the contrary, CUR is more stable in acidic pH condition which may be contributed by the conjugated diene structure (15). The oxidative degradation of CUR in phosphate buffer (pH 7.4) can be blocked by the presence of antioxidants such as ascorbic acid, N-acetylcysteine, or glutathione (25). Therefore, curcumin would be stable in the stomach but degrades in the small intestine before being absorbed. Degradation pathways of CUR are depicted in **Figure 3**.

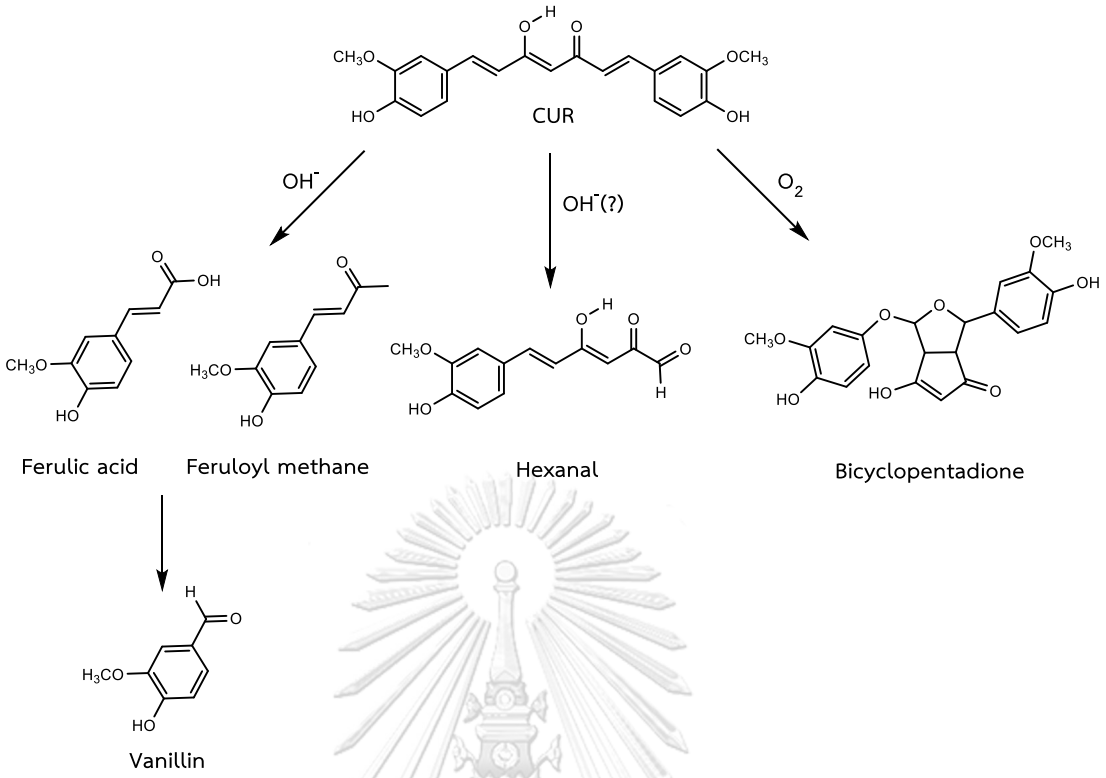

Figure 3 Degradation products of CUR from alkaline hydrolysis and autoxidation. The degradation pathway to hexanal (pathway with a question mark) has not been confirmed (26).

Pharmacokinetic properties of CUR including poor absorption and extensive metabolism also affect its oral bioavailability. For example, after oral administration of CUR to Sprague-Dawley rats at a dose of 1 g/kg, infinitesimal amounts of CUR were detected in rat plasma but 75% of CUR was found in feces. These might be due to the poor absorption from the gastrointestinal tract (27). Shoba et al. compared pharmacokinetics of CUR in rats and human volunteers. Rats were administered orally with CUR in the dose of 2 g/kg while the volunteers were administered at a dose of 2 g. In rats, a maximum serum concentration of 1.35 ± 0.23 μg/mL was achieved in 0.83 h with an elimination half-life of 1.70 ± 0.58 h. In human, however, very low or undetectable amounts of CUR were observed with a maximum serum concentration of 0.006 ± 0.005 μg/mL in 1 h (28).

CUR undergoes extensive metabolism in the alimentary tract especially in liver and intestine. Metabolism of CUR in human and rat hepatocytes and rats *in vivo* was investigated. In hepatocyte suspensions, 35% of initial amounts of CUR was

found in human hepatocyte suspensions after 2 h of incubation and the level of CUR in rat hepatocyte suspensions was near the detection limit at the same incubation time. These results suggest that CUR undergoes more extensive metabolism in rat hepatocytes than in human. The hepatocytic metabolism of CUR yields reduced metabolites including hexahydroCUR and octahydroCUR as major metabolites. On the contrary, CUR glucuronide and CUR sulfate are the predominant metabolites found in rat plasma after oral or intravenous administration (29). There is an *in vitro* study demonstrating metabolism of curcumin in subcellular fractions of rat and human intestines. HexahydroCUR and CUR sulfate were found in cytosolic fraction of both species whereas CUR glucuronide was detected in microsomal fractions (30). Asai and Miyazawa demonstrated that CUR glucuronide and CUR glucuronide/sulfate conjugates were present in rat plasma after oral administration of commercial CUR. They postulated that glucuronidation of CUR took place in the intestinal mucosa and would be subsequently conjugated with sulfate in liver (31). Glutathione conjugation of CUR via a Michael reaction was also demonstrated in human intestinal cytosol, liver cytosol and Caco-2 cells (32). The summarized metabolic pathways of CUR are illustrated in **Figure 4**.

2.2 Succinate ester prodrugs of CUR

Prodrug design is an approach that the structure of the parent compound is modified by conjugation with a pro-moiety via a covalent bond. The prodrug itself has no pharmacologically activities. However, it is biotransformed by chemical or enzymatic processes in biological systems. The purpose of prodrug design is to improve physicochemical and biopharmaceutical properties such as water solubility, stability and permeability of the parent compound.

Wichitnithad et al. synthesized six succinate ester prodrugs of curcuminoids and tested their cytotoxicity against Caco-2 cells (17). Among the six prodrugs, CDD, an ethyl succinyl ester prodrug of CUR, demonstrated the most potent cytotoxic activity with the IC_{50} value of 1.84 μM. The encapsulation of CDD in chitosan/alginate nanoparticles significantly enhances the cytotoxicity of CDD against breast cancer (MDA-MB-231) cells (33). CDD showed higher stability in phosphate buffer pH 7.4 in comparison with CUR. Besides, CDD exhibited antinociceptive effects in mice (19). It

showed the analgesic activity at both supraspinal and spinal levels with the dose of 25 mg/kg administered orally. At the dose of 200 mg/kg, CDD demonstrated the analgesic effect in a visceral inflammation pain model. The pharmacokinetics of CDD was also evaluated in rats by Bangphumi et al. (20). CDD gave superior tissue distribution with higher tissue to plasma ratio of CUR and CUR glucuronide in several organs after i.v. administration at 1 and 4 h compared to the direct i.v. CUR. Unfortunately, pharmacokinetic parameters of CDD in rats could not be calculated due to the unquantifiable amount of CDD in the study samples.

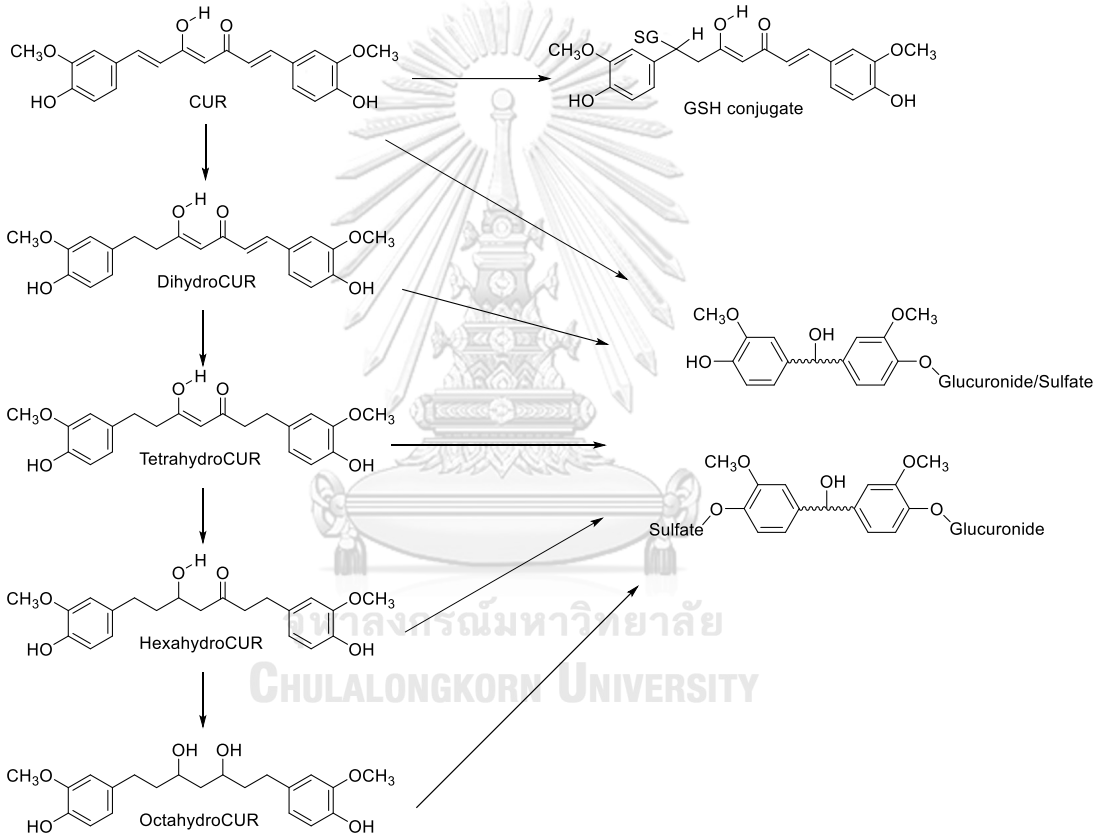

Figure 4 Reductive and conjugative metabolism of CUR (26).

2.3 Stability of drug candidates in buffers

Stability of drug candidates in buffers with different pH values is essential during drug development. The pH values of gastrointestinal (GI) tract range from pH 1.2 in the stomach to pH 8.0 in colon. Acceptable stability of drug candidates over the pH range of the GI tract is desirable to assure that the drugs achieve satisfactory oral bioavailability. The chemical stability in aqueous solutions of some

pharmaceuticals is pH-dependent. The degradation rate constant may dramatically change when the pH is altered by 1 unit (34). Temperatures also affect the degradation rates of drugs as described by Arrhenius equation. Elevating the temperature increases the rate of drug degradation and vice versa. The instability of a drug in aqueous solutions also can cause negative impacts on the sample analysis due to the degradation during sample handling and preparation. In addition, stability data of a drug in aqueous solutions is necessary for the preparation of drug formulations in the solution form. For example, Fubara and Notari studied the influence of pH and temperature on the degradation kinetic of cefepime in aqueous solutions (35). They found that cefepime was most stable in the pH range of 4-6, which was a pH-independent region under the studied conditions. They also demonstrated the temperature dependency for the degradation rate constants of cefepime in various buffers. Subsequently, they could establish equations to predict degradation rate constants of cefepime under the studied conditions which would be of benefit for the preparation of cefepime aqueous formulations. Thus, the evaluation on the effects of pH and temperature on the stability of drug candidates is essential for pharmaceutical development.

2.3 Metabolism of ester drugs in plasma and plasma esterases

Blood is another matrix that plays an important role in xenobiotic metabolism especially for ester-containing molecules. Due to the presence of esterases, several ester-based drugs are degraded in blood. Unlike other ester drugs, the cleavage of an ester bond to liberate the active metabolite *in vivo* is desired for an ester prodrug. Although the hydrolytic cleavage of an ester bond of ester prodrugs is desirable for exerting pharmacological actions, this hydrolysis reaction may render the difficulties for pharmacokinetic studies because of *ex vivo* metabolism taking place in the collected samples. The *ex vivo* hydrolysis of ester prodrugs could lead to under- or overestimation of pharmacokinetic parameters and lack of reproducibility in sample analysis (36).

Important plasma esterases that participate in the hydrolysis of ester prodrugs are carboxylesterase, acetylcholinesterase, butyrylcholinesterase, paraoxonase (or arylesterase) and albumin (37, 38). They have been divided into A-esterases, B-

esterases and C-esterases based on their substrate specificity. A-esterases are esterases that cleave aromatic esters such as organophosphates rapidly. Paraoxonase falls into this category. On the other hand, B-esterase enzymes including carboxylesterase, acetylcholinesterase and butyrylcholinesterase are inhibited by carbamate, organophosphate and organosulfur compounds. Additionally, carboxylesterase, acetylcholinesterase and butyrylcholinesterase are members of serine hydrolase superfamily. Interestingly, the amino acid sequences necessary for the hydrolytic cleavage at the catalytic triad of the active site (Glu, His and Ser) are highly conserved among carboxylesterase, acetylcholinesterase and butyrylcholinesterase. Lastly, C-esterases are not inhibited by organophosphate esters and do not hydrolyze them. However, the role of C-esterases in drug metabolism has not been reported. To date, the above esterase classification is not widely used because the more accurate and precise classification has been established.

The species differences in the expression and activities of blood esterases have been studied and reported (39, 40). **Table 1** shows a summary of relative activity of esterases found in plasma rat, dog and human. Rat and dog are animals that are typically used in drug discovery and development as representative rodent and non-rodent species. The differences in the expression and enzyme activity of plasma esterases can contribute to the metabolism of ester-based prodrugs. Understanding the interspecies differences in the expression and activity of plasma esterases lead to the selection of appropriate preclinical species for pharmacokinetic studies. Therefore, it is worthy for pharmaceutical scientists to investigate effects of the interspecies differences on the hydrolysis of ester prodrugs *in vitro* during the early phase of drug development in order to selecting appropriate animal models for *in vivo* studies. The details for each plasma esterase are described below.

Table 1 Summary of esterases existed in plasma of rat, dog and human (40)

Animal species	Esterases found	Enzyme activity
Rat	Carboxylesterase	+++
	Butyrylcholinesterase	+
	Paraoxonase	+++
	Other (e.g. albumin)	++
Dog	Butyrylcholinesterase	++
	Paraoxonase	+++
	Other (e.g. albumin)	+
Human	Butyrylcholinesterase	+++
	Paraoxonase	+++
	Other (e.g. albumin)	++

2.3.1 Carboxylesterase

Carboxylesterases (CES, EC 3.1.1.1) involve in the metabolism of various type of compounds including ester, amide and carbamate. CES enzymes are generally localized in the luminal side of the membrane of endoplasmic reticulum (ER). They are categorized into 5 families which are CES1, CES2, CES3, CES4 and CES5. However, the most important isoforms of CES that play role in drug metabolism are CES1 and CES2. CES1 family is mainly expressed in liver while CES2 isozymes are mainly expressed in small intestine (41). Generally, CES1 hydrolyzes ester compounds that contain a small alcohol group and large acyl group while features of CES2 substrates are molecules with a large alcohol group and small acyl group. Example drugs that are substrates for CES1 and CES2 are oseltamivir and prasugrel, respectively (38).

There are several literatures demonstrate that the expression of CES in plasma differs among animal species (39, 40, 42). Rat plasma has a high CES activity while this enzyme is absent in dog and human plasma. This is because most CES enzymes including human CES and dog CES contain the tetrapeptide HXEL sequence on the carboxy-terminal, where X is threonine (T), isoleucine (I) or valine (V). These HXEL-COOH motif is essential for the retention of CES enzymes within the luminal

side of the endoplasmic reticulum (ER) via the binding to KDEL receptor on the ER membrane as shown in **Figure 5**. However, rat CES1G1 and mouse CES1G2 have the HTEHK sequence on the carboxy-terminal instead of the HXEL sequence. The HTEHK-COOH cannot bind to the KDEL receptor, resulting in the secretion of CES1G1 and CES1G2 from liver to the blood stream (41).

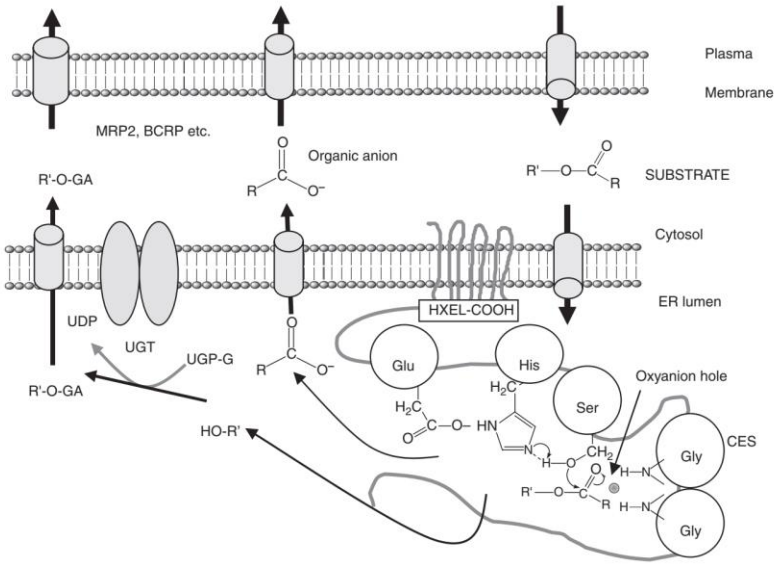

Figure 5 Interaction between CES and UDP-glucuronosyltransferase (UGT) in the luminal side of the ER membrane. An ester substrate is hydrolyzed by CES, giving two hydrolytic products: alcohol or phenol and carboxylate anion. The released alcohol or phenol undergo subsequent glucuronidation by UGT. The glucuronide conjugate and the carboxylate anion are the substrates of organic anion transporter e.g. multidrug resistance-associated protein 2 (MRP2) and breast cancer resistance protein (BCRP). Reproduced with permission from (41).

The proposed catalytic mechanism of CES is depicted in **Figure 6**. Initially, the substrate is positioned in the correct orientation for subsequent reaction. Then, the oxygen atom of the hydroxyl group of Ser attacks on the carbonyl carbon of the ester bond. The nucleophilic attack of the hydroxyl group of Ser is facilitated by the interaction between Glu, His and Ser in the catalytic triad. The negative charge on the oxygen of the tetrahedral intermediate is stabilized by the N-H groups of the nearby Gly residues. This configuration is called an oxyanion hole. As the general acid-catalyzed hydrolysis, the ester bond breaks and the leaving group (alcohol or

phenol) takes a proton from the imidazolium ring of His. The acyl part of the original ester is bonded with the enzyme as an acyl-enzyme complex. Subsequently, a water molecule attacks to the carbonyl carbon of the acyl-enzyme intermediate. The reaction takes place similar to the cleavage of ester bond of the original ester. Finally, His protonates the oxygen atom of Ser followed by the liberation of acyl part as a free acid and the enzyme is ready for the next hydrolysis (41).

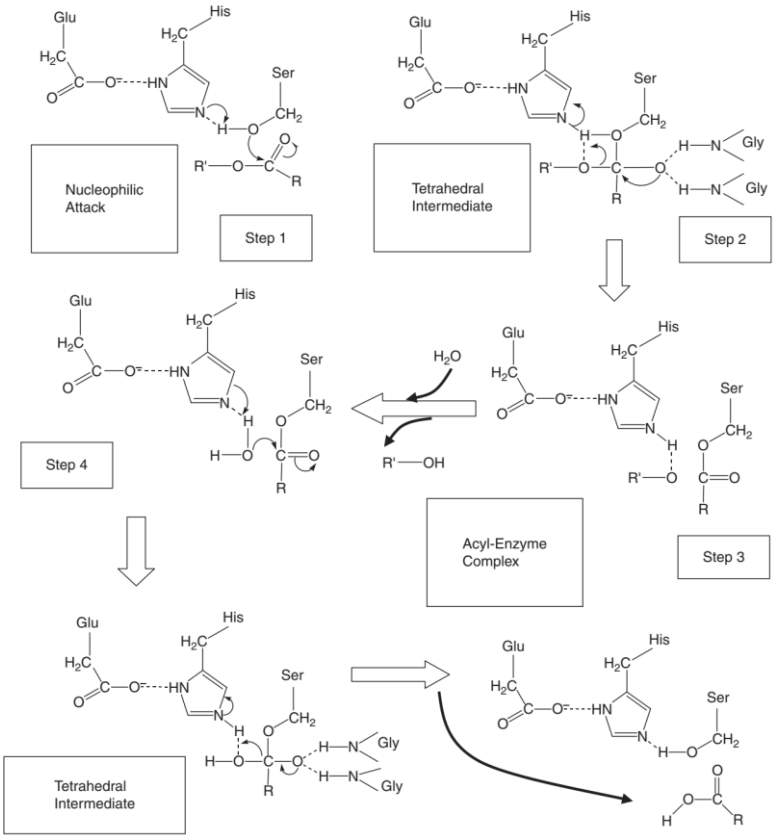

Figure 6 Proposed mechanism for the catalytic action of CES. Reproduced with permission from (41).

2.3.2 Acetylcholinesterase

Acetylcholinesterase (AChE, EC 3.1.1.7) has important roles in the regulation of cholinergic system. AChE hydrolyzes the acetylcholine at the cholinergic synapse and neuromuscular junctions resulting in the termination of neurotransmission. In addition to the skeletal muscles and nervous systems, AChE is also found in non-attached cells like red blood cells and white blood cells (43). However, a negligible amount of AChE in human plasma is reported (39). AChE has a

small catalytic gorge and limited hydrophobic residues (two aromatic residues) for substrate binding, resulting in the high substrate discrimination and specificity. It has been reported to involve in the biotransformation of ester prodrugs such as phenylbutyryl ester prodrugs of propranolol and cefpodoxime proxetil (44, 45).

2.3.3 Butyrylcholinesterase

Butyrylcholinesterase (BChE, EC 3.1.1.8) is a glycosylated globular protein that is synthesized in liver and secreted into the bloodstream. It is also expressed in other tissues including lung, brain, heart, skeletal muscle and pancreas (46). BChE can metabolize a broader substrate specificity than AChE due to its larger acyl binding pocket in the active site (43). However, its physiological functions are not completely explored (37). It is believed that BChE serves as a back-up for AChE in the case that acetylcholine evades the nerve synapses. It has also been reported for a role in fat metabolism, detoxification of poisons and drug metabolism (46). Several ester prodrugs e.g. bambuterol and methylprednisolone acetate have been reported to be metabolized by BChE to their active forms (43).

The species differences in the activity of plasma BChE have also been reported. Berry and colleagues examined the BChE activity in plasma, liver and intestine of mouse, rat, dog, monkey and human (40). They found that the plasma BChE activity was high and comparable among the tested species except for rat which had the noticeably low BChE activity. They also showed that the activity of BChE in liver was lower than that in plasma except for rat, which BChE activity in liver was absent. Interestingly, the BChE activity could be detected in the rat intestine though it was lacking in the liver. The intestinal BChE activity was absent in mouse and dog.

2.3.4 Paraoxonase

Paraoxonase (PON, EC 3.1.8.1) is a family of hydrolases comprising of PON1, PON2 and PON3. Unlike the three previously mentioned hydrolases, PON is not a serine hydrolase but has a catalytic dyad consisting of two histidine residues (42). Among the 3 isoforms, only PON1 possesses arylesterase (ArE) activities (37, 43). PON1 requires the presence of calcium ion to exert the enzymatic activity and

maintain structural stability (38, 47). **Figure 7** illustrates the proposed hydrolysis mechanism of PON1 on ester substrates. PON1 and PON3 are primarily synthesized in liver and secreted into the blood stream while PON2 can be found in several tissues except plasma (38). PON1 has been found to associate with a specific HDL subspecies containing apolipoprotein A-1 and clusterin (48). PON1 is capable to hydrolyze aromatic carboxylic acid esters, carbamate ester and organophosphates such as prulifloxacin (49) and olmesartan medoxomil (50). PON3 hydrolyzes mainly the drugs containing a lactone ring such as lovastatin and simvastatin (37). PON1 also hydrolyzes lactone-containing drugs with different substrate specificity to that of PON3. The reasons for the differences in substrate specificity are still unclear (38). There is no report for PON2 on its involvement in drug metabolism and the roles of PON3 in the hydrolysis of xenobiotics are less investigated in comparison with PON1. Therefore, more investigation of the roles of PON2 and PON3 in drug metabolism is required.

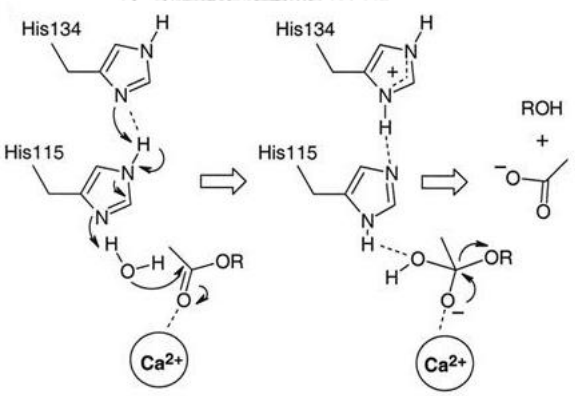

Figure 7 The proposed hydrolysis mechanism of PON1 on ester substrates. Adapted with permission from (51)

2.3.5 Serum albumin

Serum albumin is a soluble protein synthesized and secreted from liver. It is the most abundant plasma protein with a concentration of 0.6 mM (52). It has been well known as the depot and transport protein for endogenous substances and xenobiotics including pharmaceuticals. Interestingly, albumin also possesses the esterase-like activity and it involves in the hydrolysis of several drugs. Tyr-411 and Lys-199 residues are essential for the esterase-like activity of serum albumin whereas

a free Cys-34 residue is responsible for the thioesterase or thiol-disulfide exchange activity (52). For instance, it has been shown that human serum albumin was capable to metabolize an angiotensin II receptor blocker olmesartan medoxomil via the hydrolysis reaction (53). The hydrolytic cleavage of olmesartan medoxomil by human serum albumin followed Michaelis-Menten kinetics. Lys-199, Trp-214 and Tyr-411 were found to play important roles in the bioactivation of olmesartan medoxomil.

2.4 Esterase inhibitors

The conversion of ester prodrugs or ester-containing molecules to their corresponding metabolites by esterase enzymes can be inhibited by esterase inhibitors. Each inhibitor has different selectivity and inhibitory effect on the target enzymes. There are several specific esterase inhibitors available as shown in **Table 2** (36). Using these specific inhibitors, esterase(s) involving the hydrolysis of a drug or a drug candidate can be determined. In addition, the use of an appropriate esterase inhibitor during bioanalytical method development for ester-based prodrug to prevent *ex vivo* hydrolysis enables the analyst to measure the level of an ester prodrug in plasma with accuracy and precision.

Table 2 List of the esterase inhibitors with their target enzymes

Enzymes	Inhibitors
Carboxylesterase	Prazosin, Thenoyltrifluoroacetone, Bis(4-nitrophenyl)-phosphate, Phenylmethylsulfonyl fluoride, 2,2-Dichlorovinyl dimethyl phosphate (Dichlorvos)
Phosphodiesterase	BNPP
Arylesterase/Paraoxonase	5, 5'-Dithio-bis-2-nitrobenzoic acid, ethylene diamine tetraacetic acid, ethylene glycol tetraacetic acid
Acetylcholinesterase	Neostigmine, Dichlorvos, BW284c51, Paraoxon, Eserine
Butyrylcholoinesterase	Ethopropazine, Tetraisopropyl pyrophosphoramide
Serine hydrolase	Phenylmethylsulfonyl fluoride, 4-(2-aminoethyl-) benzenesulphonyl floride hydrochloride, Tosyl-L-lysyl-chloromethyl ketone
Non-specific	NaF

CHAPTER III

MATERIALS AND METHODS

3.1 Materials

3.1.1 Equipment and instruments

- Analytical balance (Sartorius BA 210S, Germany)
- Elga Maxima 21F Water purification system (Veolia Water Technologies, UK)
- Freezer (-40°C)
- Heating magnetic stirrer (Velp Scientifica, model ARE, Italy)
- High-performance liquid chromatograph (Agilent 1200 series, USA)
- Liquid chromatograph-tandem mass spectrometer (LC part: Ekspert UltraLC 100, Detector: Mass spectrometer AB SCIEX QTRAP® 6500, USA)
- Nuclear magnetic resonance spectrometer (Bruker Spectrospin AG 300 MHz/52 mm, Switzerland)
- Refrigerated centrifuge (Hettich Mikro 22R, Germany)
- Refrigerator (beko, Turkey)
- Rotary evaporator (Buchi R-200, Switzerland)
- Fume hood
- Thin-layer chromatography plate (Merck, Germany)
- Magnetic bar
- Heating magnetic stirrer (VELP Scientifica, Italy)
- Digital dry bath (Labnet, USA)
- Rainin pipettes 2-20, 20-200, 100-1,000 and 500-5,000 µL (Mettler Toledo, USA)
- Micropipette tips 20, 200, 1,000 and 5,000 µL (Mettler Toledo, USA)
- Microcentrifuge tubes 1.7 mL (Corning Inc., USA)
- Centrifuge tube 15 mL (Corning Inc., USA)
- CLARIOstar microplate reader (BMG LABTECH, Germany)
- 96-well plates (Corning Inc., USA)

- Vortex mixer VORTEX GENIE 2® Model (Scientific Industries, Inc., USA)
- Duran bottles (Schott Duran, Denmark)
- pH meter (Mettler Toledo, USA)
- Silicagel 60 RP-18 (40-63 μm) per HPLC preparative (Merck, Germany)

3.1.2 Chemicals and reagents

- Formic acid, 98-100% (Merck, Germqny)
- HPLC grade acetonitrile (Burdick & Jackson, Korea)
- Acetylacetone (Sigma-Aldrich, USA)
- Bis-*p*-nitrophenyl phosphate (BNPP; Tokyo Chemical Industry, Japan)
- Boric anhydride (Sigma-Aldrich, USA)
- *n*-Butylamine (Sigma-Aldrich, USA)
- Chloroform-*d* (Merck, Germany)
- 4-(*N*,*N*-dimethylamino)pyridine (DMAP; Sigma-Aldrich, USA)
- Commercial grade dichloromethane (RCI Labscan, Thailand)
- Commercial grade ethyl acetate (RCI Labscan, Thailand)
- Ethyl-4-chloro-4-oxobutyrate (Sigma-Aldrich, USA)
- Hydrochloric acid, 36.5-38 % (Fisher Scientific, USA)
- Commercial grade methanol (RCI Labscan, Thailand)
- Phenylmethylsulfonyl floride (PMSF; Sigma-Aldrich, USA)
- Sodium bicarbonate (Sigma-Aldrich, USA)
- Sodium fluoride (BDH Merck, UK)
- Sodium sulfate anhydrous (Merck, Germany)
- Tributyl borate (Sigma-Aldrich, USA)
- Vanillin (Sigma-Aldrich, USA)
- 4-(2-aminoethyl-)benzenesulphonyl floride hydrochloride (Pefabloc® SC; Sigma-Aldrich, USA)
- 1,5-Bis(4-allyldimethylammoniumphenyl)pentan-3-one dibromide (BW284C51; Sigma-Aldrich, USA)
- 5,5′-Dithiobis-2-nitrobenzoic acid (DTNB; Sigma-Aldrich, USA)
- Heparinized rat plasma (The National Laboratory Animal Center at Mahidol University, Thailand)

- Heparinized dog plasma (Innovative Research, USA)
- Heparinized human plasma (Innovative Research, USA)
- Ethylenediamine tetraacetic acid disodium (Na_2EDTA; Ajax Finechem, Australia)
- Ethyleneglycol-bis(2-aminoethylether)-tetraacetic acid (EGTA; Sigma-Aldrich, USA)
- *p*-Nitrophenyl acetate (*p*-NPA; Sigma-Aldrich, USA)
- *p*-Nitrophenol (*p*-NP; Sigma-Aldrich, USA)
- Tetra isopropyl pyrophosphoramide (iso-OMPA; Sigma-Aldrich, USA)
- *N*-α-tosyl-l-lysine chloromethylketone hydrochloride (TLCK; Sigma-Aldrich, USA)
- Sodium chloride (Scharlau, Spain)
- Potassium dihydrogen phosphate (Merck, Germany)
- Potassium chloride (Sigma-Aldrich, USA)
- 3,4-Dimethoxybenzaldehyde (Sigma-Aldrich, USA)
- Sodium hydroxide (Carlo Erba, Italy)
- Glacial acetic acid (Scharlau, Spain)
- Sodium acetate (Scharlau, Spain)

Preparation of solutions used in this study can be found in **APPENDIX A**.

3.2 Methods

3.2.1 Synthesis of curcumin, dimethylcurcumin, monoethylsuccinyl curcumin and curcumin diethyl disuccinate

3.2.1.1 Synthesis of curcumin and dimethylcurcumin

Curcumin (CUR) were synthesized using the previously published method with some modifications (17). Birefly, 1.03 mL of acetylacetone (MW 100.12; d 0.972; 10 mmol) and 0.348 g of boron oxide (MW 69.62; 5 mmol) were mixed in a round-bottom flask containing 10 mL of ethyl acetate. This reaction mixture was heated at 50 ºC for 30 min or until a milky mixture formed, which indicates the formation of boron-acetylacetone complex. Simultaneously, 3.04 g of vanillin (MW 152.15; 20 mmol) and 10.8 mL of tributyl borate (MW 230.15; d 0.853; 40 mmol) were dissolved in 20 mL of ethyl acetate in another round-bottom flask at room

temperature. Then, the milky mixture was gradually transferred to the clear solution of vanillin and tributyl borate and stirred until a clear solution was achieved. Subsequently, 0.1 mL of *n*-butylamine (MW 73.14; d 0.740; 2 mmol) was added dropwise to the reaction mixture. The mixture would become more yellow. Stirring was continued overnight at room temperature. The reaction was stopped by adding 100 mL of 0.5 N HCl and stirred for 30 min to break the boron complex. The organic layer was separated, and the aqueous fraction was extracted with ethyl acetate twice. The combined organic layer was washed with deionized water and saturated saline solution, respectively. Then, the combined organic layer was dried over anhydrous sodium sulfate before being evaporated by rotary evaporator to obtain the crude product. Finally, the crystalline CUR was obtained by crystallization in methanol .

For synthesis of Dimethylcurcumin (DMC), all steps were as same as the synthesis of CUR except 3,4-dimethoxybenzaldehyde (MW 166.17; 3.32 g; 20 mmol) was used instead of vanillin.

3.2.1.2 Synthesis of monoethylsuccinyl curcumin

CUR (2g, 5.43mmol) and 4-(*N*,*N*-dimethylamino) pyridine (DMAP, 0.663 mg, 5.43 mmol) were dissolved in 500 mL of dichloromethane. The mixture was stirred at room temperature until both compounds dissolved completely. Then, the reaction mixture was slowly added with ethyl-4-chloro-4-oxobutyrate (95% assay, 814.3 µL, 5.43 mmol) at room temperature. After stirring for 2 h, 100 mL of 0.1 N HCl was added and the mixture was stirred for 5 min. The organic layer was washed with deionized water three times to remove residual acids. The residual water in the organic phase was removed using anhydrous sodium sulfate and the organic layer was concentrated by rotary evaporator. The concentrated mixture was purified by reverse phase C-18 column chromatography eluted with 80% methanol and 20% water. Subsequently, the combined eluate was dried by rotary evaporator and crude product was crystallized in methanol yielding ethyl (4-((1E,3Z,6E)-3-hydroxy-7-(4-hydroxy-3-methoxyphenyl)-5-oxohepta-1,3,6-trien-1-yl)-2-methoxyphenyl) succinate or monoethylsuccinyl curcumin (MSCUR).

3.2.1.3 Synthesis of curcumin diethyl disuccinate

Curcumin diethyl disuccinate (CDD) was synthesized using the previously reported method with some modifications (17). In brief, a round-bottomed flask was charged with 0.185 g of CUR (MW 368.13; 0.5 mmol) and 0.147 g of 4-(*N*,*N*-dimethylamino) pyridine (DMAP; MW 122.17; 1.2 mmol), followed by the addition of 40 mL of dichloromethane. The mixture was stirred at room temperature until both compounds dissolved completely. Then, the reaction mixture was slowly added with 180 µL of ethyl-4-chloro-4-oxobutyrate (MW 164.59; d 1.155; %assay 95; 1.2 mmol) at room temperature. After stirring for 2 h, 50 mL of 0.01 N HCl was added to the reaction mixture. Then, the aqueous phase was removed, and the organic layer was washed with 25 mL of 0.5% sodium bicarbonate. The aqueous layer was separated, and the organic layer was washed with deionized water. Then, the residual water in the organic phase was removed using saturated saline solution and anhydrous sodium sulfate. The organic layer was evaporated by rotary evaporator to obtain the crude product. The crude product was crystallized in methanol to give the CDD as pale yellowish solids.

3.2.2 Characterization of CUR, DMC, MSCUR and CDD

3.2.2.1 Mass spectrometry

The synthesized CUR, DMC, MSCUR and CDD were characterized by AB SCIEX QTRAP® 6500 mass spectrometer at the Faculty of Pharmaceutical Sciences, Chulalongkorn University using positive ion mode.

3.2.2.2 Nuclear magnetic resonance (NMR) spectroscopy

20 mg of CUR, DMC, MSCUR and CDD were dissolved with $CDCl_3$. The solutions were analyzed by a nuclear magnetic resonance spectrometer (300 MHz) at the Faculty of Pharmaceutical Sciences, Chulalongkorn University. The ^{1}H-NMR spectrum for each compound were recorded.

3.2.3 Assessment of the chemical stability of CDD in buffers

The chemical stability of CDD was carried out in buffer solutions with the pH of 1.2, 4.5, 6.8, 7.4, and 8.0, which mimic the pH of several biological fluids in the body such as gastric fluid and intestinal fluids. The reaction was initiated by adding 20 µL of the SS-CDD 01 into a 980 µL of phosphate buffer solution to obtain

a final concentration of 1.5 µM. The reaction was incubated at 4, 25 and 37 ºC for 12 h. The remaining amount of CDD was determined at 0 min, 15 min, 30 min, 45 min, 1 h, 1.5 h, 2 h, 4 h, 6 h, 8 h, 10 h and 12 h using HPLC. The experiment was performed in triplicates. The determination of reaction order is described in **Appendix E**. The pseudo-first-order kinetic model (**scheme 1**) was used to fit the data.

$$A \xrightarrow{k_{app}} B$$

Scheme 1 Consecutive pseudo-first order kinetic model

The apparent degradation rate constants of CDD (k_{app}) at different temperatures was calculated from Eq. 1 using nonlinear regression analysis.

$$CDD_t = CDD_0 e^{-k_{app}t} \quad \text{Eq. 1}$$

The degradation half-lives ($t_{1/2}$) were calculated from the following equation:

$$t_{1/2} = \frac{\ln 2}{k_{app}} \quad \text{Eq. 2}$$

3.2.4 Study on the *in vitro* metabolism of CDD in plasma

3.2.4.1 Quantification of plasma proteins

The total protein concentrations of plasma of the tested species were determined using Bicinchoninic acid (BCA) assay. The 10 µL of plasma was mixed with 990 µL of deionized water. Then, 10 µL of the diluted plasma was mixed with 200 µL of the BCA working solution in a microplate and incubated at 37 ºC. After incubation for 30 min, the reaction plate was cooled to room temperature. The amounts of proteins in the plasma samples were measured by a microplate reader (CLARIOstar®, BMG LABTECH, Ortenberg, Germany) at 562 nm and calculated against the standard curve constructed from serial dilutions of bovine serum albumin.

3.2.4.2 Assay of plasma esterase activity using *p*-nitrophenyl acetate

The combined plasma esterase activity in the tested species was determined by the previous reported kinetic assay with some modifications (54). The blank plasma of each tested species was diluted 100 times with PBS buffer (pH

7.4). The 190 µL of the diluted plasma from each studied species was mixed with 10 µL of 50 mM p-nitrophenyl acetate (*p*-NPA) solution (in methanol), a non-specific esterase substrate, in wells of a 96-well plate. Then, the change in the absorbance at 405 nm was monitored every 10 s over 3 min by CLARIOstar® microplate reader. The temperature for the assays was set at 30 ºC. The measurement was recorded by MARS Data Analysis Software. Plasma samples spiked with 10 µL of methanol were used as blank samples. The esterase activities were expressed as units per milligram of protein, where one unit represents the formation of 1 µmol of *p*-nitrophenol from *p*-NPA catalyzed by esterase per minute at 30 ºC.

3.2.4.3 Evaluation of kinetics of *in vitro* metabolism of CDD in plasma

The *in vitro* metabolism of CDD in plasma was investigated in rat, dog and human plasma. The stock solution of CDD was prepared in acetonitrile. Rat, dog and human plasma were pre-incubated at 4, 25 and 37 ºC for 10 minutes. The reaction was initiated by adding 18 µL of SS-CDD 01 into the 882 µL pre-incubated plasma to obtain a final concentration of 1.5 µM. The incubation temperature was maintained during the study. CDD was incubated in rat plasma for 0 s, 3 s, 5 s, 10 s, 15 s, 30 s, 45 s, 1 min, 3 min, 5 min, 10 min, 15 min, 30 min, 45 min and 1 h. For dog plasma, the incubation times were 0 s, 5 s, 15 s, 30 s, 1 min, 5 min, 15 min, 30 min, 1 h, 1.5 h, 2 h, 2.5 h, 3 h, 3.5 h and 4 h. In human plasma, the incubation times were 0 s, 5 s, 15 s, 30 s, 45 s, 1 min, 5 min, 15 min, 30 min, 45 min, 1 h, 1.5 h, 2 h, 2.5 h and 3 h. A 50 µL of plasma sample at each time point was combined with 250 µL of acetonitrile containing 0.6 µM of DMC (an internal standard, IS) to stop the reaction. The plasma samples were then centrifuged at 4000 rpm at 4 ºC for 5 min. The amounts of CDD from extracted samples were determined by HPLC. The experiment was performed in triplicates. The determination of reaction order is described in **Appendix E**. Peak area ratios between the analytes and DMC were fit to the consecutive pseudo-first order kinetic model (**scheme 2**).

$$A \xrightarrow{k_1} B \xrightarrow{k_2} C$$

Scheme 2 Consecutive pseudo-first order kinetic model

Peak area ratios between analytes (CUR, MSCUR and CDD) and DMC were plotted against time. Degradation rate constants of CDD (k_1) and M2 metabolite (k_2) were extracted from Eq. 1 and Eq. 3 using nonlinear least square regression analysis. The $t_{1/2}$ of CDD and time to reach the maximum of MSCUR (t_{max}) were calculated from Eq. 2 and Eq. 4, respectively.

$$[B]_t = [A]_0 \left(\frac{k_1}{k_2 - k_1}\right)\left(e^{-k_1 t} - e^{-k_2 t}\right) \qquad \text{Eq. 3}$$

$$t_{max} = \frac{1}{k_1 - k_2} \cdot \ln \frac{k_1}{k_2} \qquad \text{Eq. 4}$$

3.2.4.4 Identification of hydrolytic metabolites in plasma by LC-MS/MS

CDD with the final concentration of 15 µM was incubated in rat, dog, and human plasma at 37 ºC for 10 s, 15 min and 5 min, respectively. The reaction was stopped by adding 250 µL of acetonitrile to a 50 µL of each sample. The resulting mixtures were subjected to centrifugation at 4,000 rpm at 5 ºC for 5 min. Subsequently, the supernatants were diluted 20 times with acetonitrile and transferred to HPLC vials for LC-MS/MS analysis.

3.2.4.5 Investigation of esterase enzymes involved in the metabolism of CDD in plasma

Rat, dog and human plasma were pre-incubated at 37 ºC with various esterase inhibitors for 30 min. The names of esterase inhibitors with target enzymes were shown in **Table 3** and their final concentrations used in this study were based on reported literatures (54-56). Then, an appropriate volume of SS-CDD 01 was spiked into plasma samples to obtain a final concentration of 1.5 µM. The reaction mixtures were incubated at 37 ºC for 5 sec, 5 min and 15 min for rat, human and dog plasma, respectively. The plasma samples spiked with solvents of esterase inhibitors were used as positive controls.

Table 3 List of esterase inhibitors used in this study

Inhibitors	Target enzymes	Final concentrations
Eserine	Non-specific ChE	10 and 100 μM
BW284c51	AChE	10 and 100 μM
Iso-OMPA	BChE	0.1 and 1 mM
BNPP	CES	0.1 and 1 mM
TLCK	Serine hydrolase	0.1 and 1 mM
PMSF	Serine hydrolase	0.1 and 1 mM
Pefabloc® SC	Serine hydrolase	0.1 and 1 mM
DTNB	Arylesterase	0.1 and 1 mM
EDTA	PON	5 and 10 mM
EGTA	PON	5 and 10 mM
NaF	Non-specific esterases	5 and 10 mM

The reaction was terminated by adding 250 μL of acetonitrile containing 0.6 μM DMC to 50 μL of each sample. The % inhibition was used to indicate the type of plasma esterase involved in the hydrolysis of CDD which was calculated as follows:

$$\% \text{ Inhibition} = [1-(D_{\text{with inhibitor}} / D_{\text{without inhibitor}})] \times 100 \qquad \text{Eq. 5}$$

Where D is the decrease of CDD in the samples.

3.2.4.6 Chromatographic conditions of HPLC analysis

The chromatographic analysis was performed on an Agilent 1200 series liquid chromatographic system consisting of degasser unit, quaternary pump and UV detector. The HPLC system and data processing were operated using ChemStation software. The separation of analytes was achieved by a Halo C18 column (4.6 x 50 mm, 2.7 μm). The injection volume was 10 μL and the temperature of column oven was maintained at 35 ºC. The autosampler temperature was set at 10 ºC. The mobile phase was delivered in an isocratic mode comprising of acetonitrile and 0.2% formic acid in water (70:30, v/v) at a flow rate of 0.5 mL/min.

The UV detection was set at 400 nm and the total run time was 5 min for each injection.

3.2.4.7 LC-MS/MS conditions for metabolite identification

The chromatographic separation was performed on an Eskpert UltraLC 100 system. The separation of analytes was achieved on a Halo C18 column (4.6 x 50 mm, 2.7 µm) with an isocratic mobile phase consisting of acetonitrile-0.2% formic acid in water (70:30 v/v) at a flow rate of 0.5 mL/min. The injection volume was 10 µL and the column oven temperature was set at 40 ºC. The autosampler temperature was set at 10 ºC. The sampling needle was washed with mobile phase between each injection.

The MS/MS analysis was conducted in an AB SCIEX QTRAP® 6500 mass spectrometer using positive ion electrospray mode for characterizing the metabolites and obtaining mass spectra of CUR and CDD standards. Analyst software (ver. 1.6) was used in the LC-MS/MS system control, data acquisition, and processing. The spray voltage was set at 3 kV and the ion spray temperature was maintained at 250 ºC. Collisionally activated dissociation (CAD) gas was set at a medium level. Curtain gas, ion source gases 1 and 2 were supplied at 40, 40 and 50 psi, respectively. Enhanced mass spectrum (EMS) was employed to obtain MS^1spectra of CUR, CDD, and metabolites. Declustering potential (DP) and entrance potential (EP) were set at 80 and 5 V, respectively. MS^2 spectra were collected by enhanced product ion (EPI) mode using DP and EP of 100 and 10 V, respectively. Collision energy (CE) and collision energy spread (CES) were set at 40 and 15 eV, respectively.

CHAPTER IV

RESULTS

4.1 Synthesis of CUR, DMC, MSCUR and CDD

4.1.1 Synthesis and characterization of CUR and DMC

CUR and DMC were synthesized via aldol condensation reaction. The reaction yields for CUR and DMC were 2.014 g (51.2% yield) and 1.440 g (33.3% yield), respectively. The chemical structures of CUR and DMC were confirmed by ^{1}H-NMR and mass spectrometric techniques. The ^{1}H-NMR and mass spectra of CUR and DMC are shown in **Figure 8-11**. CUR showed ^{1}H-NMR signals (300 MHz, $CDCl_3$) at δ 7.61 (d, J = 15.8 Hz, 1H), 7.19 – 7.04 (m, 2H), 6.95 (d, J = 8.2 Hz, 1H), 6.49 (d, J = 15.8 Hz, 1H), 5.84 (d, J = 14.4 Hz, 1H), 3.99 (s, 3H). The molecular ion of CUR showed a m/z at 369 $[M+H]^{+}$.

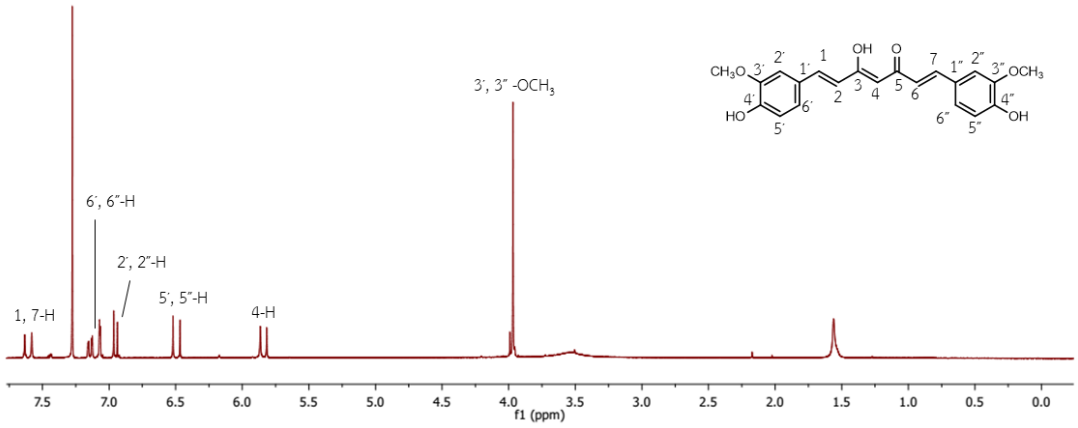

Figure 8 ^{1}H-NMR spectrum of CUR

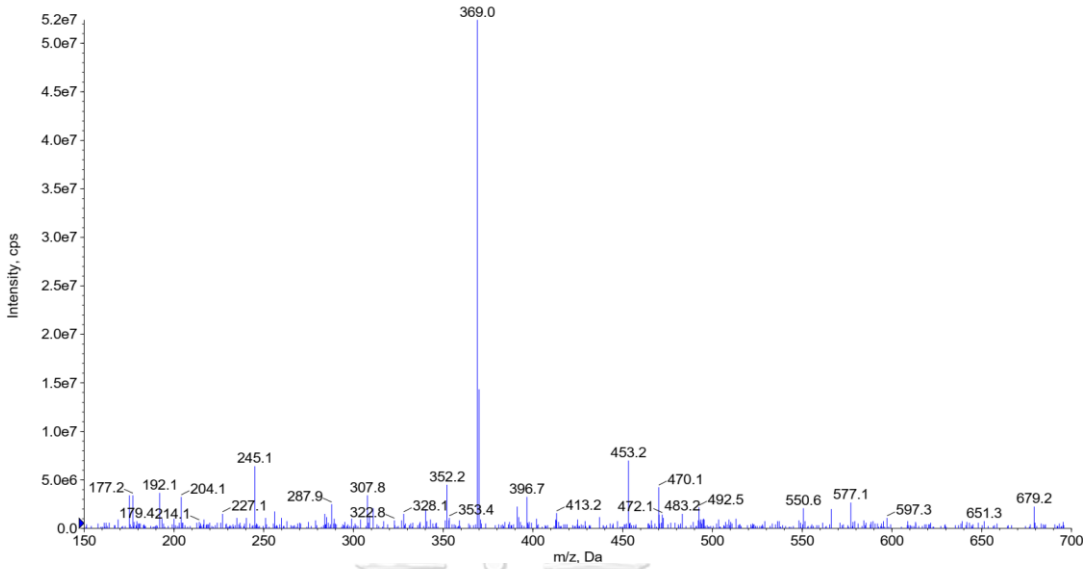

Figure 9 Mass spectrum of CUR

For DMC, its ^{1}H-NMR signals (300 MHz, $CDCl_3$) appeared at δ 7.63 (d, J = 15.8 Hz, 2H), 7.23 – 6.99 (m, 4H), 6.90 (d, J = 8.3 Hz, 2H), 6.52 (d, J = 15.8 Hz, 2H), 5.84 (s, 1H), 3.95 (d, J = 3.8 Hz, 11H) and it produced a molecular ion with m/z 397 $[M+H]^{+}$.

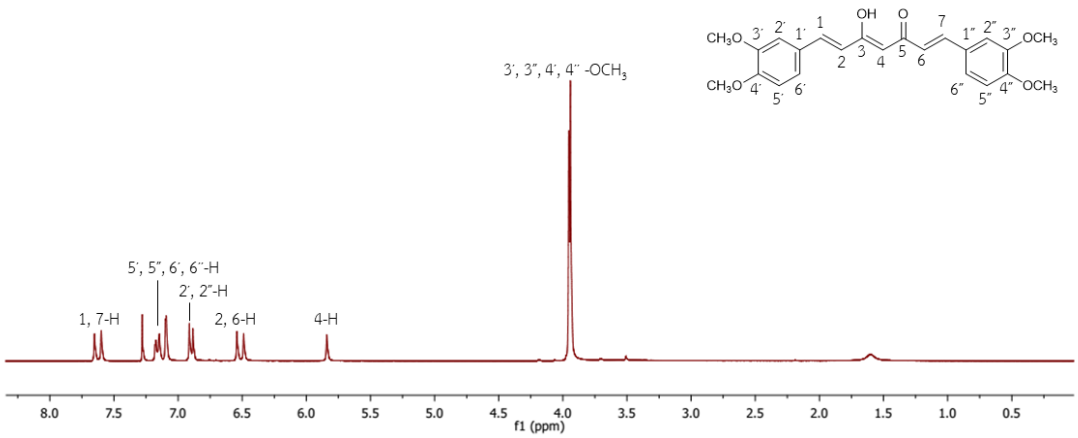

Figure 10 ^{1}H-NMR spectrum of DMC

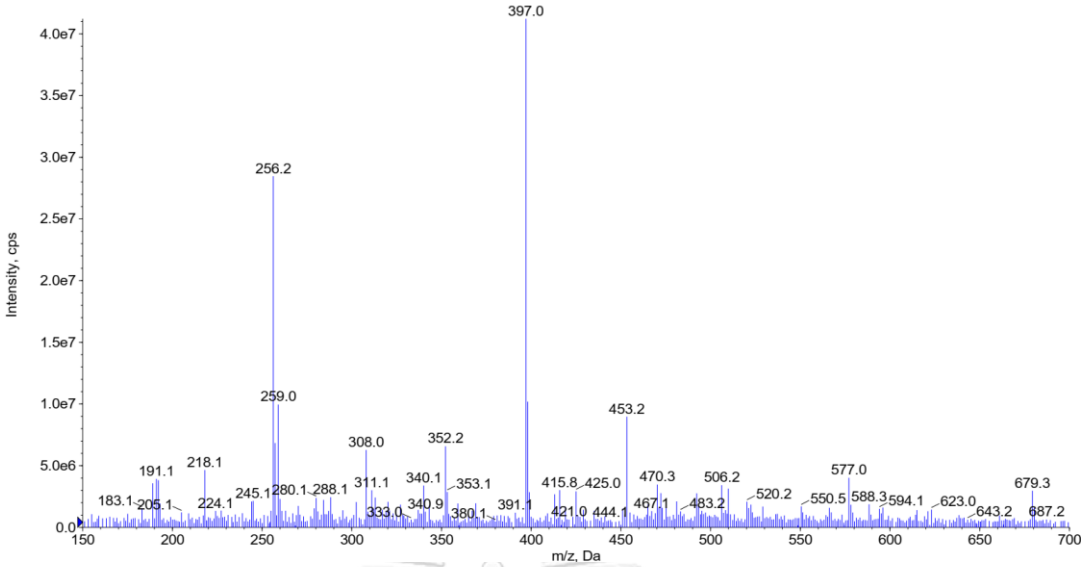

Figure 11 Mass spectrum of DMC

4.1.2 Synthesis and characterization of MSCUR and CDD

MSCUR and CDD were prepared via esterification reaction between CUR and ethyl-4-chloro-4-oxobutyrate using DMAP as a catalyst. The reaction yields for MSCUR and CDD were 239.7 mg (8.84% yield) and 230.0 mg (73.6% yield), respectively. The purified products were structurally confirmed by ^{1}H-NMR spectroscopy and mass spectrometry. The ^{1}H-NMR and mass spectra of MSCUR and CDD are depicted in **Figure 12-15**. MSCUR exhibited ^{1}H-NMR (300 MHz, CDCl3) signals at δ 7.62 (dd, J = 15.8, 3.6 Hz, 2H), 7.21 – 7.00 (m, 5H), 6.95 (d, J = 8.2 Hz, 1H), 6.53 (t, J = 16.1 Hz, 2H), 5.84 (s, 1H), 4.20 (q, J = 7.1 Hz, 2H), 3.96 (s, 3H), 3.88 (s, 3H), 2.95 (t, J = 6.8 Hz, 2H), 2.76 (t, J = 6.9 Hz, 2H), 1.29 (t, J = 7.1 Hz, 3H). The molecular ion of MSCUR has a m/z 497 $[M+H]^{+}$. For CDD, ^{1}H-NMR (300 MHz, CDCl3) spectrum shows signals at δ 7.63 (d, J = 15.8 Hz, 2H), 7.24 – 7.04 (m, 6H), 6.58 (d, J = 15.8 Hz, 2H), 5.87 (s, 1H), 4.20 (q, J = 7.1 Hz, 4H), 3.89 (s, 6H), 2.95 (t, J = 6.9 Hz, 4H), 2.76 (t, J = 6.9 Hz, 4H), 1.29 (t, J = 7.1 Hz, 6H). The m/z of the molecular ion of CDD is 625 $[M+H]^{+}$.

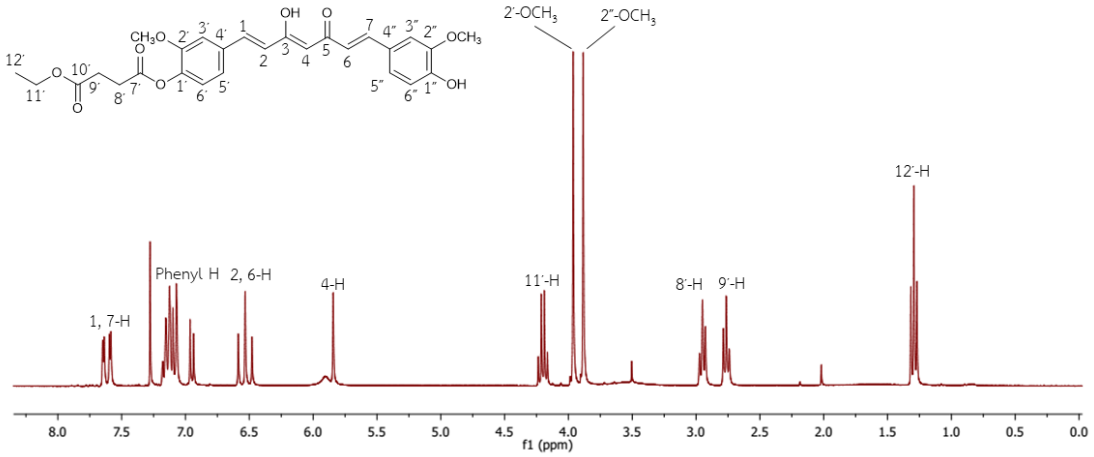

Figure 12 ^{1}H-NMR spectrum of MSCUR

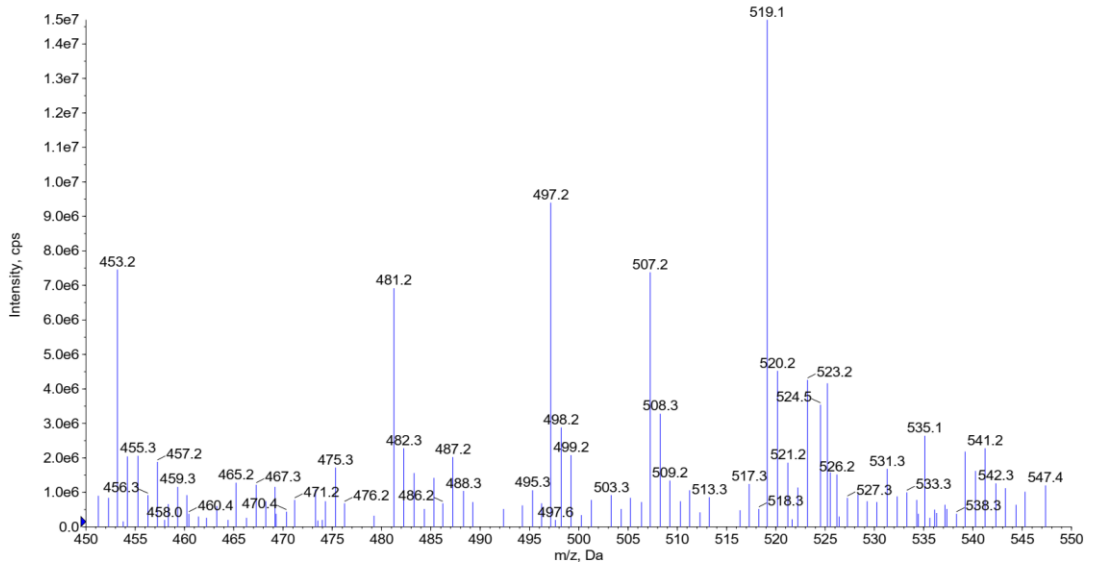

Figure 13 Mass spectrum of MSCUR

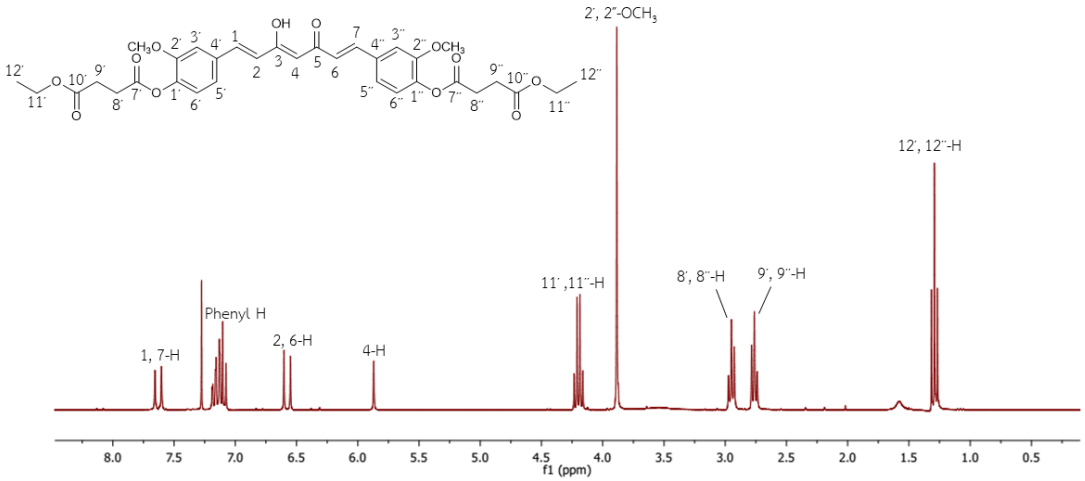

Figure 14 ^{1}H-NMR spectrum of CDD

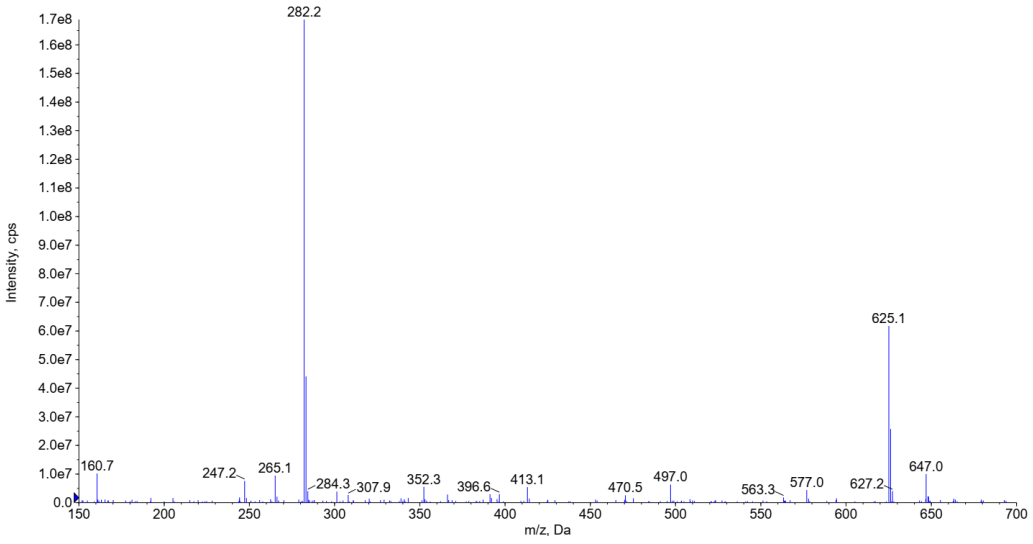

Figure 15 Mass spectrum of CDD

4.2 Chemical stability of CDD in buffer solutions

The chemical stability of CDD was assessed as functions of pH and temperature. The degradation kinetic parameters are presented in **Table 4**. As demonstrated in **Figure 16**, the remained amounts of CDD in all pH at 4 °C are more than 50%. It was found that CDD was least stable in acetate buffer (pH 4.5) at all tested temperatures.

Table 4 Summary of kinetic parameters of CDD stability in buffers as functions of pH and temperature (n =3)

pH	Temperatures (°C)	k_1 (min^{-1})	$t_{1/2}$ (min)
1.2	4	N/A	> 720
	25	1.10 ± 0.21 (× 10^{-3})	644.75 ± 111.12
	37	1.27 ± 0.10 (× 10^{-3})	548.26 ± 43.81
4.5	4	N/A	> 720
	25	1.38 ± 0.51 (× 10^{-3})	567.41 ± 263.05
	37	3.33 ± 1.03 (× 10^{-3})	224.61 ± 79.73
6.8	4	N/A	> 720
	25	1.23 ± 0.32 (× 10^{-3})	592.36 ± 161.78
	37	1.47 ± 0.57 (× 10^{-3})	531.05 ± 230.55
7.4	4	N/A	> 720
	25	1.01 ± 0.09 (×10^{-3})	688.56 ± 58.89
	37	1.43 ± 0.28 (×10^{-3})	499.11 ± 107.58
8.0	4	N/A	> 720
	25	N/A	> 720
	37	1.95 ± 0.26 (×10^{-3})	358.89 ± 48.67

N/A = Not applicable

4.3 Verification of plasma esterases activity

The BCA assay showed that rat, dog and human plasma contains proteins at the concentrations of 60.4, 42.6 and 53.6 mg/mL, respectively. The specific activities of plasma esterases from the *p*-NPA assay were found to be 15.1 units/mg protein for rat, 12.2 units/mg protein for dog, and 11.4 units/mg protein for human.

4.4 Metabolic stability of CDD in plasma

Representative chromatograms of CDD hydrolysis in plasma at 37 °C (**Figure 17**) shows the change in analytes' profile over incubation time. CDD, the peak at 3.80 min, was gradually decreasing while the peak at 2.05 min has emerged. The peak at 2.05 min was assigned as M2. The peak at 1.36 min, which was designated as M1,

appeared after the emergence of M2. It was expected that M1 was converted from M2. These two metabolites were characterized using LC-MS/MS as described in the subsequent section.

The consecutive pseudo-first order kinetic parameters of CDD hydrolysis in plasma of rat, dog, and human are summarized in **Table 5**. CDD underwent rapid hydrolysis in plasma especially in rat plasma. The k_1 values are far higher than the degradation rate constants of CDD in phosphate buffer pH 7.4 at all tested temperatures, suggesting the involvement of plasma esterases in the hydrolysis of CDD. At 4 ℃, the k_1 value in human is 210 times lower than rat while it is 3 times higher than dog. The difference between the k_1 values in human and rat at 25 ℃ and 37 ℃ is lower in comparison with that of 4 ℃ (60 and 50 times, respectively). The difference between the k_1 values in human and dog at 25 ℃ remains the same as that at 4 ℃ but this difference decreases to 1.6 times higher at 37 ℃.

Table 5 The consecutive pseudo-first order kinetic parameters of CDD metabolism in plasma at various temperature (n =3).

Species	k_1 (min^{-1})	k_2 (min^{-1})	$t_{1/2}$ (min)	t_{max} (min)
Rat				
4 ℃	5.13 ± 0.83	5.79 ± 1.99	0.14 ± 0.02	0.19 ± 0.04
25 ℃	5.56 ± 0.39	12.72 ± 2.85	0.13 ± 0.01	0.12 ± 0.02
37 ℃	7.61 ± 0.50	14.97 ± 0.44	0.09 ± 0.01	0.092 ± 0.003
Dog				
4 ℃	0.76 ± 0.03 ($\times 10^{-2}$)	0.41 ± 0.02 ($\times 10^{-2}$)	89.35 ± 2.91	174.94 ± 7.88
25 ℃	2.95 ± 0.37 ($\times 10^{-2}$)	1.45 ± 0.09 ($\times 10^{-2}$)	23.71 ± 2.99	47.60 ± 4.60
37 ℃	8.97 ± 1.26 ($\times 10^{-2}$)	4.91 ± 0.60 ($\times 10^{-2}$)	7.82 ± 1.02	14.97 ± 1.59
Human				
4 ℃	0.024 ± 0.001	0.019 ± 0.002	29.11 ± 1.57	47.04 ± 3.29
25 ℃	0.090 ± 0.023	0.091 ± 0.008	8.01 ± 1.80	11.29 ± 1.77
37 ℃	0.147 ± 0.027	0.220 ± 0.007	4.85 ± 0.95	5.58 ± 0.57

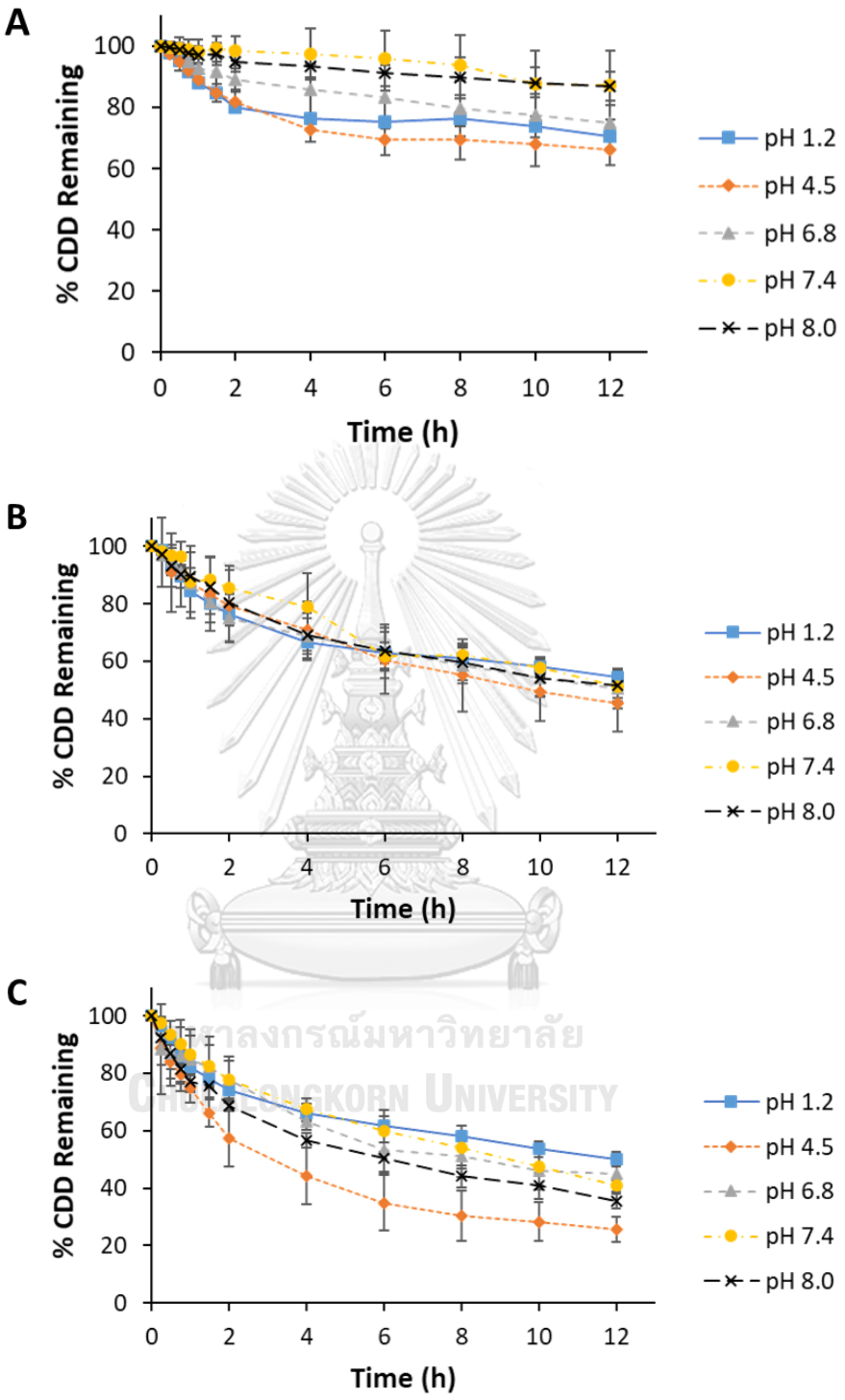

Figure 16 Time profiles of CDD degradation in buffers as functions of pH at (A) 4 °C (B) 25 °C and (C) 37 °C

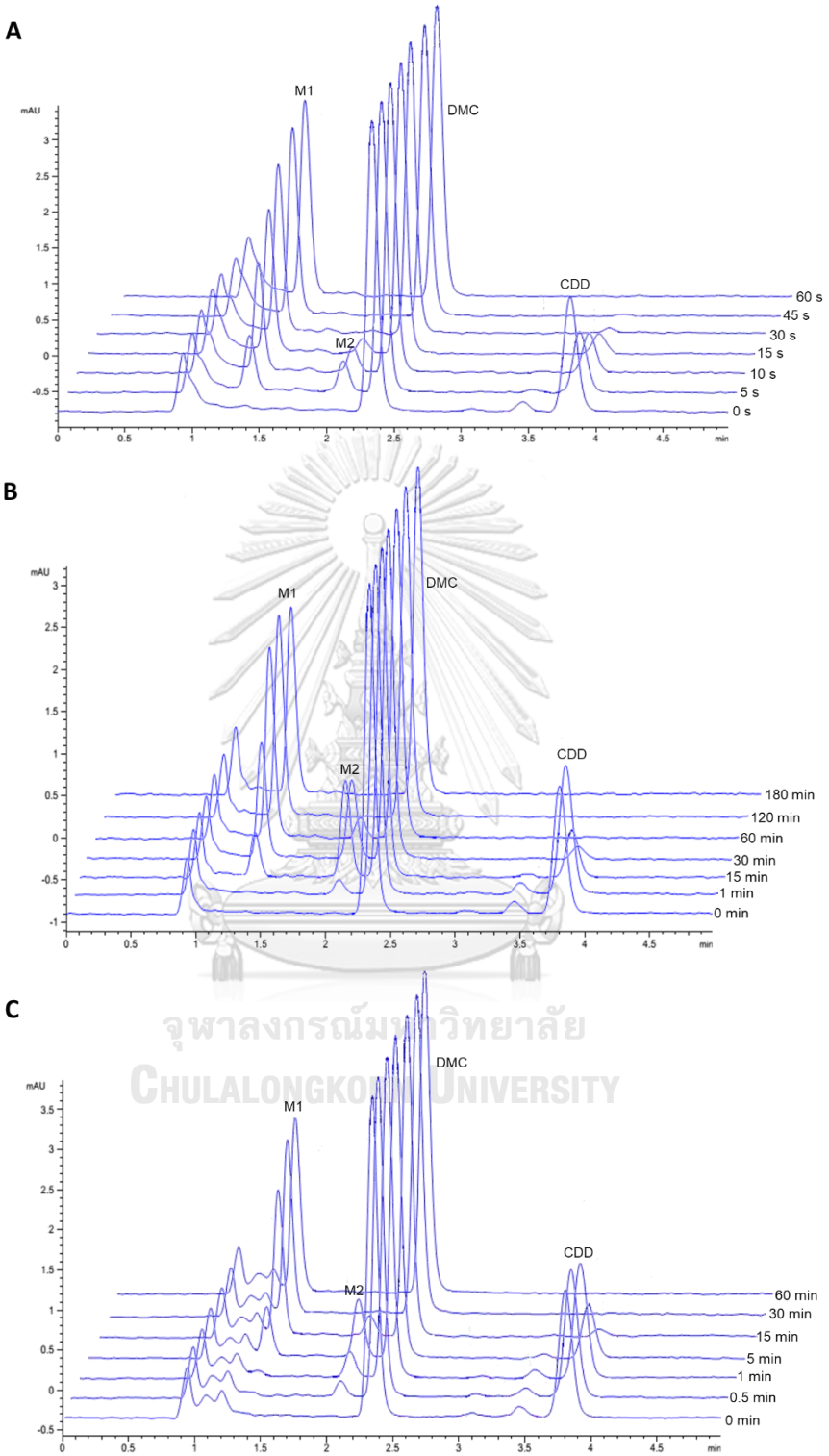

Figure 17 Representative chromatograms of CDD hydrolysis at 37 °C in (A) rat plasma (B) dog plasma and (C) human plasma

The degradation rate constants of M2 (k_2) were also calculated using the consecutive pseudo-first order kinetic model. The trend for k_2 differs among the tested species. For rat, the k_2 values are approximately 2 times higher than the k_1 values at 25 and 37 ℃. In contrast, the k_2 values in dog are approximately 2 times lower than the k_1 values at all tested temperatures. However, the k_1 and k_2 values in human are comparable.

4.5 Metabolite identification

The information for the measured m/z and characteristic product ions of CUR, MSCUR, CDD, M1, and M2 are summarized in **Table 6**. CUR, MSCUR and CDD exhibited ions at m/z 369 $[M+H]^+$, m/z 497 $[M'+H]^+$ and m/z 625 $[M''+H]^+$, respectively. Sodium adducts of CDD and MSCUR were also found at m/z 647 $[M''+Na]^+$ and 519 $[M'+Na]^+$, respectively. Fragmentation of CUR produced several characteristic ions including m/z 285 $[M+H-C_4H_4O_2]^+$, m/z 177 $[M+H-C_{11}H_{12}O_3]^+$ and m/z 175 $[M+H-C_{10}H_{10}O_4]^+$ as demonstrated in its MS^2 spectrum (**Figure 18**).

Table 6 Chromatographic and mass spectrometric information for CUR, MSCUR, CDD, M1 and M2

ID	Retention time (min)	Measured m/z	Characteristic product ions (m/z)
CDD	3.80	625, 647 (Na^+ adduct)	497, 369, 285, 177
CUR	1.36	369	285, 245, 177, 175
MSCUR	N.D.	497, 519 (Na^+ adduct)	369, 285, 245, 177
M1	1.36	369	285, 175, 177
M2	2.05	497, 519	369, 285, 245, 177

N.D. = Not determined

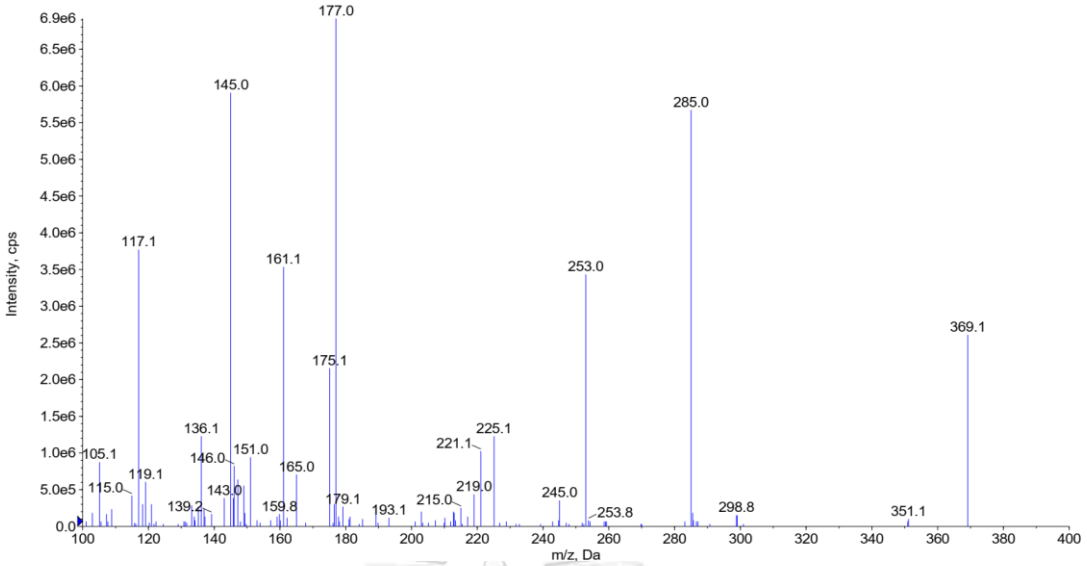

Figure 18 MS^2 spectrum of standard CUR

In case of MSCUR, the MS^2 spectrum shows that it loses an ethyl succinyl group resulting in the formation of CUR ion (m/z 369 $[M'+H-C_6H_8O_3]^+$). Additionally, it underwent further fragmentation to yield several product ions similar to those of CUR e.g. m/z 285, 177 and 175 (**Figure 19**). For CDD, further fragmentation of m/z 625 $[M''+H]^+$ generated the peak at m/z 497 $[M''+H-C_6H_8O_3]^+$ as the major product ion. The molecular ion of CDD also loses two acyl groups yielding a product ion with m/z 369 $[M''+H-2C_6H_8O_3]^+$ (**Figure 20**).

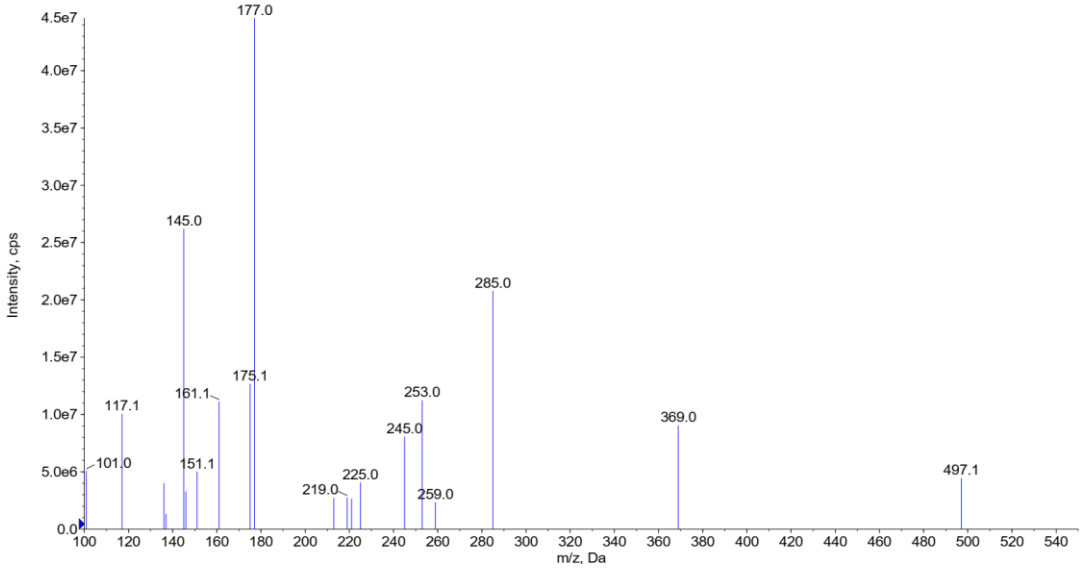

Figure 19 MS^2 spectrum of standard MSCUR

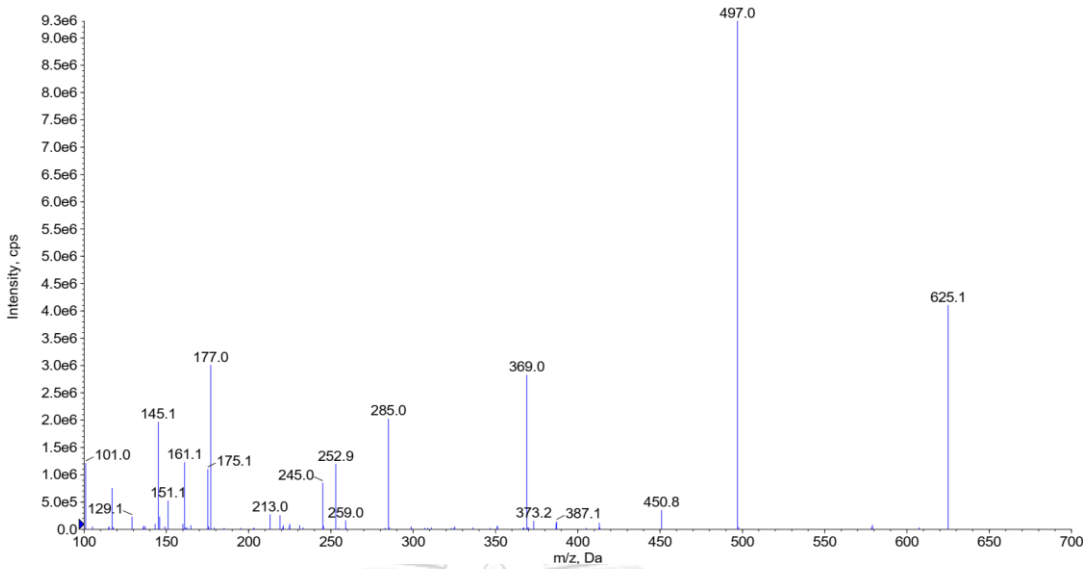

Figure 20 MS^2 spectrum of standard CDD

In the mass chromatograms, M1 was eluted at the same retention time as CUR standard (**Figure 21**). It produced a molecular ion at m/z 369 $[M1+H]^+$. Its MS^2 spectrum shows several product ions similar to those of CUR including m/z 285, m/z 177 and m/z 175 (**Figure 22**), indicating that M1 is CUR. M2 metabolite, which is a peak at 2.00 min (**Figure 23**), has a m/z of 497 $[M2+H]^+$. Fragmentation of M2 ion generated product ions at m/z 369, m/z 285, m/z 177 and m/z 175 (**Figure 24**). Therefore, M2 was identified as MSCUR. The proposed fragmentations of CUR, MSCUR, and CDD are depicted in **Figure 25**.

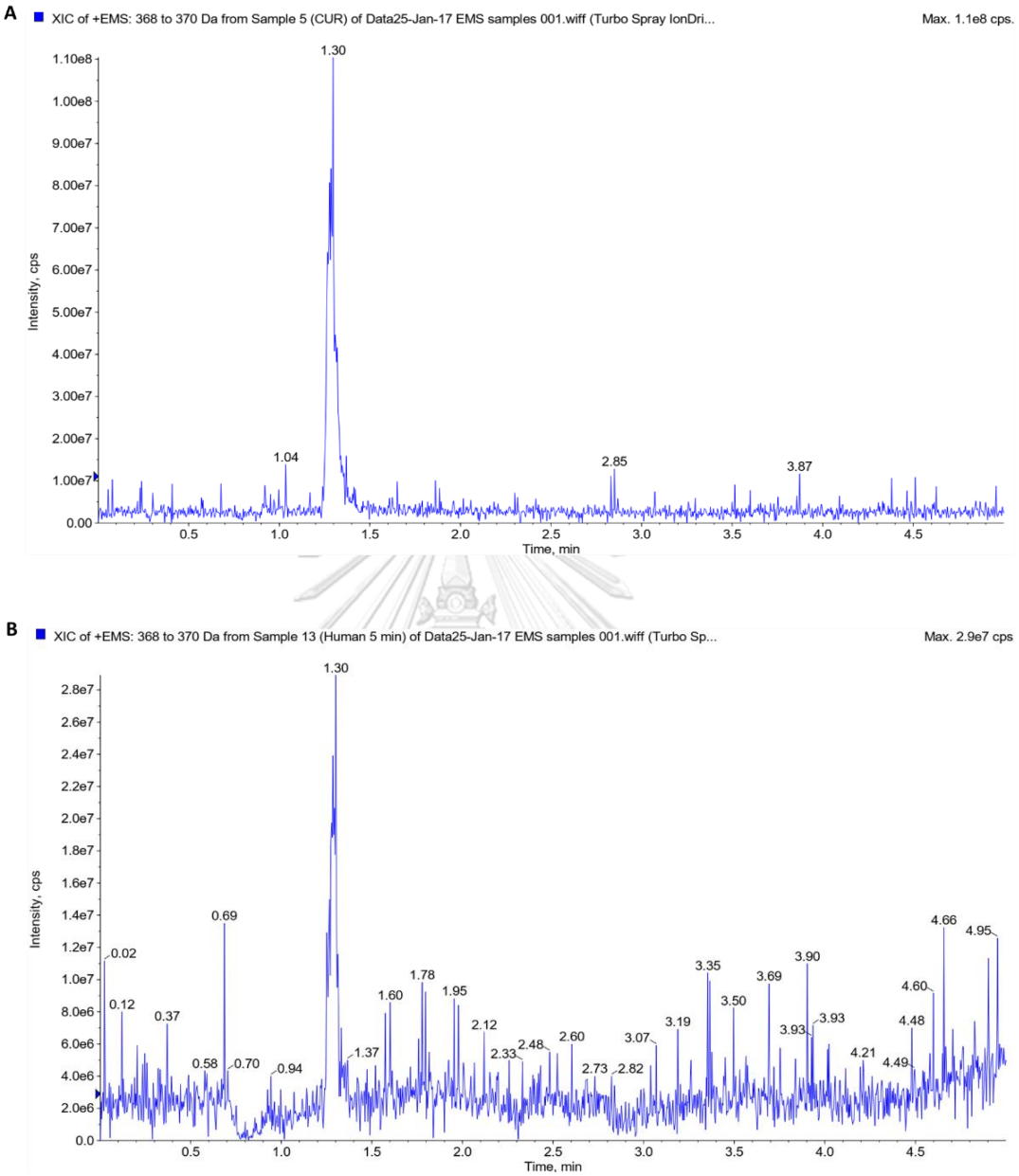

Figure 21 Representative extracted ion chromatograms (m/z 368 – 370) of (A) CUR standard and (B) CDD-spiked human plasma after incubation for 5 min.

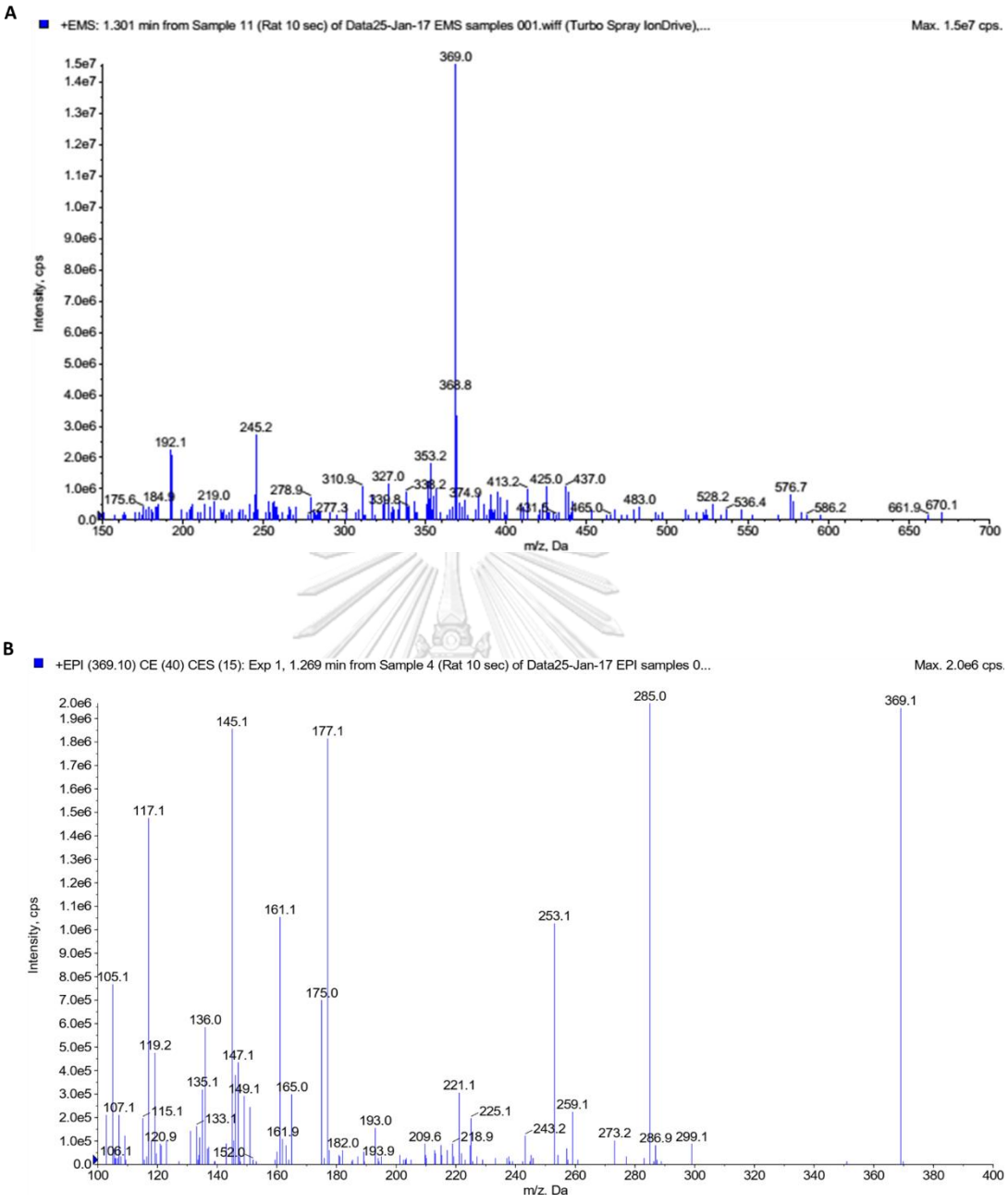

Figure 22 Mass spectra of M1 (A) MS spectrum of M1 and (B) MS^2 spectrum of M1

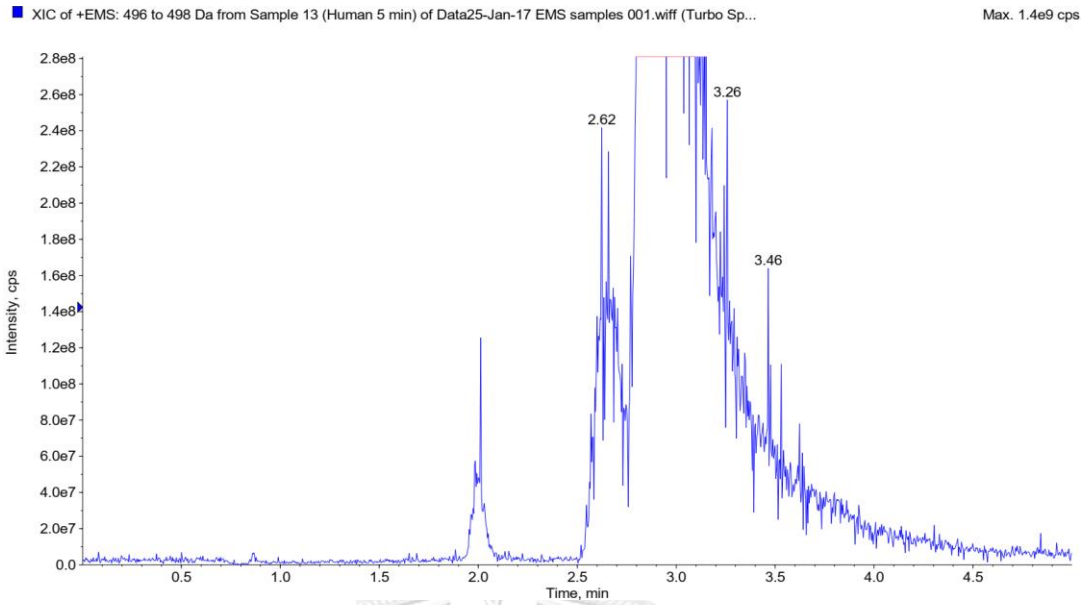

Figure 23 Representative extracted ion chromatogram (m/z 496-498) of M2

4.6 Identification of plasma esterases involving the hydrolysis of CDD

Various types of esterase inhibitors were used to determine esterases involved in the ester hydrolysis of CDD in plasma. The effect of esterase inhibitors is expressed as % inhibition and is summarized in **Table 7.**

In rat plasma, BNPP and iso-OMPA showed strong inhibition against the CDD hydrolysis even at 0.1 mM (>80% inhibition). PMSF and Pefabloc® SC strongly inhibited the hydrolytic cleavage of CDD (>90% inhibition) at concentration of 1 mM. NaF partially prevented CDD hydrolysis at 10 mM. BW284c51, eserine, TLCK, EDTA and DTNB did not prevent the hydrolysis of CDD.

BNPP, PMSF, Pefabloc® SC, TLCK, iso-OMPA and EGTA exhibited small inhibition against the hydrolysis of CDD in dog plasma. DTNB showed moderate inhibition at 1 mM. However, BW284c51, eserine, EDTA and NaF has no inhibition in dog plasma.

In human plasma, BNPP and DTNB at 1 mM moderately inhibited the hydrolysis of CDD. EGTA showed partial inhibition on CDD hydrolysis. BW284c51, eserine, TLCK, PMSF, Pefabloc® SC, iso-OMPA, EDTA and NaF did not inhibit the CDD hydrolysis.

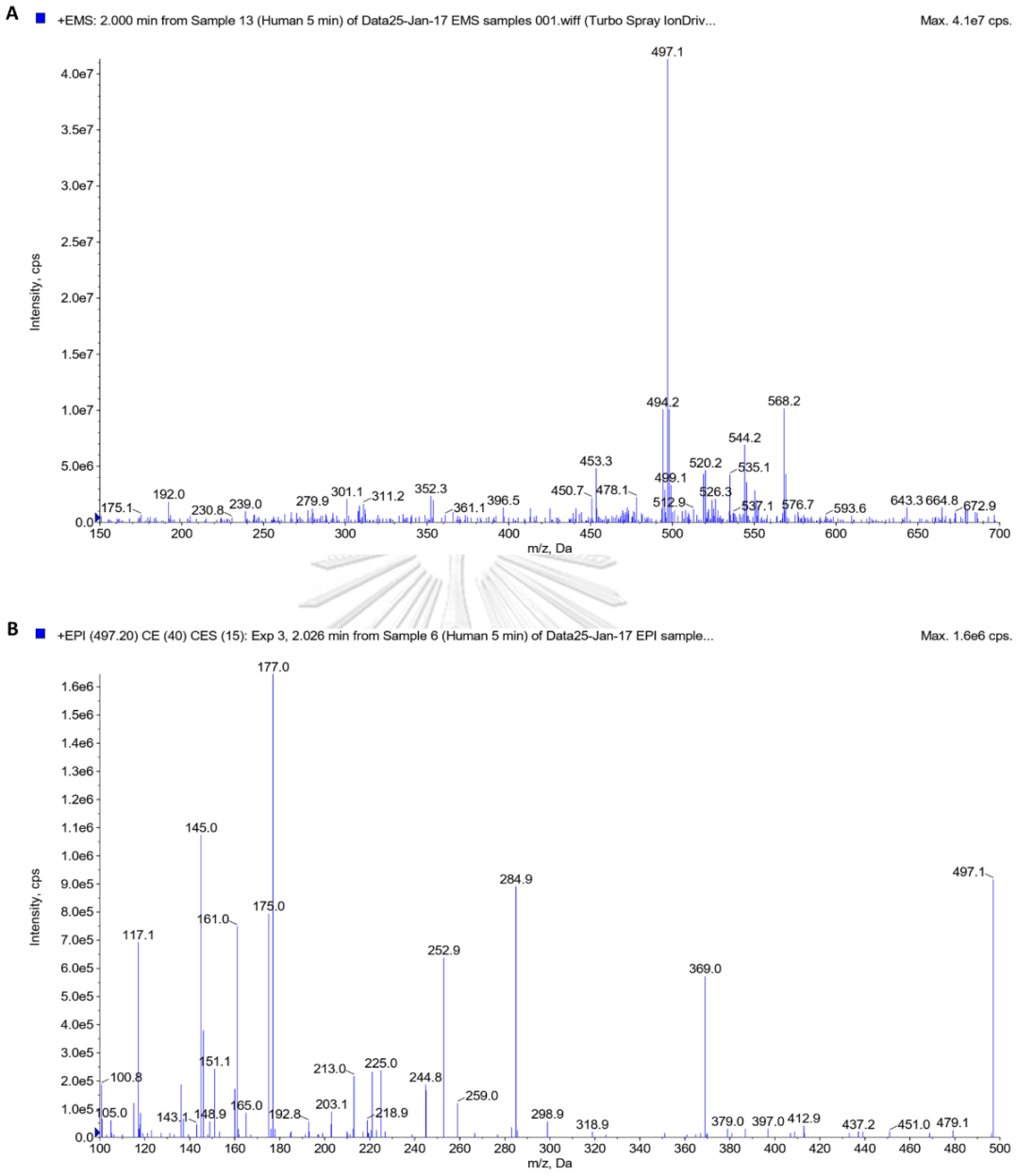

Figure 24 Mass spectra of M2 (A) MS spectrum of M2 and (B) MS^2 spectrum of M2

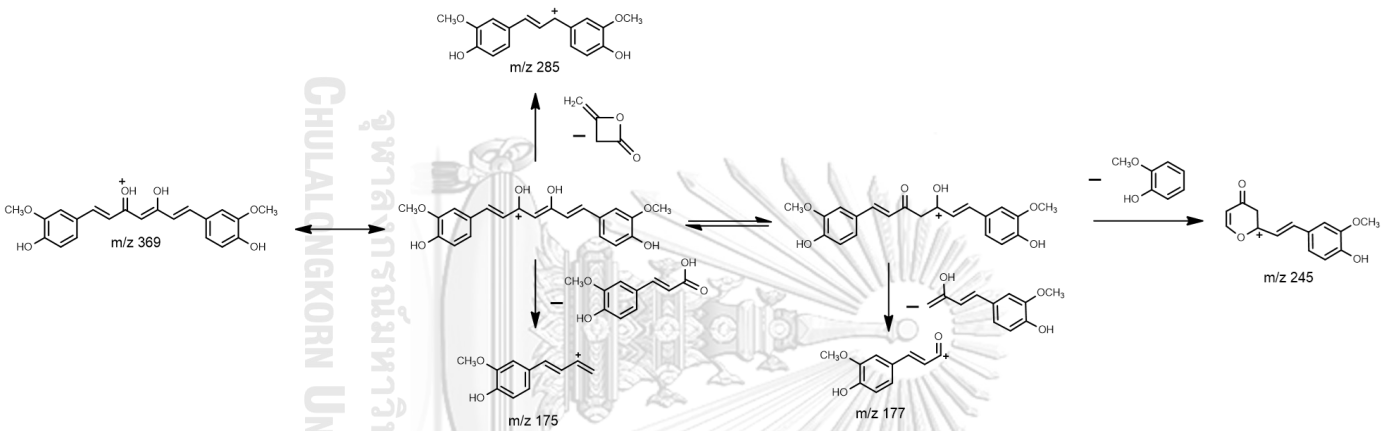

Figure 25 Proposed mass fragmentation of CUR

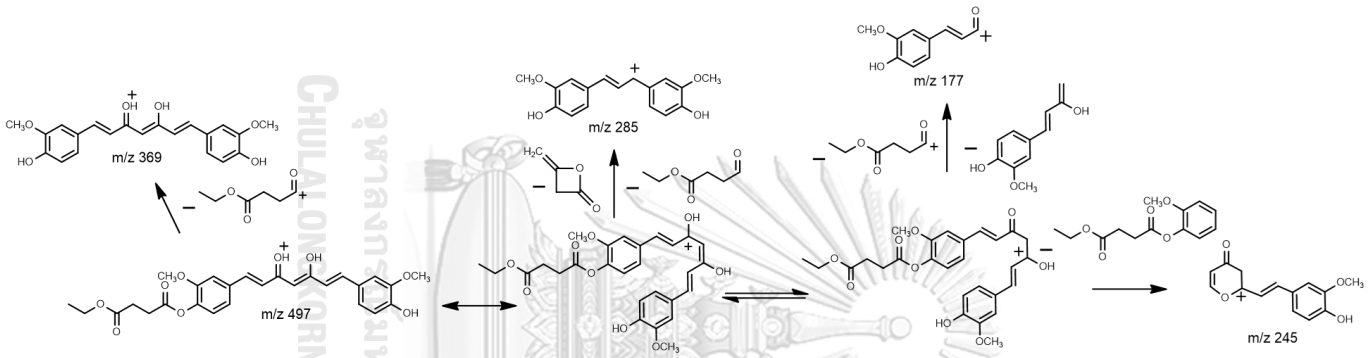

Figure 26 Proposed mass fragmentation of MSCUR

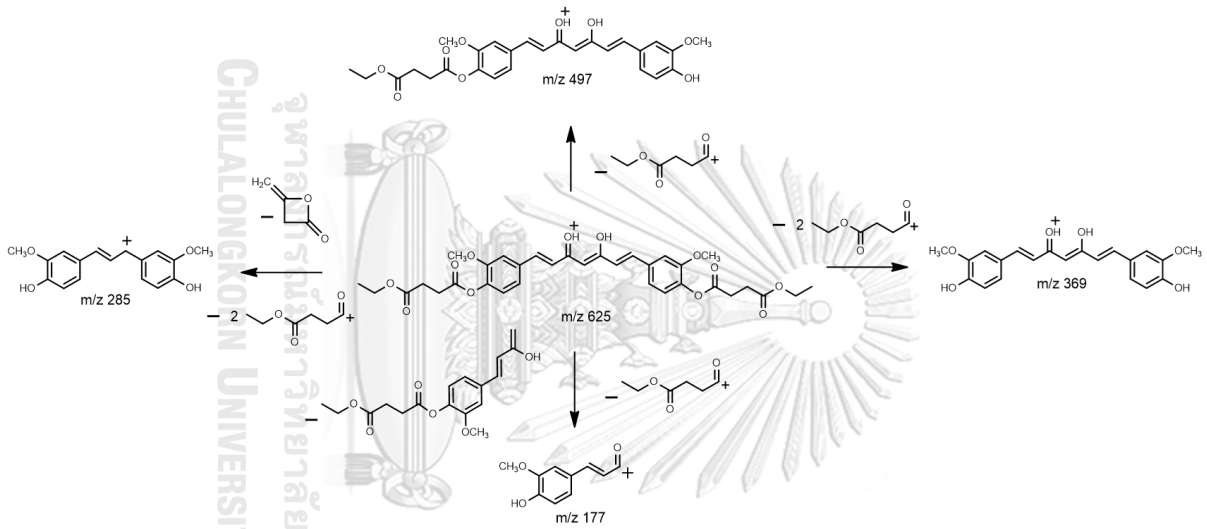

Figure 27 Proposed mass fragmentation of CDD

Table 7 Inhibition of CDD hydrolysis in rat, dog, and human plasma by esterase inhibitors

Inhibitors	Target	Concentration	% Inhibition*		
			Rat	Dog	Human
BNPP	CES	0.1 mM	83.0 ± 8.9	16.6 ± 8.2	<10%
		1 mM	97.0 ± 7.7	63.6 ± 1.8	42.2 ± 6.7
BW284c51	AChE	10 μM	<10%	<10%	<10%
		100 μM	<10%	<10%	<10%
Iso-OMPA	BChE	0.1 mM	99.5 ± 11.2	16.9 ± 7.1	<10%
		1 mM	108.3 ± 5.2	17.6 ± 6.7	<10%
Eserine	ChE	10 μM	<10%	<10%	<10%
		100 μM	<10%	<10%	<10%
TLCK	Serine hydrolase	0.1 mM	<10%	<10%	<10%
		1 mM	<10%	17.0 ± 10.3	<10%
PMSF	Serine hydrolase	0.1 mM	<10%	<10%	<10%
		1 mM	96.0 ± 9.2	29.6 ± 5.3	<10%
Pefabloc® SC	Serine hydrolase	0.1 mM	19.4 ± 2.1	<10%	<10%
		1 mM	99.8 ± 7.9	25.8 ± 3.1	<10%
DTNB	Arylesterase	0.1 mM	<10%	<10%	<10%
		1 mM	<10%	47.8 ± 0.83	52.0 ± 1.5
EDTA	PON	5 mM	<10%	<10%	<10%
		10 mM	<10%	<10%	<10%
EGTA	PON	5 mM	<10%	17.3 ± 6.1	23.2 ± 11.4
		10 mM	<10%	19.9 ± 8.0	26.5 ± 3.6
NaF	Non-specific	5 mM	<10%	<10%	<10%
		10 mM	24.4 ± 7.1	<10%	<10%

*%inhibition < 10% is considered as no inhibition.

CHAPTER V
DISCUSSION AND CONCLUSION

During drug development, investigating stability of drug candidates is important because instability of test compounds can lead to the improper interpretation of bioassay results, undesired pharmacokinetic properties or difficulty in drug formulation. Stability of a compound depends on its chemistry nature (e.g. functional groups presented in the molecule), chemical and biological properties of the sample matrices (e.g. pH, the presence of enzymes) and physical properties of the storage conditions (e.g. temperature). Ester-containing molecules are prone to the hydrolytic cleavage in aqueous solutions and the hydrolysis reaction biological matrices (e.g. blood, plasma) can be accelerated by the presence of esterase enzymes. Instability of esters due to hydrolysis can lead to under-estimation of the actual compound concentration in biological samples. As part of the ADMET assay, studying the *in vitro* hydrolysis of ester compounds will provide useful information and assist the ester-containing drug development.

The determination of the stability of drug candidates in buffers at pH values of GI fluids is essential for drug development. It provides useful information about the structural integrity of drug candidates under conditions of the GI tract. Also, evaluating the effects of different temperatures on drug stability is of benefit for compound handling during the preparation of drug formulations or sample for analyses. As expected, the degradation of CDD in buffers is temperature-dependent. At 4 °C, it seems that CDD is more stable in slightly alkaline solutions (pH 7.4 and 8.0) with more than 80% of CDD remained in the solutions at 12 h. The degradation of CDD at 25 °C, which is the general room temperature, took place at similar extent between the tested pH values with the % CDD remaining of 50-60% at 12 h. It was found that, at usual body temperature (37 °C), CDD was most stable in HCl buffer (pH 1.2) but least stable in acetate buffer (pH 4.5). Although the results at 37 °C showed that CDD degraded extensively at 12 h, this time point is far beyond the emptying time of a drug in the GI tract. Generally, it takes about 1.5 h for a drug to move along

the GI tract under fasting condition (57). Considering the % CDD remaining at 37 °C in **Figure 16C**, 65-85% of CDD remained in the buffers with pH values similar those of GI fluids at 1.5 h. These results suggest that CDD may survive in the GI fluids and provide sufficient amount of curcumin to systemic circulation for exerting pharmacological actions. Previously, CDD was shown for a significant analgesic response in mouse tail-flick test even at a dose of 25 mg/kg (19). This finding implies that the remained amount of CDD after pre-systemic degradation is sufficient for exerting certain biological activities.

The stability data of CDD obtained in this study can be used in the formulation of oral dosage forms for CDD. As shown in **Figure 16C**, about 35% of CDD was degraded in the buffer pH 4.5 which is the pH of duodenum. One may formulate CDD modified-release tablets to release CDD in the lower part of the GI tract e.g. ileum or colon. For example, methacrylic acid-based polymers such as poly(methacrylic acid-co-methyl methacrylate) or Eudragit L (dissolution pH = 5.5 – 7.0) have been used in the fabrication of enteric-coated tablets (58). Thus, the incorporation of CDD into a delivery vehicle coated with Eudragit L would avoid or reduce the degradation of CDD in the GI tract once it is orally administered.

One limitation of this study is that it cannot explain why CDD is the least stable in acetate buffer (pH 4.5) in all studied temperatures. At a constant temperature, the degradation of CDD in the buffers was compared as a function of the concentration of hydronium ion (or pH). The effects of buffer concentration and ionic species cannot be assessed since only one buffer salt was used in each tested pH value. It has been reported that types and concentrations of buffers impact the stability of pharmaceuticals at different degree. For example, Fubara and Notari demonstrated that the degradation rate constant of cefepime increased when the concentration of buffers was increased. They also found that the basic species of the buffers including borate, phosphate, acetate and formate affected the degradation rate constant of cefepime at different extent (35). Therefore, the evaluation of the effects of ionic species and concentrations of buffers over a wider range of pH values on the degradation of CDD should be further investigated to elaborate the chemical

stability information of CDD in solutions for other applications such as drug formulations.

Another limitation for the study of CDD degradation in buffer solutions is that the use of HPLC-UV. The detection wavelength used in this study was set at 400 nm which is the λ_{max} of CDD. The use of the detection wavelength at 400 nm could not detect degradation products with disrupted chromophore which generally cannot absorb the light at 400 nm. Alternative detectors such as diode array detector (DAD) or mass spectrometer could be used to solve this problem. The DAD is better than the UV detector because DAD can detect analytes (or degradation products in this case) that may escape the detection at 400 nm by setting the detection at other wavelengths such as 260 or 280 nm. However, both DAD and UV detector cannot give structural information of the generated degradation products. Mass spectrometer provides better information both quantitatively and qualitatively. LC-MS/MS is a more sensitive analytical method than HPLC-UV and HPLC-DAD because mass spectrometer dose not measure the interaction between light and substance but mass-to-charge ratio, which is the unique properties of each analyte. It can detect the minor degradation products of CDD generated during degradation in the buffers. In addition, LC-MS/MS can perform mass fragmentation that provides putative structural information of the degradation products. Therefore, the future works should use HPLC-DAD, LC-MS/MS or combination of both techniques as analytical tools to extensively investigate the stability of CDD.

The hydrolytic cleavage of an ester prodrug to its active metabolite in blood or plasma is desirable. Blood (or plasma) is the first and important matrix in the bioactivation of ester prodrugs administered intravenously. This study showed that CDD was hydrolyzed rapidly in rat, dog, and human plasma.The rate constants for the hydrolysis could be calculated from consecutive pseudo-first order kinetic model using nonlinear regression analysis. The calculations show that the $t_{1/2}$ values of CDD in dog and human plasma are obviously different from that in rat. The k_1 values for the stability of CDD in plasma are in the following order: rat >> human > dog. This order shows the same trend as other ester-based compounds e.g. clevidipine,

oseltamivir, and WS070117 (42, 56, 59). These data indicate that the clearance of CDD in dog plasma is much closer to human than rat.

Though the k_2 values in phosphate buffer (pH 7.4) could not be established, the obtained k_2 values in plasma of the tested species suggested that plasma esterases also involved in the conversion of M2 (MSCUR) to M1 (CUR). Interestingly, the k_2 values at 25 and 37 ℃ in rat plasma are two times higher than k_1 values and the t_{max} values are extremely low. This data supports the previous study which showed that CDD was rapidly metabolized to CUR in rat following intravenous administration (21). These results imply that esterases in rat plasma may preferential hydrolyze MSCUR over CUR. The k_2 values in human plasma is slightly higher than the k_1 but vice versa in dog, suggesting that CDD and MSCUR are hydrolyzed by plasma esterases at the comparable rate in both species. Therefore, the interspecies differences in metabolic rate of CDD in plasma should be considered when conducting pharmacokinetic studies in the future.

The knowledge of the rate of bioconversion of CDD

Because CDD has four ester bonds, there are five possible metabolites that can be formed in the plasma. However, the LC-MS/MS analysis showed that only two hydrolytic metabolites were generated similar to those found by HPLC analysis. Mass fragmentation was subsequently performed to obtain mass fragmental profiles of standards and the metabolites. Mass spectrometric analyses confirm that M1 metabolite is CUR because CUR and M1 share the same m/z and product ions (**Figure 9, Figure 18** and **Figure 22**) and as reported in the literature (60). For M2, it was identified as MSCUR because it has the same m/z to the standard MSCUR and the major product ion of CDD (m/z 497, **Figure 13 and 24A**). The MS^2 spectrum of M2 (**Figure 24B**) shows the fragmental profile similar to that of MSCUR (**Figure 19**). MSCUR is the only intermediate metabolite detected in the study samples. It might be derived from the stronger electron-withdrawing effect of the phenolic group of CDD in comparison with the ethoxy group. This effect makes the carbonyl carbon adjacent to the phenolic group more electrophilic and susceptible towards nucleophilic attack by nucleophilic groups within the catalytic site of esterases than that of the ethoxy group. Additionally, the phenolate anion is a more stable leaving

group than an ethoxide anion due to the lower pK_a value. Therefore, the cleavage of ester bonds of CDD would be preferred to occur at the carbonyl carbons of the phenolate esters.

The use of esterase inhibitors is one of the approaches employed to determine plasma esterases involving the ester hydrolysis of xenobiotics (55, 56, 61, 62). The absence of inhibition by BW284c51 in all species indicated that AChE did not involve in the CDD hydrolysis. In rat, the inhibition by BNPP, PMSF and Pefabloc® SC supported the involvement of CES in the hydrolytic cleavage of CDD. Surprisingly, iso-OMPA, which is a BChE inhibitor, also inhibited the hydrolysis of CDD at comparable extent to BNPP. This observation is consistent with the previous study showing that iso-OMPA could inhibit plasma CES in rats which is required for the detoxification of soman, a toxic organophosphate ester (63). However, eserine (or physostigmine), a cholinesterase inhibitor, did not prevent the cleavage of CDD. Thus, it could be concluded that BChE was not responsible for the metabolism of CDD. Although TLCK is a serine hydrolase inhibitor, it weakly reduced the hydrolytic cleavage of CDD. This could be derived from the different alkylation site (alkylates the His residue) in the catalytic triad of serine hydrolases (64). PON and ArE did not participate in the hydrolysis of CDD because DTNB, EDTA and EGTA did not show inhibition.

In dog plasma, iso-OMPA, PMSF and Pefabloc® SC partly inhibit the hydrolysis of CDD. In contrast, they did not prevent the cleavage of CDD in human plasma. These results suggest that BChE participates, at small extent, in the hydrolytic cleavage of CDD in dog plasma but not in human. PON may play a minor role in the metabolism of CDD in dog and human plasma as suggested by the small inhibition of EGTA. The moderate inhibition by DTNB implies that ArE contributed to CDD hydrolysis in dog and human plasma. Though BNPP showed the inhibition against CDD hydrolysis in dog and human plasma, CES is not present in dog and human plasma (40, 42). It can be hypothesized that BNPP acted on serum albumin. Serum albumin has been demonstrated for its esterase-like activity. It has been reported that serum albumin was capable to hydrolyze several ester-containing molecules e.g. organophosphate pesticides, aspirin and ester-based prodrugs (53, 65-68). BNPP, an

organophosphate, may alkylate the Tyr411 residue of serum albumin like other organophosphate compounds (68). Also, serum albumin has been reported for its thioesterase activity (52). The reactive Cys34 residue of serum albumin is responsible for thiol-disulfide exchange with thiol-containing molecules including disulfiram (69), 2,2′-dithiodipyridine (70) and DTNB (71, 72). Therefore, the action of DTNB in the reduction of CDD hydrolysis could be derived from the inhibition on serum albumin in addition to ArE. In dog and human plasma, serum albumin and ArE might play a main role in the metabolism of CDD. The mechanistic investigation of esterases responsible for CDD hydrolysis should be further performed using purified or recombinant enzymes. However, the application of esterase inhibitors allows the proper selection of purified esterases that might involve in the hydrolytic cleavage of CDD for future studies. The proposed metabolism map of CDD in plasma of the investigated species is depicted in **Figure 26**.

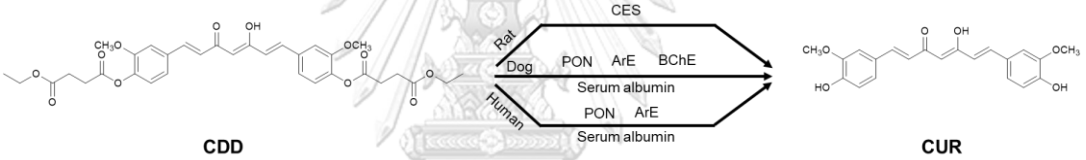

Figure 28 Summary of esterases involved in the plasma metabolism of CDD

In conclusion, CDD undergoes hydrolytic cleavage under non-enzymatic and enzymatic conditions at different extent. The hydrolysis of CDD in plasma of rat, dog and human is more pronounced than in buffer solutions. The marked interspecies differences in the rate of conversion could be observed. The rapid metabolism of CDD in plasma of rat, dog, and human is mediated by plasma esterases. The application of different esterase inhibitors provides useful information regarding plasma esterases involving the deacylation of CDD. Considering the degradation rate constants and the types of plasma esterases participating the hydrolysis, the metabolism of CDD in dog is closer to human than rat. The discrepancy in the metabolism of CDD in plasma of the tested species could be derived from the difference in types of existed esterases and the structural differences of the same enzymes. The stability of CDD in aqueous media should be taken into consideration in future *in vitro* and *in vivo* experiments. This study provides useful information for

future *in vivo* pharmacokinetic studies and further development of CDD as pharmaceutical products.

REFERENCES

1. Epstein J, Sanderson IR, MacDonald TT. Curcumin as a therapeutic agent: the evidence from in vitro, animal and human studies. British Journal of Nutrition. 2010;103(11):1545-57.

2. Ak T, Gülçin İ. Antioxidant and radical scavenging properties of curcumin. Chemico-Biological Interactions. 2008;174(1):27-37.

3. Chaniad P, Morales Noppawan P, Rojsitthisak P, Luechapudiporn R. Effects of turmeric extract on hemin-induced low-density lipoprotein oxidation. Journal of Food Biochemistry. 2018;0(0):e12507.

4. Lantz RC, Chen GJ, Solyom AM, Jolad SD, Timmermann BN. The effect of turmeric extracts on inflammatory mediator production. Phytomedicine. 2005;12(6):445-52.

5. Buadonpri W, Wichitnithad W, Rojsitthisak P, Towiwat P. Synthetic curcumin inhibits carrageenan-induced paw edema in rats. Journal of Health Research. 2009;23(1):11-6.

6. Shao ZM, Shen ZZ, Liu CH, Sartippour Maryam R, Go Vay L, Heber D, et al. Curcumin exerts multiple suppressive effects on human breast carcinoma cells. International Journal of Cancer. 2001;98(2):234-40.

7. Wichitnithad W, Nimmannit U, Callery PS, Rojsitthisak P. Effects of different carboxylic ester spacers on chemical stability, release characteristics, and anticancer activity of mono-PEGylated curcumin conjugates. Journal of Pharmaceutical Sciences. 2011;100(12):5206-18.

8. Shimada K, Ushijima K, Suzuki C, Horiguchi M, Ando H, Akita T, et al. Pulmonary administration of curcumin inhibits B16F10 melanoma lung metastasis and invasion in mice. Cancer Chemotherapy and Pharmacology. 2018.

9. Ono K, Hasegawa K, Naiki H, Yamada M. Curcumin has potent anti-amyloidogenic effects for Alzheimer's β-amyloid fibrils in vitro. Journal of Neuroscience Research. 2004;75(6):742-50.

10. Begum AN, Jones MR, Lim GP, Morihara T, Kim P, Heath DD, et al. Curcumin

structure-function, bioavailability, and efficacy in models of neuroinflammation and Alzheimer's disease. Journal of Pharmacology and Experimental Therapeutics. 2008;326(1):196.

11. Ishrat T, Hoda MN, Khan MB, Yousuf S, Ahmad M, Khan MM, et al. Amelioration of cognitive deficits and neurodegeneration by curcumin in rat model of sporadic dementia of Alzheimer's type (SDAT). European Neuropsychopharmacology. 2009;19(9):636-47.

12. Nemmar A, Subramaniyan D, Ali BH. Protective effect of curcumin on pulmonary and cardiovascular effects induced by repeated exposure to diesel exhaust particles in mice. PLOS One. 2012;7(6):e39554.

13. Chandran B, Goel A. A randomized, pilot study to assess the efficacy and safety of curcumin in patients with active rheumatoid arthritis. Phytotherapy Research. 2012;26(11):1719-25.

14. Dhillon N, Aggarwal BB, Newman RA, Wolff RA, Kunnumakkara AB, Abbruzzese JL, et al. Phase II trial of curcumin in patients with advanced pancreatic cancer. Clinical Cancer Research. 2008;14(14):4491.

15. Wang Y-J, Pan M-H, Cheng A-L, Lin L-I, Ho Y-S, Hsieh C-Y, et al. Stability of curcumin in buffer solutions and characterization of its degradation products. Journal of Pharmaceutical and Biomedical Analysis. 1997;15(12):1867-76.

16. Liu W, Zhai Y, Heng X, Che FY, Chen W, Sun D, et al. Oral bioavailability of curcumin: problems and advancements. Journal of Drug Targeting. 2016;24(8):694-702.

17. Wichitnithad W, Nimmannit U, Wacharasindhu S, Rojsitthisak P. Synthesis, characterization and biological evaluation of succinate prodrugs of curcuminoids for colon cancer treatment. Molecules. 2011;16(2).

18. Bhunchu S, Rojsitthisak P, Rojsitthisak P. Effects of preparation parameters on the characteristics of chitosan–alginate nanoparticles containing curcumin diethyl disuccinate. Journal of Drug Delivery Science and Technology. 2015;28:64-72.

19. Wongsrisakul J, Wichitnithad W, Rojsitthisak P, Towiwat P. Antinociceptive effects of curcumin diethyl disuccinate in animal models. Journal of Health Research. 2010;24(4):175-80.

20. Bangphumi K, Kittiviriyakul C, Towiwat P, Rojsitthisak P, Khemawoot P.

Pharmacokinetics of curcumin diethyl disuccinate, a prodrug of curcumin, in Wistar rats. European Journal of Drug Metabolism and Pharmacokinetics. 2016;41(6):777-85.

21. Ratnatilaka Na Bhuket P, Niwattisaiwong N, Limpikirati P, Khemawoot P, Towiwat P, Ongpipattanakul B, et al. Simultaneous determination of curcumin diethyl disuccinate and its active metabolite curcumin in rat plasma by LC–MS/MS: Application of esterase inhibitors in the stabilization of an ester-containing prodrug. Journal of Chromatography B. 2016;1033-1034:301-10.

22. Jang GR, Harris RZ, Lau DT. Pharmacokinetics and its role in small molecule drug discovery research. Medicinal Research Reviews. 2001;21(5):382-96.

23. Muangnoi C, Jithavech P, Ratnatilaka Na Bhuket P, Supasena W, Wichitnithad W, Towiwat P, et al. A curcumin-diglutaric acid conjugated prodrug with improved water solubility and antinociceptive properties compared to curcumin. Bioscience, Biotechnology, and Biochemistry. 2018:1-8.

24. Griesser M, Pistis V, Suzuki T, Tejera N, Pratt DA, Schneider C. Autoxidative and cyclooxygenase-2 catalyzed transformation of the dietary chemopreventive agent curcumin. Journal of Biological Chemistry. 2011;286(2):1114-24.

25. Oetari S, Sudibyo M, Commandeur JNM, Samhoedi R, Vermeulen NPE. Effects of curcumin on cytochrome P450 and glutathione S-transferase activities in rat liver. Biochemical Pharmacology. 1996;51(1):39-45.

26. Metzler M, Pfeiffer E, Schulz Simone I, Dempe Julia S. Curcumin uptake and metabolism. BioFactors. 2012;39(1):14-20.

27. Wahlström B, Blennow G. A study on the fate of curcumin in the rat. Acta Pharmacologica et Toxicologica. 1978;43(2):86-92.

28. Shoba G, Joy D, Joseph T, Majeed M, Rajendran R, Srinivas PSSR. Influence of piperine on the pharmacokinetics of curcumin in animals and human volunteers. Planta Medica. 1998;64(04):353-6.

29. Ireson C, Orr S, Jones DJL, Verschoyle R, Lim C-K, Luo J-L, et al. Characterization of metabolites of the chemopreventive agent curcumin in human and rat hepatocytes and in the rat in vivo, and evaluation of their ability to inhibit phorbol ester-induced prostaglandin E2 production. Cancer Research. 2001;61(3):1058.

30. Ireson CR, Jones DJL, Orr S, Coughtrie MWH, Boocock DJ, Williams ML, et al.

Metabolism of the cancer chemopreventive agent curcumin in human and rat intestine. Cancer Epidemiology Biomarkers & Prevention. 2002;11(1):105.

31. Asai A, Miyazawa T. Occurrence of orally administered curcuminoid as glucuronide and glucuronide/sulfate conjugates in rat plasma. Life Sciences. 2000;67(23):2785-93.

32. Usta M, Wortelboer HM, Vervoort J, Boersma MG, Rietjens IMCM, van Bladeren PJ, et al. Human glutathione S-transferase-mediated glutathione conjugation of curcumin and efflux of these conjugates in Caco-2 cells. Chemical Research in Toxicology. 2007;20(12):1895-902.

33. Bhunchu S, Muangnoi C, Rojsitthisak P, Rojsitthisak P. Curcumin diethyl disuccinate encapsulated in chitosan/alginate nanoparticles for improvement of its in vitro cytotoxicity against MDA-MB-231 human breast cancer cells. Die Pharmazie - An International Journal of Pharmaceutical Sciences. 2016;71(12):691-700.

34. Di L, Kerns EH. Stability challenges in drug discovery. Chemistry & Biodiversity. 2009;6(11):1875-86.

35. Fubara JO, Notari RE. Influence of pH, temperature and buffers on cefepime degradation kinetics and stability predictions in aqueous solutions. Journal of Pharmaceutical Sciences. 2000;87(12):1572-6.

36. Li W, Zhang J, Tse Francis LS. Strategies in quantitative LC-MS/MS analysis of unstable small molecules in biological matrices. Biomedical Chromatography. 2010;25(1-2):258-77.

37. Liederer BM, Borchardt RT. Enzymes involved in the bioconversion of ester-based prodrugs. Journal of Pharmaceutical Sciences. 2006;95(6):1177-95.

38. Fukami T, Yokoi T. The emerging role of human esterases. Drug Metabolism and Pharmacokinetics. 2012;27(5):466-77.

39. Li B, Sedlacek M, Manoharan I, Boopathy R, Duysen EG, Masson P, et al. Butyrylcholinesterase, paraoxonase, and albumin esterase, but not carboxylesterase, are present in human plasma. Biochemical Pharmacology. 2005;70(11):1673-84.

40. Berry LM, Wollenberg L, Zhao Z. Esterase activities in the blood, liver and intestine of several preclinical species and humans. Drug Metabolism Letters.

2009;3(2):70-7.

41. Hosokawa M, Satoh T. Carboxylesterases: Overview, Structure, Function, and Polymorphism. Anticholinesterase Pesticides. 2011.

42. Bahar FG, Ohura K, Ogihara T, Imai T. Species difference of esterase expression and hydrolase activity in plasma. Journal of Pharmaceutical Sciences. 2012;101(10):3979-88.

43. Yang Y-h, Aloysius H, Inoyama D, Chen Y, Hu L-q. Enzyme-mediated hydrolytic activation of prodrugs. Acta Pharmaceutica Sinica B. 2011;1(3):143-59.

44. Udata C, Tirucherai G, Mitra Ashim K. Synthesis, stereoselective enzymatic hydrolysis, and skin permeation of diastereomeric propranolol ester prodrugs. Journal of Pharmaceutical Sciences. 2000;88(5):544-50.

45. Crauste-Manciet S, Decroix M-O, Farinotti R, Chaumeil J-C. Cefpodoxime-proxetil hydrolysis and food effects in the intestinal lumen before absorption: in vitro comparison of rabbit and human material. International Journal of Pharmaceutics. 1997;157(2):153-61.

46. Lockridge O, Duysen Ellen G, Masson P. Butyrylcholinesterase: Overview, structure, and function. Anticholinesterase Pesticides. 2011.

47. Costa Lucio G, Furlong Clement E. Paraoxonase 1: Structure, function, and polymorphisms. Anticholinesterase Pesticides. 2011.

48. Mackness MI, Mackness B, Durrington PN, Connelly PW, Hegele RA. Paraoxonase: biochemistry, genetics and relationship to plasma lipoproteins. Current Opinion in Lipidology. 1996;7(2):69-76.

49. Tougou K, Nakamura A, Watanabe S, Okuyama Y, Morino A. Paraoxonase has a major role in the hydrolysis of prulifloxacin (NM441), a prodrug of a new antibacterial agent. Drug Metabolism and Disposition. 1998;26(4):355.

50. Ishizuka T, Fujimori I, Nishida A, Sakurai H, Yoshigae Y, Nakahara K, et al. Paraoxonase 1 as a major bioactivating hydrolase for olmesartan medoxomil in human blood circulation: Molecular identification and contribution to plasma metabolism. Drug Metabolism and Disposition. 2011.

51. Harel M, Aharoni A, Gaidukov L, Brumshtein B, Khersonsky O, Meged R, et al. Structure and evolution of the serum paraoxonase family of detoxifying and anti-

atherosclerotic enzymes. Nature Structural & Molecular Biology. 2004;11:412.

52. Kragh-Hansen U. Molecular and practical aspects of the enzymatic properties of human serum albumin and of albumin–ligand complexes. Biochimica et Biophysica Acta (BBA) - General Subjects. 2013;1830(12):5535-44.

53. Ma S-F, Anraku M, Iwao Y, Yamasaki K, Kragh-Hansen U, Yamaotsu N, et al. Hydrolysis of angiotensin II receptor blocker prodrug olmesartan medoxomil by human serum albumin and identification of its catalytic active sites. Drug Metabolism and Disposition. 2005;33(12):1911-9.

54. Koitka M, Höchel J, Gieschen H, Borchert H-H. Improving the ex vivo stability of drug ester compounds in rat and dog serum: Inhibition of the specific esterases and implications on their identity. Journal of Pharmaceutical and Biomedical Analysis. 2010;51(3):664-78.

55. Tsujikawa K, Kuwayama K, Miyaguchi H, Kanamori T, Iwata YT, Inoue H. In vitro stability and metabolism of salvinorin A in rat plasma. Xenobiotica. 2009;39(5):391-8.

56. Liu Y, He J, Abliz Z, Zhu H. In vitro stability and metabolism of O2′, O3′, O5′-tri-acetyl-N6-(3-hydroxylaniline) adenosine in rat, dog and human plasma: Chemical hydrolysis and role of plasma esterases. Xenobiotica. 2011;41(7):549-60.

57. Yu LX, Amidon GL, Polli JE, Zhao H, Mehta MU, Conner DP, et al. Biopharmaceutics classification system: The scientific basis for biowaiver Extensions. Pharmaceutical Research. 2002;19(7):921-5.

58. Thakral S, Thakral NK, Majumdar DK. Eudragit®: a technology evaluation. Expert Opinion on Drug Delivery. 2013;10(1):131-49.

59. Ericsson H, Tholander B, Regårdh CG. In vitro hydrolysis rate and protein binding of clevidipine, a new ultrashort-acting calcium antagonist metabolised by esterases, in different animal species and man. European Journal of Pharmaceutical Sciences. 1999;8(1):29-37.

60. Jiang H, Somogyi Á, Jacobsen NE, Timmermann BN, Gang DR. Analysis of curcuminoids by positive and negative electrospray ionization and tandem mass spectrometry. Rapid Communications in Mass Spectrometry. 2006;20(6):1001-12.

61. Hioki T, Fukami T, Nakajima M, Yokoi T. Human Paraoxonase 1 Is the Enzyme Responsible for Pilocarpine Hydrolysis. Drug Metabolism and Disposition.

2011;39(8):1345.

62. Eichenbaum G, Skibbe J, Parkinson A, Johnson MD, Baumgardner D, Ogilvie B, et al. Use of enzyme inhibitors to evaluate the conversion pathways of ester and amide prodrugs: A case study example with the prodrug ceftobiprole medocaril. Journal of Pharmaceutical Sciences. 2012;101(3):1242-52.

63. Grubič Z, Sket D, Brzin M. Iso-OMPA-induced potentiation of soman toxicity in rat correlates with the inhibition of plasma carboxylesterases. Archives of Toxicology. 1988;62(5):398-9.

64. Powers JC, Asgian JL, Ekici ÖD, James KE. Irreversible Inhibitors of Serine, Cysteine, and Threonine Proteases. Chemical Reviews. 2002;102(12):4639-750.

65. Walker John E. Lysine residue 199 of human serum albumin is modified by acetylsalicylic acid. FEBS Letters. 1976;66(2):173-5.

66. Sogorb MA, García-Argüelles S, Carrera V, Vilanova E. Serum Albumin is as Efficient as Paraxonase in the Detoxication of Paraoxon at Toxicologically Relevant Concentrations. Chemical Research in Toxicology. 2008;21(8):1524-9.

67. Salvi A, Carrupt P-A, Mayer JM, Testa B. Esterase-like Activity of Human Serum Albumin Toward Prodrug Esters of Nicotinic Acid. Drug Metabolism and Disposition. 1997;25(4):395.

68. Lockridge O, Xue W, Gaydess A, Grigoryan H, Ding S-J, Schopfer LM, et al. Pseudo-esterase Activity of Human Albumin: SLOW TURNOVER ON TYROSINE 411 AND STABLE ACETYLATION OF 82 RESIDUES INCLUDING 59 LYSINES. Journal of Biological Chemistry. 2008;283(33):22582-90.

69. Agarwal RP, Phillips M, McPherson RA, Hensley P. Serum albumin and the metabolism of disulfiram. Biochemical Pharmacology. 1986;35(19):3341-7.

70. Overgaard PA, Jørgen J. Reactivity of the Thiol Group in Human and Bovine Albumin at pH 3–9, as Measured by Exchange with 2,2′-Dithiodipyridine. European Journal of Biochemistry. 1980;106(1):291-5.

71. Stewart Alan J, Blindauer Claudia A, Berezenko S, Sleep D, Tooth D, Sadler Peter J. Role of Tyr84 in controlling the reactivity of Cys34 of human albumin. The FEBS Journal. 2004;272(2):353-62.

72. Torres MJ, Turell L, Botti H, Antmann L, Carballal S, Ferrer-Sueta G, et al. Modulation of the reactivity of the thiol of human serum albumin and its sulfenic derivative by fatty acids. Archives of Biochemistry and Biophysics. 2012;521(1):102-10.

APPENDIX

APPENDIX A

Preparation of solutions

1. Buffer solutions

1.1. Solutions necessary for buffer preparation

1.1.1. 0.2 M Potassium Chloride (KCl) solution

A 1.491 g of KCl was dissolved in ultrapure water and adjusted to the volume with ultrapure water in a 100 mL-volumetric flask.

1.1.2. 0.2 M Hydrochloric acid (HCl) solution

A 1.97 mL of 37% HCl was transferred to a 100-mL volumetric flask containing 50 mL of ultrapure water. Then, the HCl solution was diluted with ultrapure water to 100 mL.

1.1.3. 0.2 M Monobasic potassium phosphate (KH_2PO_4) solution

A 2.722 g of KH_2PO_4 was dissolved in ultrapure water and diluted in a 100-mL volumetric flask with ultrapure water.

1.1.4. 2 M Acetic acid solution

A 11.7 mL of glacial acetic acid was transferred to a 100-mL volumetric flask containing 50 mL of ultrapure water. The acetic acid solution was then adjusted to the volume with ultrapure water.

1.1.5. 0.2 M Sodium hydroxide (NaOH) solution

A 0.8 g of NaOH pellets was dissolved in ultrapure water and subsequently made up to the volume with ultrapure water in a 100-mL volumetric flask.

1.2. Buffer solutions

1.2.1. Hydrochloric acid buffer (pH 1.2)

A 25 mL of 0.2 M KCl solution was transferred to a 100-mL volumetric flask. A 42.5 mL of 0.2 M HCl solution was added to the same volumetric flask. Then, ultrapure water was added to adjust the volume.

1.2.2. Acetate buffer (pH 4.5)

A 0.299 g of sodium acetate trihydrate was dissolved in ultrapure water. Then, the sodium acetate solution was transferred to a 100-mL volumetric flask. A 1.4 mL of 2 M acetic acid solution was added to the sodium acetate solution. Then, the pH of the solution was adjusted to 4.5, and solution was diluted with ultrapure water to 100 mL.

1.2.3. Phosphate buffers

A 25 mL of 0.2 M KH_2PO_4 solution was added to a 100-mL volumetric flask. A specified amount of 0.2 M NaOH was added as indicated below to obtain buffers with desired pH values.

pH	6.8	7.4	8.0
0.2 M NaOH (mL)	11.2	19.6	23.0

Then, the pH of each buffer was adjusted, and the phosphate solutions were made up to the volume with ultrapure water.

2. Stock and spiking solutions

2.1. Solutions of curcumin diethyl disuccinate, monoethylsuccinyl curcumin, curcumin and dimethylcurcumin

2.1.1. Stock solution of curcumin diethyl disuccinate (CDD)

A 0.010225 g of CDD powder (98.0 % purity) was transferred to a 10-mL volumetric flask. The CDD powder was dissolved in acetonitrile to obtain a stock solution of CDD (stock solution-CDD 01) at the concentration of 1604.3 µM.

2.1.2. Stock solution of curcumin (CUR)

A 0.010336 g of CUR powder (>98 % purity) was transferred to a 10-mL volumetric flask. The CUR powder was dissolved in acetonitrile to obtain a stock solution of CUR (stock solution-CUR 01) at the concentration of 2749.5 µM.

2.1.3. Stock solution of dimethyl curcumin (DMC)

A 0.009962 g of DMC powder (>98 % purity) was transferred to a 10-mL volumetric flask. The DMC powder was dissolved in acetonitrile to obtain a

stock solution of DMC (stock solution-DMC 01) at the concentration of 2462.9 µM.

2.1.4. Spiking solution of CDD for kinetic assays

A 233.75 µL of stock solution-CDD 01 was aliquoted into a 5-mL volumetric flask. Subsequently, acetonitrile was added to the volumetric flask to adjust the volume, resulting a spiking solution of CDD (SS-CDD 01) at the concentration of 75 µM.

2.1.5. Intermediate stock solution of DMC

A 1.02 mL of stock solution-DMC 01 was taken into a 50-mL volumetric flask. Then, the solution was diluted with acetonitrile to 50 mL, giving an intermediate stock solution of DMC (INT IS-01) with the concentration of 50 µM.

2.1.6. Precipitating solution

A 1.20 mL of INT IS-01 was transferred to a 100-mL volumetric flask and the solution was made up to the volume with acetonitrile. The precipitation solution contained DMC at 0.6 µM.

2.1.7. Spiking solution of CDD for system suitability test

A 156 µL of stock solution-CDD 01 was diluted in a 5-mL volumetric flask using acetonitrile. The resulting solution (SS-Sys Suit CDD 01) had the concentration of 50 µM.

2.1.8. Spiking solution of CUR for system suitability test

A 91 µL of stock solution-CUR 01 was diluted in a 5-mL volumetric flask using acetonitrile. The resulting solution (SS-Sys Suit CUR 01) had the concentration of 50 µM.

2.1.9. Spiking solution of CDD for metabolite identification

A 187 µL of stock solution-CDD 01 was transferred into a microcentrifuge tube. Then, an 813 µL of acetonitrile was added to the microcentrifuge tube yielding a spiking solution of CDD for metabolite identification (SS-Met ID 01) with the concentration of 300 µM.

2.1.10. Solutions of monoethylsuccinyl curcumin (MSCUR)

A 0.00105 g of MSCUR was transferred into a microcentrifuge tube and dissolved in a 1 mL of acetonitrile to obtain a stock solution of MSCUR (stock

solution-MSCUR 01) at the concentration of 1 mg/mL. Then, a 10 µL of stock solution-MSCUR 01 was taken to combine with a 990 µL of acetonitrile in a microcentrifuge tube. The resulting solution (INT MSCUR-01) had the concentration of 10 µg/mL. Subsequently, a 10 µL of INT MSCUR-01 was aliquoted to another microcentrifuge tube and further diluted with a 990 µL of acetonitrile to obtain a working solution of MSCUR (WS MSCUR-01) at the concentration of 100 ng/mL.

2.2. Solutions of esterase inhibitors

2.2.1. 200 mM BNPP solution

A 0.069333 g of BNPP was dissolved in a 1000 µL of methanol in a microcentrifuge tube.

2.2.2. 200 mM TLCK solution

A 0.075158 g of TLCK was dissolved in a 1000 µL of methanol in a microcentrifuge tube.

2.2.3. 200 mM PMSF solution

A 0.035207 g of TLCK was dissolved in a 1000 µL of methanol in a microcentrifuge tube.

2.2.4. 200 mM Pefabloc® SC solution

A 0.049693 g of TLCK was dissolved in a 1000 µL of methanol in a microcentrifuge tube.

2.2.5. 200 mM Iso-OMPA solution

A 0.068418 g of TLCK was dissolved in a 1000 µL of methanol in a microcentrifuge tube.

2.2.6. 200 mM DTNB solution

A 0.080847 g of TLCK was dissolved in a 1000 µL of methanol in a microcentrifuge tube.

2.2.7. 400 mM NaF solution

A 0.017508 g of NaF was dissolved in a 1000 µL of ultrapure water in a microcentrifuge tube.

2.2.8. 400 mM Na_2EDTA solution

A 0.153104 g of Na_2EDTA was dissolved in a 750 µL of ultrapure water in a microcentrifuge tube. A small amount of 0.2 M NaOH was gradually added to the solution until Na_2EDTA solids dissolved. Then, the volume of the solution was made up to 1000 µL.

2.2.9. 400 mM EGTA solution

A 0.155301 g of EGTA was dissolved in a 750 µL of ultrapure water in a microcentrifuge tube. A small amount of 0.2 M NaOH was gradually added to the solution until EGTA solids dissolved. Then, the volume of the solution was made up to 1000 µL.

2.2.10. 2 mM Eserine hemisulfate solution

A 0.006823 g of serine hemisulfate was dissolved in a 1000 µL of ultrapure water in a microcentrifuge tube.

2.2.11. 2 mM BW284c51 solution

A 0.002340 g of BW284c51 was dissolved in a 1000 µL of ultrapure water in a microcentrifuge tube.

2.2.12. 20 mM BNPP solution

A 100 µL of 200 mM BNPP solution was mixed with 900 µL of methanol in a microcentrifuge tube.

2.2.13. 2 mM BNPP solution

A 10 µL of 200 mM BNPP solution was mixed with 990 µL of methanol in a microcentrifuge tube.

2.2.14. 20 mM TLCK solution

A 100 µL of 200 mM TLCK solution was mixed with 900 µL of methanol in a microcentrifuge tube.

2.2.15. 2 mM TLCK solution

A 10 µL of 200 mM TLCK solution was mixed with 990 µL of methanol in a microcentrifuge tube.

2.2.16. 20 mM PMSF solution

A 100 µL of 200 mM PMSF solution was mixed with 900 µL of methanol in a microcentrifuge tube.

2.2.17. 2 mM PMSF solution

A 10 µL of 200 mM PMSF solution was mixed with 990 µL of methanol in a microcentrifuge tube.

2.2.18. 20 mM Pefabloc® SC solution

A 100 µL of 200 mM Pefabloc® SC solution was mixed with 900 µL of methanol in a microcentrifuge tube.

2.2.19. 2 mM Pefabloc® SC solution

A 10 µL of 200 mM Pefabloc® SC solution was mixed with 990 µL of methanol in a microcentrifuge tube.

2.2.20. 20 mM Iso-OMPA solution

A 100 µL of 200 mM Iso-OMPA solution was mixed with 900 µL of methanol in a microcentrifuge tube.

2.2.21. 2 mM Iso-OMPA solution

A 10 µL of 200 mM Iso-OMPA solution was mixed with 990 µL of methanol in a microcentrifuge tube.

2.2.22. 20 mM DTNB solution

A 100 µL of 200 mM DTNB solution was mixed with 900 µL of methanol in a microcentrifuge tube.

2.2.23. 2 mM DTNB solution

A 10 µL of 200 mM DTNB solution was mixed with 990 µL of methanol in a microcentrifuge tube.

2.2.24. 200 mM NaF solution

A 500 µL of 400 mM NaF solution was mixed with 500 µL of ultrapure water in a microcentrifuge tube.

2.2.25. 100 mM NaF solution

A 500 µL of 200 mM NaF solution was mixed with 500 µL of ultrapure water in a microcentrifuge tube.

2.2.26. 200 mM Na_2EDTA solution

A 500 µL of 400 mM Na_2EDTA solution was mixed with 500 µL of ultrapure water in a microcentrifuge tube.

2.2.27. 100 mM Na_2EDTA solution

A 500 µL of 200 mM Na_2EDTA solution was mixed with 500 µL of ultrapure water in a microcentrifuge tube.

2.2.28. 200 mM EGTA solution

A 500 µL of 400 mM EGTA solution was mixed with 500 µL of ultrapure water in a microcentrifuge tube.

2.2.29. 100 mM EGTA solution

A 500 µL of 200 mM EGTA solution was mixed with 500 µL of ultrapure water in a microcentrifuge tube.

2.2.30. 200 µM eserine hemisulfate solution

A 100 µL of 2 mM eserine hemisulfate solution was mixed with 900 µL of ultrapure water in a microcentrifuge tube.

2.2.31. 20 µM eserine hemisulfate solution

A 10 µL of 2 mM eserine hemisulfate solution was mixed with 990 µL of ultrapure water in a microcentrifuge tube.

2.2.32. 200 µM BW284c51 solution

A 100 µL of 2 mM BW284c51 solution was mixed with 900 µL of ultrapure water in a microcentrifuge tube.

2.2.33. 20 µM BW284c51 solution

A 10 µL of 2 mM BW284c51 solution was mixed with 990 µL of ultrapure water in a microcentrifuge tube.

APPENDIX B

Chromatographic purity

The synthesized standards of CUR, DMC and CDD were injected into an HPLC system to determine purity. All compounds were prepared in acetonitrile at the final concentration of 15 μM. The chromatographic conditions for the assay were described below.

Mobile phase (A:B = 30:70 v/v)	A: 0.2 % Formic acid in water
	B: Acetonitrile
Column	Halo C8 4.6 x 50 mm, 2.7 μm
Flow rate	0.5 mL/min
Autosampler temperature	4 ℃
Column oven temperature	35 ℃
Injection volume	10 μL
Detection wavelength	λ = 400 nm

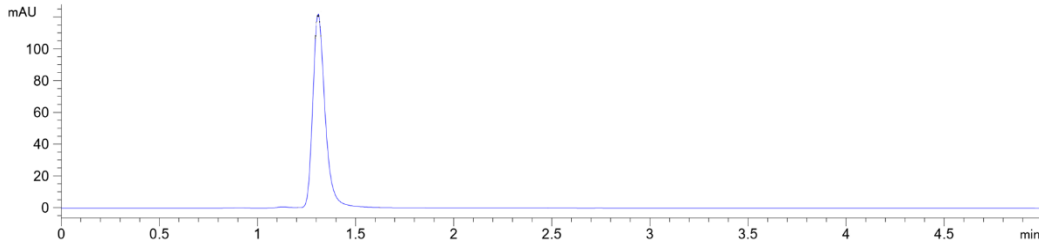

Figure B1 Chromatogram of CUR standard at 15 μM

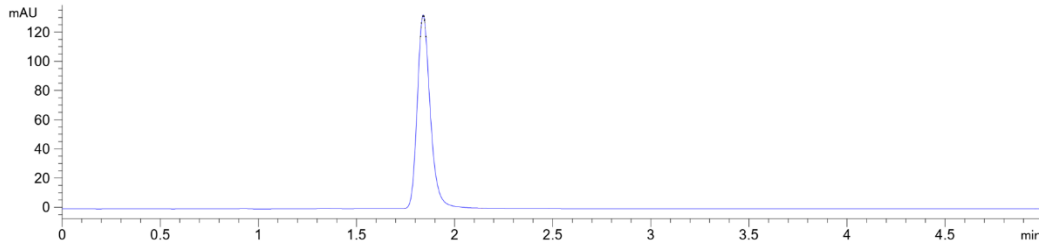

Figure B2 Chromatogram of DMC standard at 15 μM

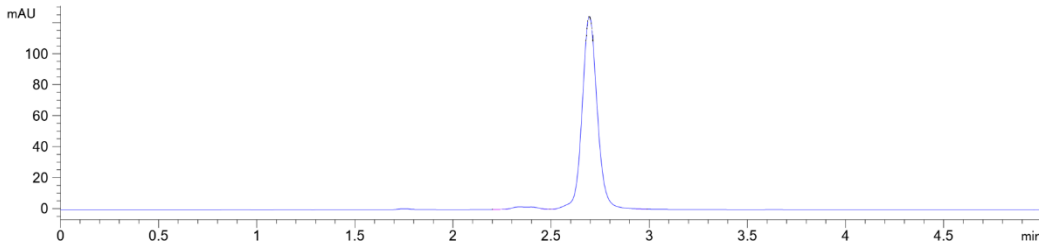

Figure B3 Chromatogram of CDD standard at 15 μM

APPENDIX C

Chromatograms of CDD hydrolysis in plasma at 4 and 25 °C

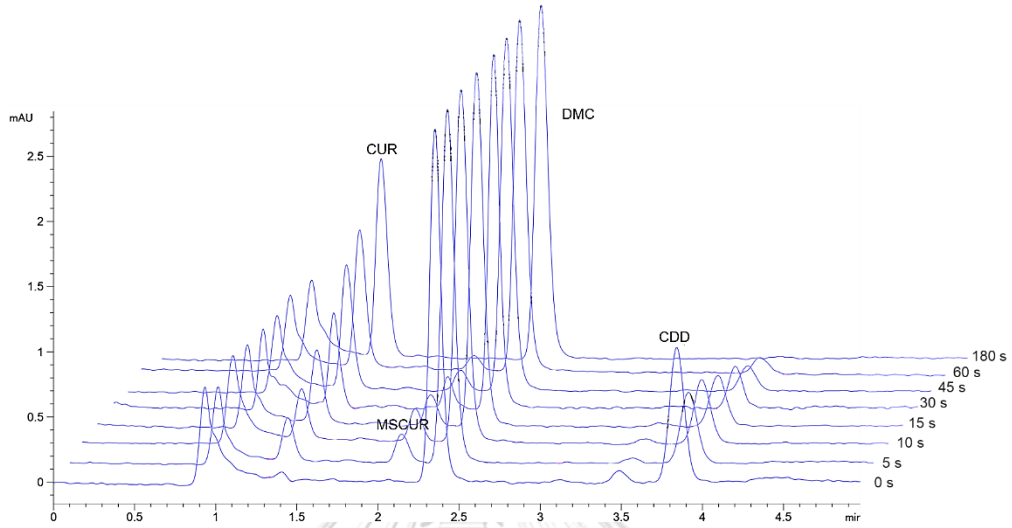

Figure C1 Representative chromatograms of CDD hydrolysis in rat plasma at 4 °C

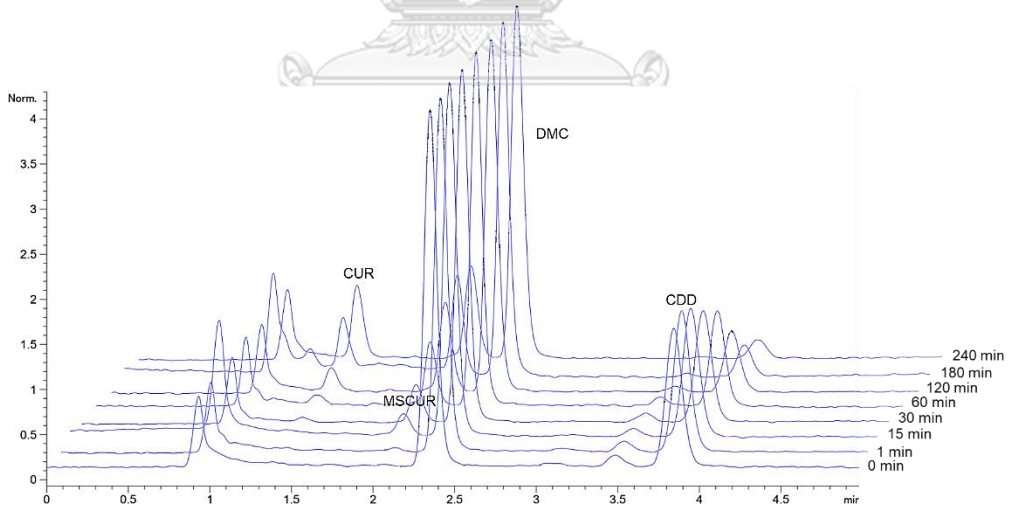

Figure C2 Representative chromatograms of CDD hydrolysis in dog plasma at 4 °C

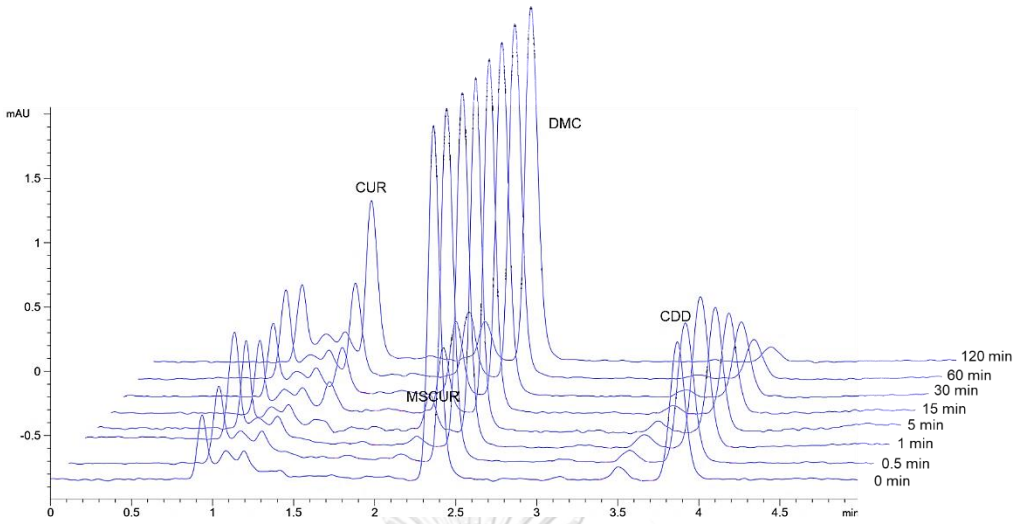

Figure C3 Representative chromatograms of CDD hydrolysis in human plasma at 4 °C

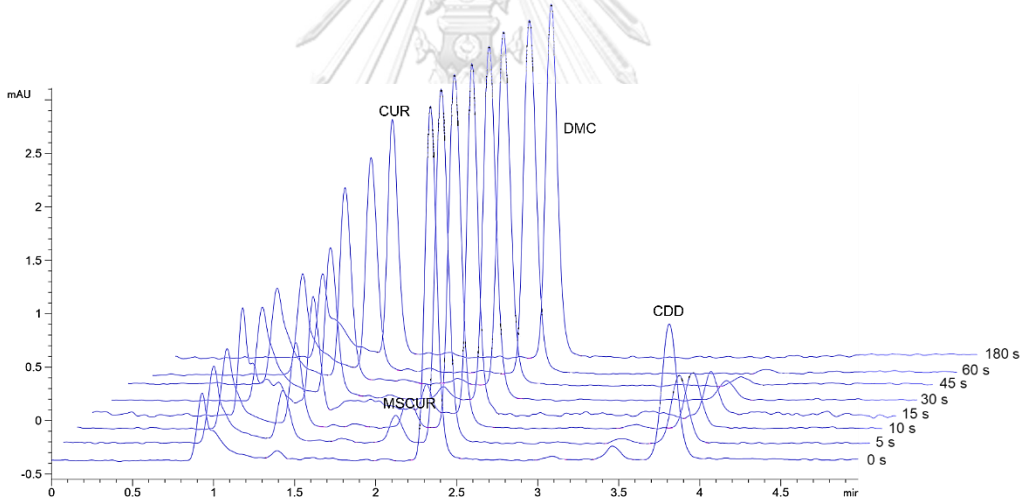

Figure C4 Representative chromatograms of CDD hydrolysis in rat plasma at 25 °C

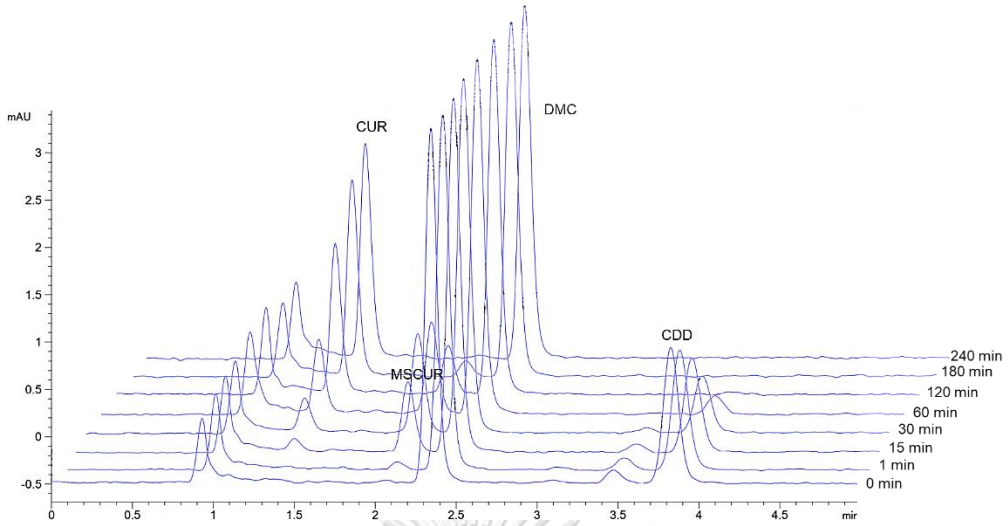

Figure C5 Representative chromatograms of CDD hydrolysis in dog plasma at 25 ℃

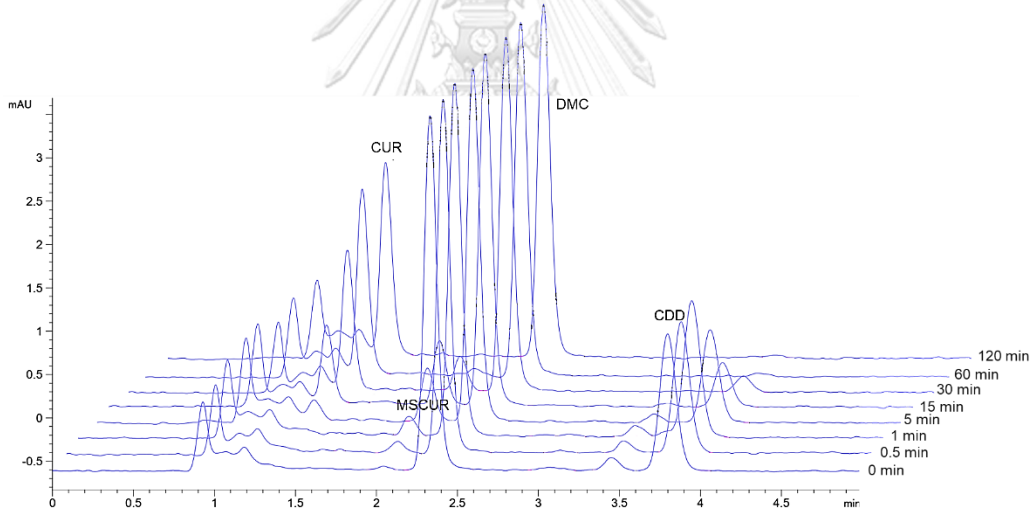

Figure C6 Representative chromatograms of CDD hydrolysis in human plasma at 25 ℃

APPENDIX D

Hydrolysis profiles of CDD in plasma

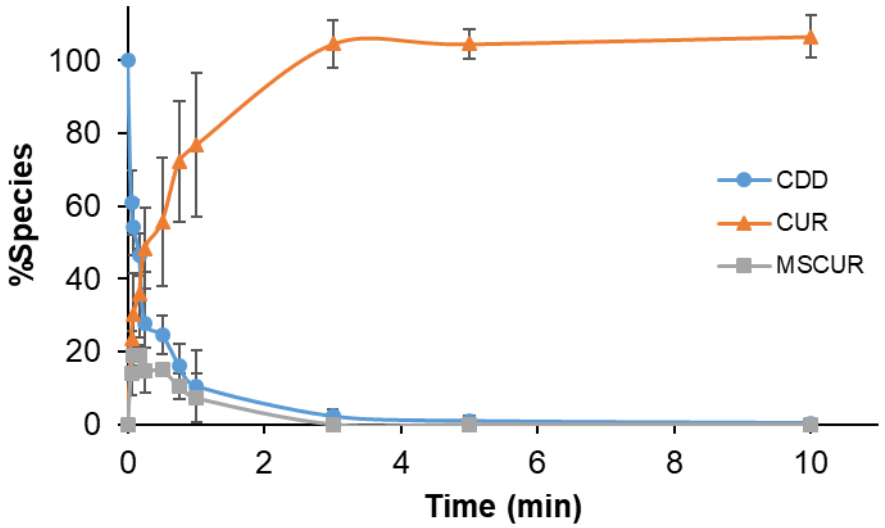

Figure D1 Hydrolysis profile of CDD in rat plasma at 4 °C

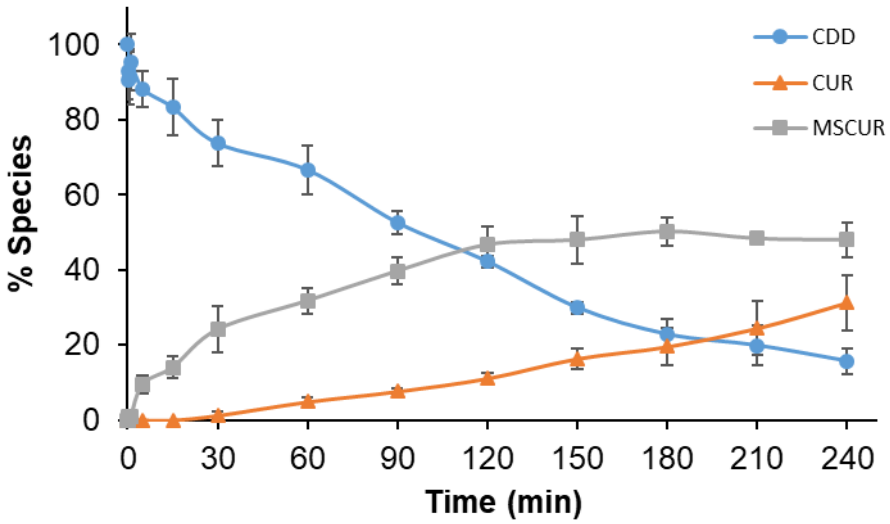

Figure D2 Hydrolysis profile of CDD in dog plasma at 4 °C

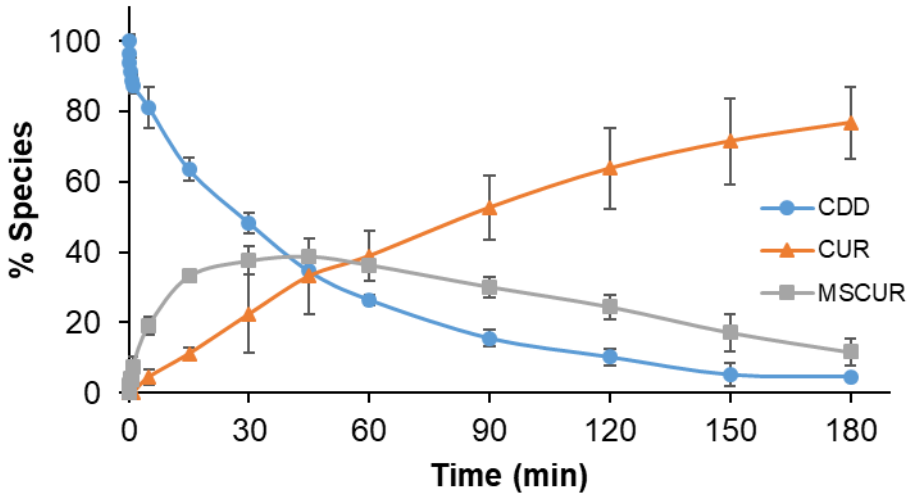

Figure D3 Hydrolysis profile of CDD in human plasma at 4 ℃

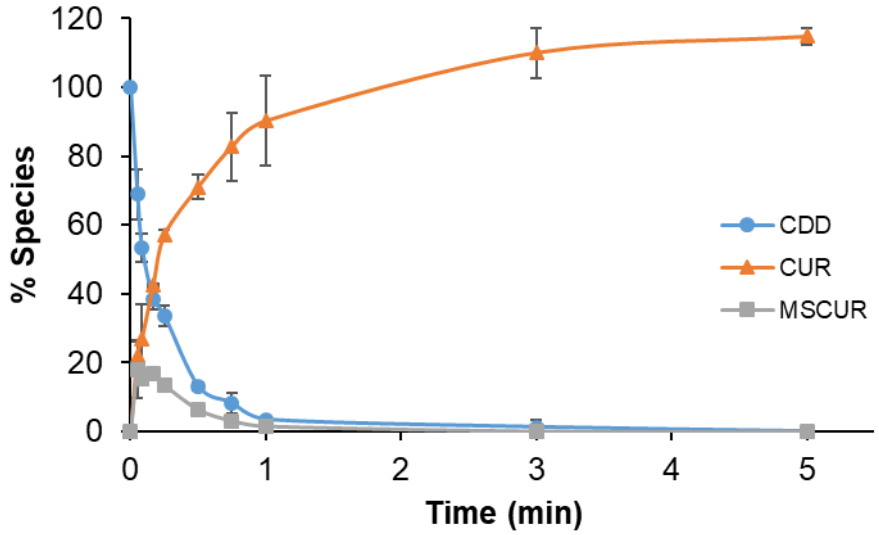

Figure D4 Hydrolysis profile of CDD in rat plasma at 25 ℃

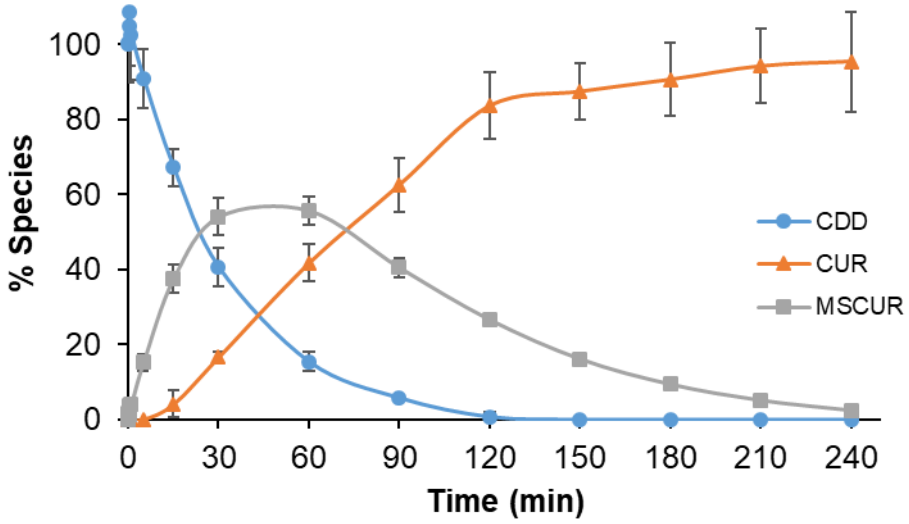

Figure D5 Hydrolysis profile of CDD in dog plasma at 25 °C

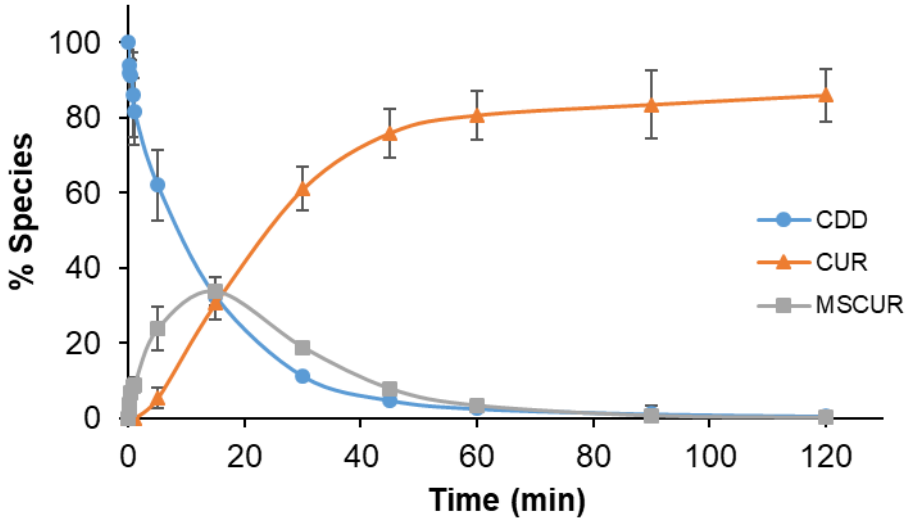

Figure D6 Hydrolysis profile of CDD in human plasma at 25 °C

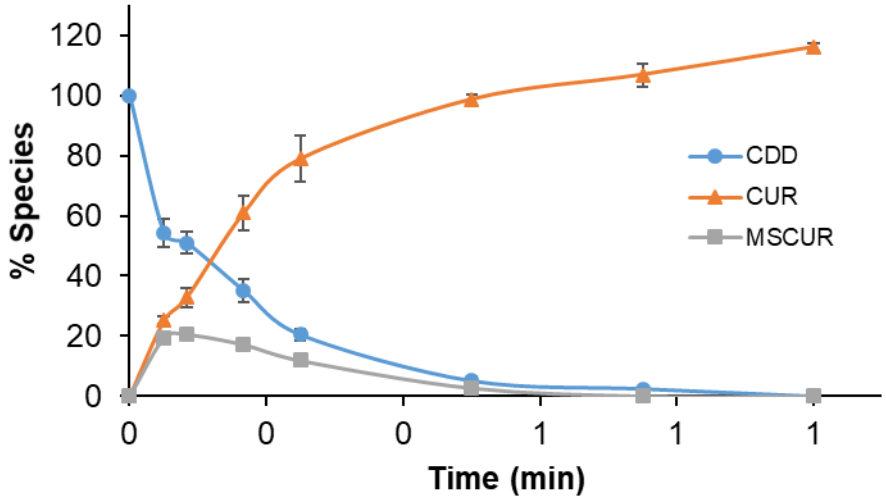

Figure D7 Hydrolysis profile of CDD in rat plasma at 37 °C

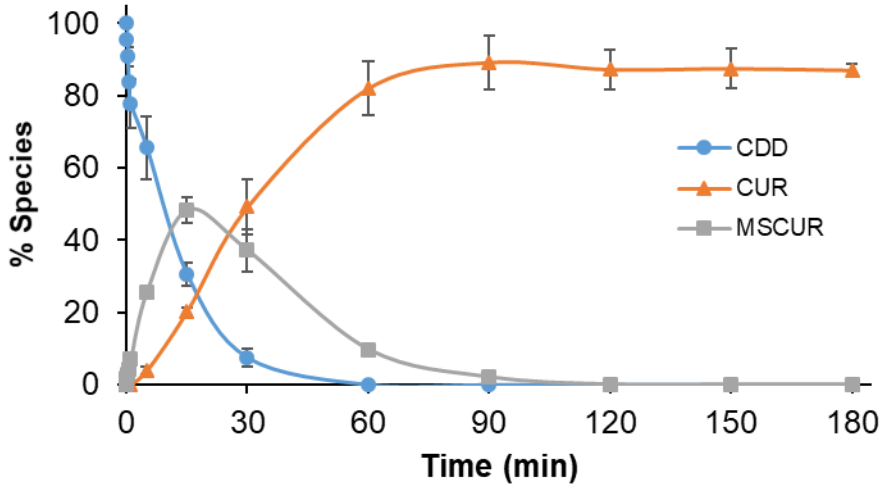

Figure D8 Hydrolysis profile of CDD in dog plasma at 37 °C

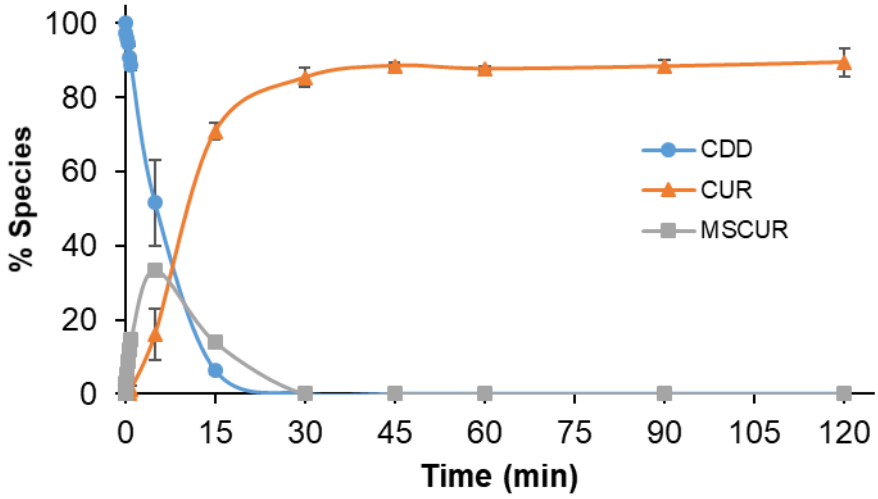

Figure D9 Hydrolysis profile of CDD in human plasma at 37 °C

APPENDIX E

Comprehensive review of chemical kinetics and regression data

The chemical instability of drug molecules contributes to the changes in their therapeutic efficacy and toxicological consequences. A knowledge of the chemical stability of drugs is therefore crucial in the development of medicinal products. In this section, the overview on the orders of reaction and equations for calculating kinetic parameters are reviewed.

Basic principles of chemical kinetics

The following scheme describes the simplest model of chemical reaction of a drug D converting to a product P:

$$D \longrightarrow P$$

In general, drugs undergo degradation reactions that involve the collision between the drug D and a reactant A (so-called biomolecular reaction) to form one or multiple products as illustrated in the simplest form by the following scheme:

$$D + A \longrightarrow P$$

The speed of a reaction, or rate, is proportional to the concentration (or activity) of D and A as described by the following expression:

$$- d[D]/dt \propto [D][A]$$

When the proportional constant is included, we obtain the following equation:

$$- d[D]/dt = k[D][A] \qquad \text{Eq. E1}$$

where k is the proportional constant or usually designated as the rate constant. In this case, the rate of reaction (- d[D]/dt) is said to be first-order in D and first-order in A. The overall order for this case is said to be second order (from the sum of the orders of all the components).

The effect of molecular structure in the chemical kinetics

The molecular structure of a drug molecule determines its degradation pathways and the substituents around the reaction site can influence the chemical reactivity. For instance, a drug with an electron-withdrawing group close to its ester

bond is more susceptible to the nucleophilic attack by hydroxide ion than a similar ester without an electron-withdrawing group and hence having the faster rate of reaction. The presence of an electron-withdrawing group makes the carbonyl carbon to be more electrophilic, stabilize the generated reaction intermediate, thus decreasing the activation energy (E_a). In contrast, the presence of a bulky group or electron-donating group increases the E_a of the reaction, hence retarding the hydrolysis rate.

Rate equations and kinetic models

Drug substances are degraded through several mechanisms and pathways depending on their chemical structures. The degradation rate is determined by factors contributing to the rate equations. The degradation of pharmaceuticals generally follows pseudo-zero, pseudo-first, or pseudo-second order kinetics. The degradation at higher order is rare. Some drugs may undergo complex degradation pathways involving consecutive reactions. When a drug D degrades in solution via a pathway involving several reactants A, B,...., the degradation rate is usually contributed by A, B, ... and D as shown in Eq. E2, assuming that all reactants involve in the rate-limiting step.

$$- d[D]/dt = k_0[D]^m[A]^a[B]^b \cdots \qquad \text{Eq. E2}$$

If the concentration of reactants A, B,..... are constant or in excess of D (the change in their concentrations is negligible), the rate equation can be simplified to:

$$- d[D]/dt = k[D]^m \qquad \text{Eq. E3}$$

When *m* equals 0, 1, or 2, the reaction is considered to be pseudo-zero, pseudo-first, or pseudo-second order reactions, respectively.

<u>Simple pseudo-first order and zero-order reactions</u>

$$D \xrightarrow{k_{app}} P$$

The differential equation for the pseudo-1st order reaction is:

$$- d[D]/dt = k_{app}[D] \qquad \text{Eq. E4}$$

The integrated form of this equation is:

$$[D] = [D]_0 e^{-k_{app}t} \qquad \text{Eq. E5}$$

Where $[D]_0$ is the initial concentration of the drug and k_{app} is the apparent rate constant. Most degradation kinetics in solutions obey the pseudo-1st order reaction.

The rate equations for pseudo-zero order kinetics are:

$$- d[D]/dt = k \qquad \text{Eq. E6}$$

$$[D] = [D]_0 - kt \qquad \text{Eq. E7}$$

For the pseudo-zero order kinetics, the degradation rate does not depend on the drug concentration. A specific example of this type of reaction order is a drug degradation in suspensions because the concentration of a drug in solution is maintained constant from the solid phase.

Simple pseudo-second order reactions

$$D + A \xrightarrow{k} P \quad \text{or} \quad 2D \xrightarrow{k} P$$

The changes in the rate and concentration when the drug D react with a reactant A are described by:

$$- d[D]/dt = k[D][A] \qquad \text{Eq. E8}$$

$$\ln ([D]/[A]) = ([D]_0 - [A]_0)k_0t + \ln ([D]_0/[A]_0) \qquad \text{Eq. E9}$$

where $[A]_0$ is the initial concentration of A, $[D]_0$ is the initial concentration of D. The following equations are established when the drug D undergoes the bimolecular reaction with itself.

$$- d[D]/dt = k[D]^2 \qquad \text{Eq. E10}$$

$$[D] = [D]_0/(1+ kt[A]_0) \qquad \text{Eq. E11}$$

Pseudo-first order consecutive reactions

$$D \xrightarrow{k_1} I \xrightarrow{k_2} P$$

Eq. E12 and Eq. E13 represent the case when the drug D converts to intermediate I which is subsequently converted to P according to the pseudo-1st order reactions.

$$- d[D]/dt = k_1[D] \qquad \text{Eq. E12}$$

$$d[I]/dt = k_1[D] - k_2[P] \qquad \text{Eq. E13}$$

Integration of Eq. E12 and Eq. E13 yields Eq. E14 and Eq. E15 as shown below.

$$[D] = [D]_0 e^{-k_1 t} \qquad \text{Eq. E14}$$

$$[I] = [D]_0 \left(\frac{k_1}{k_2 - k_1}\right)\left(e^{-k_1 t} - e^{-k_2 t}\right) \qquad \text{Eq. E15}$$

Half-lives

The half-life ($t_{1/2}$) of a drug substance is defined as the time required for a drug to decompose to one-half of the initial concentration. We can obtain half-lives for each reaction order by substituting $t = t_{1/2}$ and $[D] = ½ [D]_0$ into the integrated rate equations (Eq. E5, E7, E11 and E14) as shown below.

Zero-order reaction: $t_{1/2} = [D]_0/2k$ Eq. E16

First-order reaction: $t_{1/2} = \ln 2/k$ Eq. E17

Second-order reaction: $t_{1/2} = 1/k[D]_0$ Eq. E18

Determination of reaction order

The order of reaction can be determined by several method as described below.

Substitution method

The data obtain from a kinetic study can be substituted in the integrated rate equations. When the equation is found in which the calculated *k* values remain constant after substituting several experimental data, the reaction is considered to be of that order.

Graphic method

A plot of the data according to the integrated rate equations can be used to ascertain the reaction order. If a straight-line is obtained when concentrations are plotted against time, the reaction is zero order. The reaction is first order if the log [D] vs time plot yields a straight line. It is considered to be second order if the 1/[D] vs time plot gives a straight line (in the case in which the initial concentrations are equal).

Half-life method

The investigation of the behavior of the $t_{1/2}$ as the reaction proceeds is another method to determine the reaction order. We can measure a series of successive $t_{1/2}$ values. T = 0 is used as the start time to measure the first $t_{1/2}$

(designated as $t_{1/2}$ (1)). Then $t_{1/2}$ (1) is used as the start time to measure the second $t_{1/2}$ (designated as $t_{1/2}$ (2)), and so on. For the zero-order reaction, the successive $t_{1/2}$ will decrease by a factor of two. For the first-order reaction, the $t_{1/2}$ is constant since it is concentration independent. In case of the second-order reaction, the successive $t_{1/2}$ will be doubled.

In this work, the graphic method was used to determine the reaction order. The experimental data from each one replicate of CDD degradation in phosphate buffer pH 7.4 and in human plasma at 37 °C was plotted according to the integrated rate equations. The plots are shown below.

Zero-order

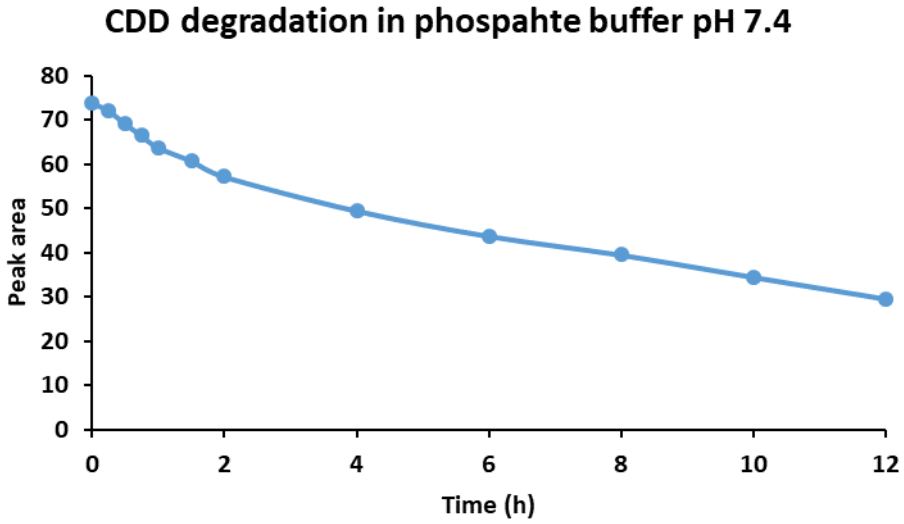

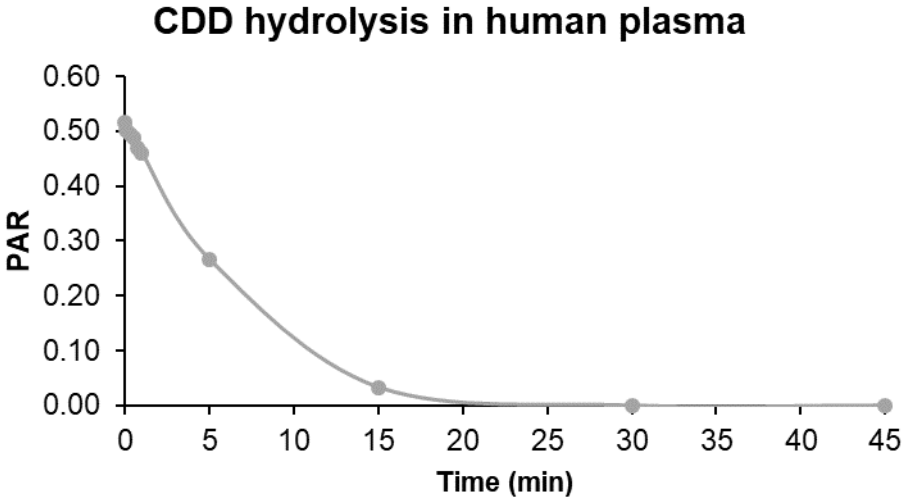

Pseudo-first order

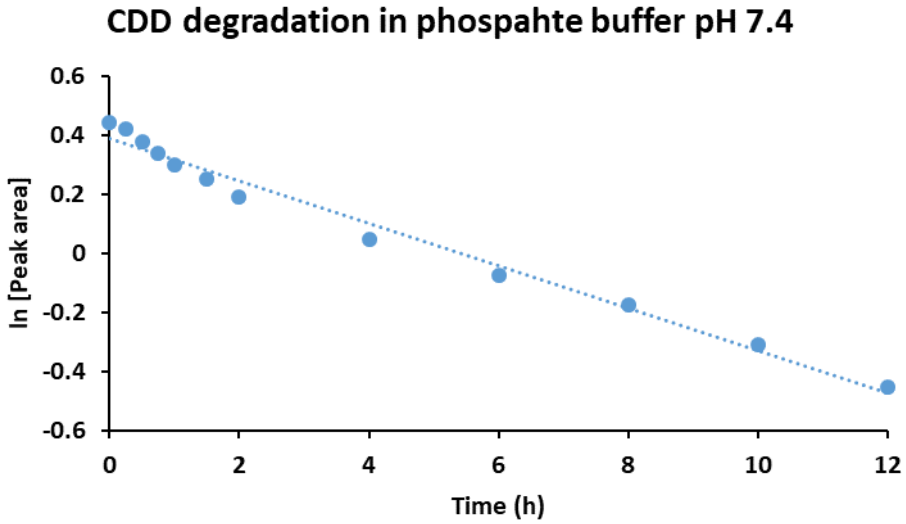

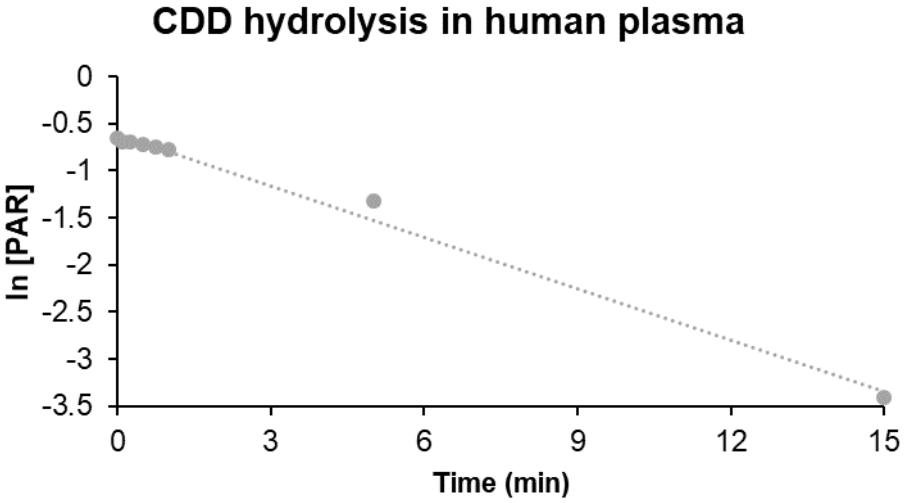

Second-order

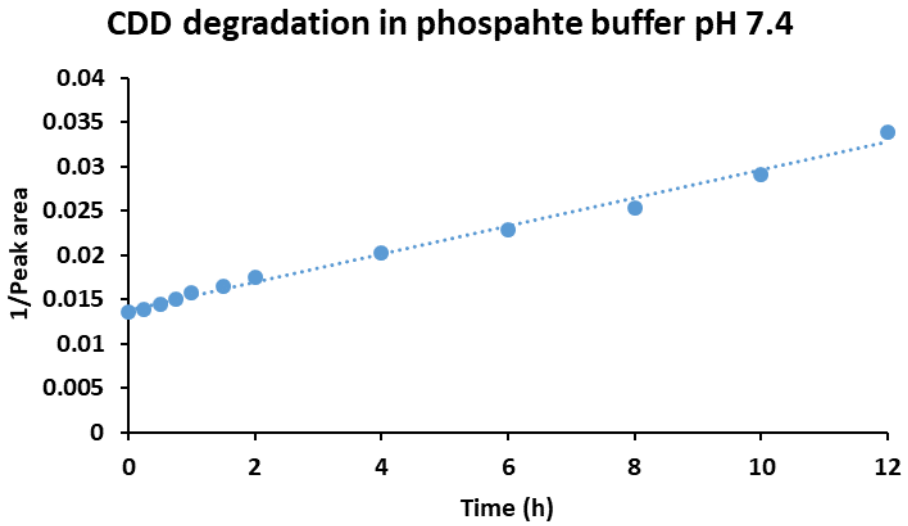

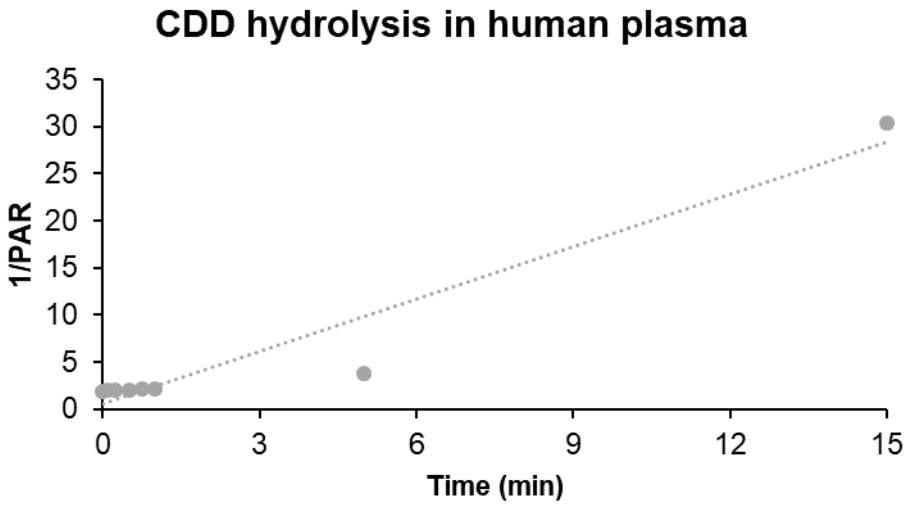

From the plots above, it is clearly seen that the hydrolysis of CDD in plasma follows pseudo-1st order reaction. However, the HPLC chromatograms show that CDD was converted to an intermediate MSCUR (M2) which was subsequently converted to CUR (M1). Therefore, the data from plasma metabolism of CDD was fitted using pseudo-first order consecutive kinetic model. For CDD stability in buffer, the experimental data was fitted to the pseudo-first order kinetic model since the CDD degradation profile in phosphate buffer pH 7.4 was similar to that of human plasma. Unfortunately, the pseudo-first order consecutive kinetic model could not be used because there was no M2 detected in the HPLC analysis.

Regression data

1. Nonlinear least square fit for CDD degradation in buffer pH 1.2

1.1 At 4 °C

- N1

Time (h)	Peak area	Fitted y	residuals	$(residuals)^2$	$(y-y_{mean})^2$	Upper CI	Lower CI
0	68.33717	68.33717	0	0	149.2869771	80.98340195	55.69093805
0.25	66.04562	67.60018269	1.554562694	2.416665168	98.54046483	80.24641464	54.95395075
0.5	65.36757	66.87114348	1.503573482	2.260733215	85.53854418	79.51737543	54.22491153
0.75	61.48628	66.14996665	4.663686648	21.74997315	28.80914378	78.7961986	53.5037347
1	58.96809	65.4365674	6.468477399	41.84119986	8.118083101	78.08279935	52.79033545
1.5	56.21416	64.03276705	7.818607051	61.13061621	0.009081137	76.678999	51.3865351
2	52.64996	62.65908221	10.00912221	100.1825274	12.0333019	75.30531416	50.01285026
4	49.5266	57.45278277	7.926182773	62.82437335	43.45795783	70.09901472	44.80655082
6	50.31995	52.67907112	2.359121125	5.565452482	33.62741518	65.32530307	40.03283918
8	48.57354	48.30200385	-0.271536152	0.073731882	56.93192936	60.9482358	35.6557719
10	48.36674	44.28862404	-4.078115961	16.63102979	60.09544202	56.93485599	31.64239209
12	47.5707	40.60871316	-6.961986842	48.46926078	73.07112487	53.25494511	27.96248121
Average	56.118865		SSR	363.1455633	649.5194652		

k_1 (h^{-1})	k_1 (min^{-1})	$t_{1/2}$ (min)	r^2	df	S.E. of y	Critical t	CI
0.043372598	0.000722877	958.8733967	0.440901185	11	5.745714318	2.20098516	12.64623195

-N2

Time (h)	Peak area	Fitted y	residuals	$(residuals)^2$	$(y-y_{mean})^2$	Upper CI	Lower CI
0	68.09438	68.09438	0	0	202.3003072	98.734391	37.454369
0.25	51.16776	66.5643614	15.3966014	237.0553347	7.308310734	97.2043724	35.9243504
0.5	47.64007	65.06872092	17.42865092	303.757873	38.82634239	95.70873192	34.42870992
0.75	45.98809	63.60668612	17.61859612	310.4149294	62.14261526	94.24669712	32.96667512
1	43.88492	62.17750191	18.29258191	334.618553	99.72476465	92.81751291	31.53749091
1.5	42.45342	59.41474935	16.96132935	287.6866932	130.3645298	90.05476035	28.77473835
2	40.43632	56.77475504	16.33843504	266.9444595	180.4946235	87.41476604	26.13474404
4	39.01706	47.33684057	8.319780571	69.21874874	220.6439526	77.97685157	16.69682957
6	37.48978	39.46783167	1.978051674	3.912688423	268.3492421	70.10784267	8.827820673
8	40.02894	32.90692235	-7.122017649	50.72313539	191.6067431	63.54693335	2.266911351
10	38.33062	27.43666152	-10.89395848	118.6783313	241.5080338	58.07667252	-3.203349478
12	35.07162	22.87574594	-12.19587406	148.739344	353.4222812	53.51575694	-7.764265058
Average	53.87114875		SSR	2131.750091	1996.691746		

k_1 (h^{-1})	k_1 (min^{-1})	$t_{1/2}$ (min)	r^2	df	S.E. of y	Critical t	CI
0.090901455	0.001515024	457.5155666	-0.067641059	11	13.92104388	2.20098516	30.640011

-N3

Time (h)	Peak area	Fitted y	residuals	$(residuals)^2$	$(y-y_{mean})^2$	Upper CI	Lower CI
0	68.39687	68.39687	0	0	700.8349069	101.6530728	35.14066717
0.25	47.98001	66.56203299	18.58202299	345.2915783	36.68030397	99.81823582	33.30583015
0.5	44.88269	64.77641792	19.89372792	395.7604104	8.756312265	98.03262075	31.52021508
0.75	43.68391	63.03870435	19.35479435	374.6080642	3.098749973	96.29490718	29.78250151
1	42.26441	61.34760725	19.08319725	364.1684174	0.116162817	94.60381009	28.09140442
1.5	41.01267	58.10029385	17.08762385	291.9868889	0.829763101	91.35649669	24.84409102
2	38.25115	55.02487052	16.77372052	281.3577	13.48676659	88.28107335	21.76866769
4	36.72406	44.26717737	7.543117366	56.8986196	27.03504289	77.5233802	11.01097453
6	36.04618	35.61267793	-0.433502069	0.187924044	34.54386994	68.86888076	2.356475098
8	36.27766	28.65018519	-7.627474809	58.17837196	31.87645029	61.90638802	-4.606017642
10	34.35772	23.04890166	-11.30881834	127.8893723	57.24228798	56.30510449	-10.20730117
12	33.20567	18.54270275	-14.66296725	215.0026086	76.00201289	51.79890558	-14.71350008
Average	41.92358333		SSR	2511.329956	990.5026296		

k_1 (h^{-1})	k_1 (min^{-1})	$t_{1/2}$ (min)	r^2	df	S.E. of y	Critical t	CI
0.108770895	0.001812848	382.3525678	-1.53540968	11	15.10968971	2.20098516	33.25620283

1.2 At 25 °C

- N1

Time (h)	Peak area	Fitted y	residuals	$(residuals)^2$	$(y-y_{mean})^2$	Upper CI	Lower CI
0	68.33717	68.33717	0	0	111.2675559	82.78622	53.88812
0.25	68.00705	66.98254	-1.02451	1.049626564	104.4120966	81.43159	52.53348
0.5	60.97424	65.65476	4.680517	21.90723852	10.14686076	80.10381	51.2057
0.75	57.72038	64.3533	6.632917	43.99558734	0.004684889	78.80235	49.90424
1	55.78149	63.07764	7.296146	53.23374005	4.029398821	77.52669	48.62858
1.5	51.35044	60.60167	9.251233	85.58531174	41.4528175	75.05073	46.15262
2	48.61093	58.2229	9.611968	92.38993712	84.23377958	72.67195	43.77384
4	41.84989	49.60559	7.755704	60.15094263	254.0496888	64.05465	35.15654
6	39.64031	42.2637	2.623387	6.882159905	329.3686421	56.71275	27.81464
8	38.20594	36.00844	-2.1975	4.829002509	383.4894339	50.45749	21.55939
10	36.96723	30.679	-6.28823	39.54188145	433.5388704	45.12805	16.22994
12	34.16946	26.13834	-8.03112	64.49890986	557.8744621	40.58739	11.68928
Average	57.78882625		SSR	474.0643377	2313.868291		

k_1 (h^{-1})	k_1 (min^{-1})	$t_{1/2}$ (min)	r^2	df	S.E. of y	Critical t	CI
0.080087557	0.001335	519.292	0.79512	11	6.564812105	2.200985	14.44905

-N2

Time (h)	Peak area	Fitted y	residuals	$(residuals)^2$	$(y-y_{mean})^2$	Upper CI	Lower CI
0	68.09438	68.09438	0	0	187.416853	76.90307559	59.28568441
0.25	69.7448	67.06738884	-2.677411155	7.168530494	235.3293295	75.87608444	58.25869325
0.5	66.24971	66.05588665	-0.193823355	0.037567493	140.3124943	74.86458224	57.24719105
0.75	64.66885	65.0596398	0.390789799	0.152716667	105.3599089	73.86833539	56.25094421
1	59.52231	64.07841823	4.556108226	20.75812217	26.19348897	72.88711382	55.26972264
1.5	57.5713	62.16014788	4.588847883	21.05752489	10.02955647	70.96884347	53.35145229
2	54.57385	60.29930344	5.725453443	32.78081713	0.028729403	69.10799903	51.49060785
4	46.9932	53.39656512	6.403365116	41.00308481	54.92518138	62.20526071	44.58786953
6	43.78029	47.28401496	3.503724962	12.27608861	112.870704	56.09271055	38.47531937
8	43.12241	41.87119651	-1.25121349	1.565535198	127.2822266	50.6798921	33.06250092
10	40.32918	37.07800826	-3.251171743	10.5701177	198.1104809	45.88670385	28.26931267
12	38.20195	32.83351829	-5.368431714	28.82005906	262.5178468	41.64221388	24.0248227
Average	54.4043525		SSR	176.1901642	1460.3768		

k_1 (h^{-1})	k_1 (min^{-1})	$t_{1/2}$ (min)	r^2	df	S.E. of y	Critical t	CI
0.060787066	0.001013118	684.1723676	0.879352942	11	4.002160374	2.20098516	8.808695591

-N3

Time (h)	Peak area	Fitted y	residuals	$(residuals)^2$	$(y-y_{mean})^2$	Upper CI	Lower CI
0	68.39687	68.39687	0	0	181.7181286	77.39872923	59.39501077
0.25	70.06159	67.43063842	-2.630951581	6.921906223	229.3712269	76.43249765	58.42877919
0.5	64.55338	66.47805664	1.924676636	3.704380152	92.86784999	75.47991587	57.4761974
0.75	63.35667	65.53893182	2.182261822	4.762266661	71.23506294	74.54079105	56.53707259
1	59.7625	64.61307387	4.850573874	23.52806691	23.48290834	73.6149331	55.61121464
1.5	57.25264	62.80041155	5.547771545	30.77776912	5.45716075	71.80227078	53.79855231
2	54.75294	61.03860185	6.285661846	39.50954484	0.026779141	70.04046108	52.03674262
4	48.73163	54.47195048	5.740320475	32.95127916	38.25364774	63.47380971	45.47009124
6	46.15014	48.61175222	2.461612216	6.059534704	76.85052872	57.61361145	39.60989299
8	44.58485	43.38200547	-1.202844529	1.44683496	106.7447137	52.3838647	34.38014624
10	41.97927	38.71488504	-3.264384959	10.65620916	167.3740763	47.71674427	29.71302581
12	39.41652	34.54986249	-4.866657505	23.68435528	240.2519633	43.55172173	25.54800326
Average	54.91658333		SSR	184.0021472	1233.634046		

k_1 (h^{-1})	k_1 (min^{-1})	$t_{1/2}$ (min)	r^2	df	S.E. of y	Critical t	CI
0.056910291	0.000948505	730.7787404	0.850845437	11	4.089922728	2.20098516	9.001859231

1.3 At 37 °C

- N1

Time (h)	Peak area	Fitted y	residuals	$(residuals)^2$	$(y-y_{mean})^2$	Upper CI	Lower CI
0	68.33717	68.33717	0	0	279.6381043	81.68579531	54.98854469
0.25	68.4119	67.15100989	-1.260890108	1.589843864	282.1430163	80.4996352	53.80238458
0.5	62.2548	65.98543852	3.730638518	13.91766375	113.2098837	79.33406383	52.63681321
0.75	56.1963	64.84009851	8.64379851	74.71525268	20.99026442	78.18872382	51.4914732
1	53.85732	63.7146387	9.857318702	97.16673199	5.028955751	77.06326401	50.36601339
1.5	55.62326	61.5219854	5.898725396	34.7949613	16.06785846	74.87061071	48.17336008
2	49.71406	59.4047893	9.690729295	93.91023427	3.612761861	72.75341461	46.05616398
4	46.36769	51.63996389	5.272273891	27.79687198	27.53202343	64.9885892	38.29133858
6	44.17933	44.89008213	0.710752135	0.505168597	55.28601584	58.23870745	31.54145682
8	40.36379	39.02248031	-1.341309692	1.799111689	126.584926	52.37110562	25.673855
10	38.36705	33.92183523	-4.445214775	19.75993439	175.5025268	47.27046054	20.57320991
12	35.70477	29.48789764	-6.216872359	38.64950192	253.1286303	42.83652295	16.13927233
Average	51.61478667		SSR	404.6052764	1358.724967		

k_1 (h^{-1})	k_1 (min^{-1})	$t_{1/2}$ (min)	r^2	df	S.E. of y	Critical t	CI
0.070039492	0.001167325	593.7911537	0.702216941	11	6.064841124	2.20098516	13.34862531

-N2

Time (h)	Peak area	Fitted y	residuals	$(residuals)^2$	$(y-y_{mean})^2$	Upper CI	Lower CI
0	68.09438	68.09438	0	0	338.6505647	81.31356061	54.87519939
0.25	64.12337	66.71054295	2.587172946	6.69346385	208.2667732	79.92972355	53.49136234
0.5	61.8474	65.3548287	3.507428696	12.30205606	147.7557143	78.5740093	52.13564809
0.75	59.20058	64.02666573	4.826085732	23.29110349	90.41463084	77.24584634	50.80748513
1	55.8461	62.72549414	6.879394144	47.32606379	37.87394173	75.94467475	49.50631354
1.5	50.9402	60.20194214	9.261742138	85.77986743	1.558205039	73.42112274	46.98276153
2	48.31324	57.77991687	9.466676869	89.61797094	1.900756245	70.99909747	44.56073626
4	42.30402	49.02781688	6.723796883	45.20944452	54.5810541	62.24699749	35.80863628
6	39.96677	41.60142414	1.634654137	2.672094148	94.57852631	54.82060474	28.38224353
8	38.47283	35.29992972	-3.172900281	10.06729619	125.8679617	48.51911032	22.08074911
10	34.466	29.95294185	-4.513058147	20.36769384	231.8286145	43.17212246	16.73376125
12	32.72814	25.41587852	-7.312261476	53.4691679	287.7698036	38.63505913	12.19669792
Average	49.69191917		SSR	396.7962222	1621.046546		

k_1 (h^{-1})	k_1 (min^{-1})	$t_{1/2}$ (min)	r^2	df	S.E. of y	Critical t	CI
0.082126714	0.001368779	506.3983309	0.755222191	11	6.006028957	2.20098516	13.21918061

-N3

Time (h)	Peak area	Fitted y	residuals	$(residuals)^2$	$(y-y_{mean})^2$	Upper CI	Lower CI
0	68.39687	68.39687	0	0	290.6059482	78.3145569	58.4791831
0.25	65.10813	67.10342227	1.995292269	3.981191241	189.2943502	77.02110917	57.18573537
0.5	64.61809	65.83443483	1.216344825	1.479494734	176.050129	75.75212172	55.91674793
0.75	59.72477	64.5894451	4.864675101	23.66506384	70.14176959	74.507132	54.6717582
1	58.16068	63.36799928	5.207319278	27.11617406	46.38942586	73.28568618	53.45031238
1.5	52.82671	60.99396681	8.167256807	66.70408375	2.181553617	70.91165371	51.07627991
2	52.73611	58.7088756	5.972765604	35.67392896	1.922128067	68.6265625	48.7911887
4	46.09917	50.39312581	4.293955806	18.43805646	27.56808278	60.31081271	40.47543891
6	41.46735	43.25525063	1.787900631	3.196588666	97.66087446	53.17293753	33.33756373
8	39.14842	37.12841141	-2.02000859	4.080434705	148.8712743	47.04609831	27.21072451
10	35.40798	31.86940114	-3.538578859	12.52154034	254.1384897	41.78708804	21.95171424
12	32.50214	27.35529721	-5.146842789	26.4899907	355.2305808	37.27298411	17.43761031
Average	51.34970167		SSR	223.3465475	1660.054607		

k_1 (h^{-1})	k_1 (min^{-1})	$t_{1/2}$ (min)	r^2	df	S.E. of y	Critical t	CI
0.076368073	0.001272801	544.5840052	0.865458313	11	4.506021703	2.20098516	9.917686899

2. Nonlinear least square fit for CDD degradation in buffer pH 4.5

2.1 At 4 °C

- N1

Time (h)	Peak area	Fitted y	residuals	$(residuals)^2$	$(y-y_{mean})^2$	Upper CI	Lower CI
0	68.33717	68.33717	0	0	176.8189408	81.36534835	55.30899165
0.25	63.71246	67.54407023	3.831610227	14.68123693	75.21430876	80.57224858	54.51589188
0.5	61.11937	66.76017492	5.640804922	31.81868017	36.96066476	79.78835327	53.73199657
0.75	59.49771	65.98537726	6.48766726	42.08982647	19.87259008	79.01355561	52.95719891
1	58.63447	65.21957166	6.585101656	43.36356382	12.92135285	78.24775001	52.1913933
1.5	55.97818	63.7145204	7.736340401	59.8509628	0.880478828	76.74269875	50.68634205
2	54.77766	62.24420073	7.466540733	55.74923052	0.068739226	75.27237908	49.21602238
4	49.10928	56.69448303	7.585203031	57.53530502	35.17156168	69.72266138	43.66630468
6	47.83472	51.63958037	3.804860367	14.47696241	51.91377823	64.66775872	38.61140202
8	48.42147	47.03537484	-1.386095165	1.921259805	43.80284352	60.06355319	34.00719648
10	47.63309	42.8416821	-4.791407899	22.95758965	54.85997025	55.86986045	29.81350375
12	45.42252	39.02190068	-6.400619321	40.96792769	92.49287604	52.05007903	25.99372233
Average	55.03984		SSR	385.4125453	600.978105		

k_1 (h^{-1})	k_1 (min^{-1})	$t_{1/2}$ (min)	r^2	df	S.E. of y	Critical t	CI
0.046694233	0.000778	890.6631	0.358691	11	5.919248611	2.200985	13.02818

-N2

Time (h)	Peak area	Fitted y	residuals	$(residuals)^2$	$(y-y_{mean})^2$	Upper CI	Lower CI
0	68.09438	68.09438	0	0	202.3003072	90.34708	45.84168
0.25	57.51683	66.72852	9.211691305	84.8552567	13.29099178	88.98122	44.47582
0.5	53.84418	65.39006	11.54587944	133.307332	0.000727313	87.64276	43.13736
0.75	52.39439	64.07844	11.68405486	136.517138	2.180816406	86.33114	41.82575
1	50.94657	62.79314	11.84656907	140.3411987	8.553160865	85.04584	40.54044
1.5	47.97346	60.29935	12.32589358	151.9276524	34.78273259	82.55205	38.04666
2	45.39706	57.90461	12.50754702	156.4387325	71.81018014	80.15731	35.65191
4	39.61835	49.23965	9.62130112	92.56943523	203.1422722	71.49235	26.98695
6	38.70003	41.87134	3.171305755	10.05718019	230.1628441	64.12403	19.61864
8	38.79713	35.60563	-3.191500837	10.18567759	227.2260413	57.85833	13.35293
10	38.86262	30.27753	-8.585085136	73.7036868	225.2559352	52.53023	8.024837
12	37.34435	25.74675	-11.59760324	134.5044008	273.1350769	47.99944	3.494049
Average	53.87115		SSR	1124.407691	1491.841086		

k_1 (h^{-1})	k_1 (min^{-1})	$t_{1/2}$ (min)	r^2	df	S.E. of y	Critical t	CI
0.081049	0.001351	513.1328	0.246295265	11	10.11033536	2.200985	22.2527

-N3

Time (h)	Peak area	Fitted y	residuals	$(residuals)^2$	$(y-y_{mean})^2$	Upper CI	Lower CI
0	68.39687	68.39687	0	0	382.1818099	86.29958	50.49416
0.25	60.63103	67.04115	6.410118	41.08961041	138.8539556	84.94385	49.13844
0.5	57.7391	65.7123	7.973198	63.57188558	79.06234371	83.615	47.80959
0.75	55.1683	64.40979	9.241488	85.40509605	39.95378734	82.31249	46.50708
1	52.18561	63.1331	10.94749	119.8474312	11.14365157	81.0358	45.23039
1.5	49.95968	60.65513	10.69545	114.3925625	1.237168652	78.55783	42.75242
2	48.37504	58.27442	9.899377	97.99765923	0.223123182	76.17712	40.37171
4	43.00564	49.65004	6.644405	44.14811186	34.12615016	67.55275	31.74734
6	39.26008	42.30204	3.041964	9.25354335	91.9166888	60.20475	24.39934
8	38.19254	36.04152	-2.15102	4.626901754	113.5260239	53.94422	18.13881
10	36.32924	30.70752	-5.62172	31.6037189	156.7043089	48.61023	12.80482
12	36.92566	26.16294	-10.7627	115.8362369	142.1278648	44.06564	8.26023
Average	48.8474		SSR	727.7727578	1191.056876		

k_1 (h^{-1})	k_1 (min^{-1})	$t_{1/2}$ (min)	r^2	df	S.E. of y	Critical t	CI
0.080082	0.001335	519.3284	0.388969	11	8.133951057	2.200985	17.90271

2.2 At 25 °C

- N1

Time (h)	Peak area	Fitted y	residuals	$(residuals)^2$	$(y-y_{mean})^2$	Upper CI	Lower CI
0	68.33717	68.33717	0	0	111.2675559	75.85681	60.81753
0.25	67.58383	66.6848	-0.89903	0.808259238	95.94209846	74.20444	59.16515
0.5	61.63008	65.07238	3.442299	11.84942304	14.75523037	72.59202	57.55273
0.75	59.87823	63.49895	3.620718	13.10960153	4.365608031	71.01859	55.9793
1	56.72897	61.96356	5.234593	27.40096113	1.123295271	69.48321	54.44392
1.5	54.49985	59.00327	4.503419	20.28078534	10.81736477	66.52291	51.48363
2	52.01911	56.1844	4.165293	17.34966675	33.28962561	63.70405	48.66476
4	48.13458	46.19283	-1.94175	3.770400044	93.20447066	53.71247	38.67318
6	34.73288	37.97811	3.245229	10.5315103	531.5766575	45.49775	30.45846
8	32.50729	31.22426	-1.28303	1.646172981	639.1560752	38.7439	23.70461
10	27.29164	25.67148	-1.62016	2.624920099	930.0783692	33.19112	18.15184
12	25.46792	21.10618	-4.36174	19.0247578	1044.640981	28.62583	13.58654
Average	57.78883		SSR	128.3964583	3510.217332		

k_1 (h^{-1})	k_1 (min^{-1})	$t_{1/2}$ (min)	r^2	df	S.E. of y	Critical t	CI
0.097907321	0.001632	424.7775	0.963422	11	3.416490201	2.200985	7.519644

-N2

Time (h)	Peak area	Fitted y	residuals	$(residuals)^2$	$(y-y_{mean})^2$	Upper CI	Lower CI
0	68.09438	68.09438	0	0	74.57304044	75.70449	60.48427
0.25	74.56104	67.28634	-7.274700937	52.92127372	228.0773006	74.89645	59.67623
0.5	71.33754	66.48789	-4.849653269	23.51913683	141.1041868	74.098	58.87778
0.75	70.01279	65.69891	-4.313880778	18.60956736	111.3864587	73.30902	58.0888
1	69.24441	64.91929	-4.325115897	18.70662752	95.75793474	72.5294	57.30919
1.5	66.56699	63.38771	-3.179282042	10.1078343	50.52619922	70.99782	55.7776
2	63.06317	61.89226	-1.170914767	1.371041392	12.991399	69.50236	54.28215
4	54.82068	56.25503	1.434348062	2.057354364	21.51226536	63.86514	48.64492
6	49.67778	51.13125	1.45346688	2.112565972	95.66858046	58.74136	43.52114
8	47.06459	46.47415	-0.590443642	0.348623694	153.6167307	54.08425	38.86404
10	40.94809	42.24122	1.293130613	1.672186783	342.6468166	49.85133	34.63111
12	38.11428	38.39384	0.279555255	0.078151141	455.5890321	46.00394	30.78373
Average	59.45881167		SSR	131.5043631	1783.449945		

k_1 (h^{-1})	k_1 (min^{-1})	$t_{1/2}$ (min)	r^2	df	S.E. of y	Critical t	CI
0.04775	0.000796	870.9737	0.926264057	11	3.457591951	2.200985	7.610109

-N3

Time (h)	Peak area	Fitted y	residuals	$(residuals)^2$	$(y-y_{mean})^2$	Upper CI	Lower CI
0	68.39687	68.39687	0	0	497.2306466	85.48618	51.30756
0.25	58.38123	66.66955	8.288318	68.69621067	150.8728055	83.75886	49.58023
0.5	52.72954	64.98585	12.25631	150.2170844	43.97465914	82.07516	47.89654
0.75	54.92017	63.34467	8.424499	70.97218338	77.82713998	80.43398	46.25536
1	52.86983	61.74494	8.875107	78.7675252	45.85496157	78.83425	44.65562
1.5	49.33902	58.66565	9.326634	86.98609643	10.50290887	75.75497	41.57634
2	46.56417	55.73994	9.175767	84.19470725	0.217127264	72.82925	38.65062
4	41.35854	45.42519	4.066647	16.53761909	22.46438482	62.5145	28.33587
6	37.7302	37.0192	-0.711	0.50552769	70.02343795	54.10851	19.92988
8	31.91294	30.16874	-1.7442	3.042221386	201.2216249	47.25806	13.07943
10	31.43766	24.58598	-6.85168	46.94555954	214.9314575	41.67529	7.496664
12	27.53824	20.03631	-7.50193	56.27896909	344.4721461	37.12562	2.946996
Average	46.0982		SSR	663.1437041	1679.5933		

k_1 (h^{-1})	k_1 (min^{-1})	$t_{1/2}$ (min)	r^2	df	S.E. of y	Critical t	CI
0.102315	0.001705	406.478	0.605176	11	7.764392525	2.200985	17.08931

2.3 At 37 °C

- N1

Time (h)	Peak area	Fitted y	residuals	$(residuals)^2$	$(y-y_{mean})^2$	Upper CI	Lower CI
0	68.33717	68.33717	0	0	563.7573934	79.49786	57.17648
0.25	63.36343	66.11789	2.754456	7.587028358	352.3067372	77.27858	54.95719
0.5	60.00236	63.97067	3.968315	15.7475203	237.4300645	75.13137	52.80998
0.75	56.37757	61.89319	5.515625	30.42211655	138.8620864	73.05389	50.7325
1	54.08299	59.88318	5.800192	33.64222941	90.04863328	71.04388	48.72249
1.5	48.38842	56.05687	7.668446	58.80505883	14.40070311	67.21756	44.89617
2	45.53041	52.47504	6.944627	48.22784106	0.877623906	63.63573	41.31434
4	37.3297	40.29475	2.965054	8.791547863	52.76415846	51.45545	29.13406
6	30.75439	30.94171	0.187317	0.035087823	191.523572	42.1024	19.78101
8	26.90997	23.75965	-3.15032	9.924516599	312.7105637	34.92034	12.59896
10	23.88759	18.24466	-5.64293	31.8426472	428.7386086	29.40535	7.083967
12	20.15913	14.00979	-6.14934	37.81440792	597.0430391	25.17048	2.849094
Average	44.59359		SSR	282.8400019	2980.463184		

k_1 (h^{-1})	k_1 (min^{-1})	$t_{1/2}$ (min)	r^2	df	S.E. of y	Critical t	CI
0.132058134	0.002201	314.9282	0.905102	11	5.070771879	2.200985	11.16069

-N2

Time (h)	Peak area	Fitted y	residuals	(residuals)^2	(y-y_{mean})^2	Upper CI	Lower CI
0	68.09438	68.09438	0	0	985.8742799	85.08986	51.0989
0.25	55.73534	63.91092	8.175581224	66.84012835	362.5061778	80.9064	46.91544
0.5	52.39644	59.98448	7.588038186	57.57832351	246.5118235	76.97996	42.989
0.75	51.40988	56.29926	4.88938082	23.9060448	216.5057688	73.29474	39.30378
1	46.91708	52.84045	5.923369142	35.08630199	104.4756892	69.83593	35.84497
1.5	41.61084	46.54726	4.93641939	24.36823639	24.15815886	63.54274	29.55178
2	31.69317	41.00358	9.310405706	86.68365441	25.02575663	57.99906	24.0081
4	24.43462	24.69063	0.25601116	0.065541714	150.3351863	41.68611	7.695152
6	18.63895	14.86766	-3.771288909	14.22262004	326.0478457	31.86314	-2.12782
8	17.19287	8.952681	-8.240188926	67.90071353	380.3621333	25.94816	-8.0428
10	16.46846	5.390929	-11.07753147	122.7117034	409.1430585	22.38641	-11.6046
12	15.75691	3.246191	-12.51071925	156.5180962	438.4348112	20.24167	-13.7493
Average	36.69575		SSR	655.8813643	3669.380689		

k_1 (h^{-1})	k_1 (min^{-1})	$t_{1/2}$ (min)	r^2	df	S.E. of y	Critical t	CI
0.253618	0.004227	163.9824	0.821255569	11	7.72176007	2.200985	16.99548

-N3

Time (h)	Peak area	Fitted y	residuals	(residuals)^2	(y-y_{mean})^2	Upper CI	Lower CI
0	68.39687	68.39687	0	0	843.4030108	78.74333	58.05041
0.25	62.68659	64.84396	2.157372	4.654252196	544.3412382	75.19042	54.4975
0.5	59.01919	61.47561	2.456421	6.034002801	386.6619498	71.82207	51.12915
0.75	54.86538	58.28223	3.41685	11.67486717	240.5573599	68.62869	47.93577
1	51.53304	55.25473	3.721692	13.85099059	148.2932517	65.60119	44.90827
1.5	44.45842	49.66336	5.20494	27.09140215	26.04011571	60.00982	39.3169
2	38.91952	44.63779	5.718274	32.69865819	0.190050949	54.98425	34.29133
4	27.01843	29.13193	2.113498	4.466871697	152.2025148	39.47839	18.78547
6	20.07463	19.01235	-1.06228	1.128446594	371.7507268	29.35881	8.665886
8	15.92992	12.40801	-3.52191	12.40383428	548.7563147	22.75447	2.061552
10	15.2583	8.097831	-7.16047	51.27231613	580.6735217	18.44429	-2.24863
12	14.10533	5.284881	-8.82045	77.80032204	637.5694859	15.63134	-5.06158
Average	39.35547		SSR	243.0759638	4480.439541		

k_1 (h^{-1})	k_1 (min^{-1})	$t_{1/2}$ (min)	r^2	df	S.E. of y	Critical t	CI
0.213373	0.003556	194.9113	0.945747	11	4.700831298	2.200985	10.34646

3. Nonlinear least square fit for CDD degradation in buffer pH 6.8

3.1 At 4 °C

- N1

Time (h)	Peak area	Fitted y	residuals	$(residuals)^2$	$(y-y_{mean})^2$	Upper CI	Lower CI
0	68.33717	68.33717	0	0	104.5549877	80.07761	56.59673
0.25	61.22268	67.81654	6.593861	43.47900478	9.676599657	79.55698	56.0761
0.5	60.79558	67.29988	6.504299	42.30590177	7.201834195	79.04032	55.55944
0.75	58.98985	66.78715	7.797302	60.79792619	0.770696705	78.52759	55.04671
1	58.42898	66.27833	7.849352	61.61233459	0.100503794	78.01877	54.53789
1.5	59.5471	65.27229	5.725192	32.7778274	2.059636387	77.01273	53.53185
2	57.00403	64.28152	7.277493	52.96190291	1.227501499	76.02196	52.54108
4	58.00946	60.46657	2.457109	6.037383294	0.010505567	72.20701	48.72613
6	58.26561	56.87802	-1.38759	1.925397874	0.023609347	68.61846	45.13758
8	54.9928	53.50245	-1.49035	2.221146939	9.729138311	65.24289	41.76201
10	51.85126	50.32721	-1.52405	2.32273834	39.19632275	62.06765	38.58676
12	49.89896	47.34041	-2.55855	6.546189596	67.45331425	59.08085	35.59997
Average	58.11196		SSR	312.9877537	242.0046502		

k_1 (h^{-1})	k_1 (min^{-1})	$t_{1/2}$ (min)	r^2	df	S.E. of y	Critical t	CI
0.030590801	0.00051	1359.521	-0.29331	11	5.334175864	2.200985	11.74044

-N2

Time (h)	Peak area	Fitted y	residuals	$(residuals)^2$	$(y-y_{mean})^2$	Upper CI	Lower CI
0	68.09438	68.09438	0	0	202.3003072	83.37326	52.8155
0.25	61.64977	67.2564	5.606625232	31.43424649	60.50694855	82.53527	51.97752
0.5	59.13571	66.42872	7.293012893	53.18803705	27.71560516	81.7076	51.14984
0.75	56.11439	65.61124	9.496846076	90.19008538	5.032131306	80.89011	50.33236
1	54.84898	64.80381	9.954829435	99.09862909	0.956153953	80.08269	49.52493
1.5	53.6996	63.21864	9.519042997	90.61217959	0.029428974	78.49752	47.93976
2	53.1065	61.67225	8.565751327	73.3720958	0.584687711	76.95113	46.39337
4	51.90812	55.85581	3.947687539	15.5842369	3.853481873	71.13469	40.57693
6	48.09169	50.58793	2.49623518	6.231190073	33.40214344	65.8668	35.30905
8	45.58398	45.81687	0.232888232	0.054236929	68.67716589	61.09575	30.53799
10	46.87501	41.49578	-5.379229987	28.93611525	48.94595741	56.77466	26.2169
12	44.01487	37.58222	-6.432647003	41.37894747	97.1462308	52.8611	22.30334
Average	53.87115		SSR	530.08	549.1502423		

k_1 (h^{-1})	k_1 (min^{-1})	$t_{1/2}$ (min)	r^2	df	S.E. of y	Critical t	CI
0.04953	0.000826	839.6645	0.034726821	11	6.941836278	2.200985	15.27888

-N3

Time (h)	Peak area	Fitted y	residuals	$(residuals)^2$	$(y-y_{mean})^2$	Upper CI	Lower CI
0	68.39687	68.39687	0	0	446.6262664	91.60786	45.18588
0.25	53.11312	67.02662	13.9135	193.5855251	34.2199748	90.23761	43.81563
0.5	54.78186	65.68382	10.90196	118.8528266	56.52820564	88.89482	42.47283
0.75	51.39963	64.36793	12.9683	168.1767652	17.10892943	87.57892	41.15694
1	49.69992	63.07839	13.37847	178.9835926	5.936942401	86.28939	39.8674
1.5	47.96242	60.57631	12.61389	159.1103003	0.488718672	83.78731	37.36532
2	46.20586	58.17348	11.96762	143.2239156	1.118255138	81.38447	34.96249
4	41.26018	49.4782	8.218016	67.5357805	36.03787996	72.68919	26.2672
6	40.34297	42.08261	1.73964	3.026346846	47.89146327	65.2936	18.87162
8	39.34819	35.79245	-3.55574	12.64325671	62.64953356	59.00345	12.58146
10	37.30932	30.4425	-6.86682	47.15323953	99.08243121	53.65349	7.231506
12	37.33969	25.89221	-11.4475	131.0448213	98.47874663	49.1032	2.681216
Average	47.26334		SSR	1223.33637	906.1673471		

k_1 (h^{-1})	k_1 (min^{-1})	$t_{1/2}$ (min)	r^2	df	S.E. of y	Critical t	CI
0.080949	0.001349	513.7675	-0.35001	11	10.54572886	2.200985	23.21099

3.2 At 25 °C

- N1

Time (h)	Peak area	Fitted y	residuals	$(residuals)^2$	$(y-y_{mean})^2$	Upper CI	Lower CI
0	68.33717	68.33717	0	0	111.2675559	75.50789	61.16645
0.25	65.51501	67.41588	1.900875	3.613325631	59.69391534	74.5866	60.24517
0.5	64.67902	66.50702	1.828	3.34158473	47.47476991	73.67774	59.3363
0.75	61.0943	65.61041	4.516108	20.39523383	10.92615671	72.78113	58.43969
1	60.39057	64.72588	4.335314	18.79494716	6.769070541	71.8966	57.55517
1.5	59.55582	62.99245	3.436629	11.81041649	3.122266913	70.16317	55.82173
2	55.5489	61.30544	5.756537	33.13771565	5.017269605	68.47615	54.13472
4	52.01482	54.99725	2.982432	8.89490228	33.33914818	62.16797	47.82653
6	50.0465	49.33817	-0.70833	0.501738407	59.94361576	56.50888	42.16745
8	43.97814	44.26138	0.283245	0.080227454	190.7350547	51.4321	37.09067
10	41.1268	39.70699	-1.41981	2.015852788	277.6231188	46.87771	32.53628
12	39.38571	35.62124	-3.76447	14.17125679	338.6746877	42.79195	28.45052
Average	57.78883		SSR	116.7572012	1144.58663		

k_1 (h^{-1})	k_1 (min^{-1})	$t_{1/2}$ (min)	r^2	df	S.E. of y	Critical t	CI
0.054292652	0.000905	766.0121	0.897992	11	3.257958106	2.200985	7.170717

-N2

Time (h)	Peak area	Fitted y	residuals	(residuals)^2	(y-y_{mean})^2	Upper CI	Lower CI
0	68.09438	68.09438	0	0	92.73494191	77.88468	58.30408
0.25	71.38478	67.20302	-4.181757203	17.4870933	166.934109	76.99332	57.41273
0.5	75.42906	66.32333	-9.105726516	82.91425539	287.796918	76.11363	56.53304
0.75	69.41258	65.45516	-3.957420674	15.66117839	119.8608571	75.24546	55.66486
1	68.57833	64.59835	-3.979980409	15.84024406	102.2899281	74.38865	54.80805
1.5	67.37862	62.91823	-4.460389708	19.89507635	79.46186223	72.70853	53.12793
2	63.1607	61.28181	-1.878891283	3.530232455	22.05446663	71.07211	51.49151
4	49.48925	55.15081	5.661558034	32.05323937	80.55478347	64.94111	45.36051
6	45.43009	49.63319	4.203099531	17.66604567	169.8953661	59.42349	39.84289
8	43.70438	44.66759	0.963206764	0.927767271	217.8606012	54.45788	34.87729
10	39.929	40.19877	0.269772761	0.072777343	343.5640806	49.98907	30.40848
12	39.58261	36.17705	-3.405564215	11.59786762	356.5250776	45.96734	26.38675
Average	58.46448		SSR	217.6457772	2039.532992		

k_1 (h^{-1})	k_1 (min^{-1})	$t_{1/2}$ (min)	r^2	df	S.E. of y	Critical t	CI
0.052706	0.000878	789.0747	0.893286464	11	4.448143404	2.200985	9.790298

-N3

Time (h)	Peak area	Fitted y	residuals	(residuals)^2	(y-y_{mean})^2	Upper CI	Lower CI
0	70.35748	70.35748	0	0	266.7643574	78.30527	62.40969
0.25	69.45016	69.07496	-0.375198576	0.140773972	237.9492125	77.02275	61.12717
0.5	68.09438	67.81582	-0.278558631	0.077594911	197.9599052	75.76361	59.86803
0.75	64.14456	66.57963	2.435073679	5.929583825	102.4144506	74.52742	58.63184
1	62.60388	65.36598	2.762099964	7.629196212	73.60477456	73.31377	57.41819
1.5	56.72356	63.00464	6.281078894	39.45195207	7.284614495	70.95243	55.05685
2	54.48803	60.7286	6.240571091	38.94472754	0.214806758	68.67639	52.78081
4	48.55717	52.4175	3.86032691	14.90212385	29.89232608	60.36529	44.46971
6	42.91167	45.24382	2.33215141	5.438930201	123.4962686	53.19161	37.29603
8	40.7005	39.05191	-1.648589922	2.717848731	177.5305083	46.9997	31.10412
10	37.01188	33.7074	-3.304477902	10.91957421	289.4311957	41.65519	25.75961
12	33.25142	29.09432	-4.157095192	17.28144043	431.5232416	37.04212	21.14653
Average	54.02456		SSR	143.433746	1938.065662		

k_1 (h^{-1})	k_1 (min^{-1})	$t_{1/2}$ (min)	r^2	df	S.E. of y	Critical t	CI
0.073587	0.001226	565.1642	0.925991287	11	3.611015294	2.200985	7.947791

3.3 At 37 °C

- N1

Time (h)	Peak area	Fitted y	residuals	$(residuals)^2$	$(y-y_{mean})^2$	Upper CI	Lower CI
0	68.33717	68.33717	0	0	644.4041905	91.04498	45.62936
0.25	47.82521	66.31013	18.48492	341.6923762	23.74766402	89.01795	43.60232
0.5	50.45372	64.34322	13.8895	192.9182784	56.27501528	87.05104	41.63541
0.75	48.75278	62.43466	13.68188	187.1937044	33.64843953	85.14247	39.72684
1	49.02922	60.5827	11.55348	133.4829023	36.93196482	83.29051	37.87489
1.5	47.43581	57.04196	9.60615	92.27812662	20.10408132	79.74977	34.33415
2	48.22817	53.70816	5.479988	30.03027284	27.83741587	76.41597	31.00034
4	40.56435	42.2108	1.646445	2.710781368	5.701123229	64.91861	19.50298
6	30.65673	33.17468	2.517955	6.340095848	151.1749554	55.8825	10.46687
8	29.23918	26.07294	-3.16624	10.02504912	188.0428722	48.78076	3.365131
10	27.82163	20.49148	-7.33015	53.73108511	228.929685	43.19929	-2.21633
12	27.08066	16.10485	-10.9758	120.468459	251.9010999	38.81266	-6.60297
Average	42.95205		SSR	1170.871131	1668.698507		

k_1 (h^{-1})	k_1 (min^{-1})	$t_{1/2}$ (min)	r^2	df	S.E. of y	Critical t	CI
0.12044446	0.002007	345.2947	0.298333	11	10.31711346	2.200985	22.70781

-N2

Time (h)	Peak area	Fitted y	residuals	$(residuals)^2$	$(y-y_{mean})^2$	Upper CI	Lower CI
0	68.09438	68.09438	0	0	92.73494191	77.88468	58.30408
0.25	71.38478	67.20302	-4.181757203	17.4870933	166.934109	76.99332	57.41273
0.5	75.42906	66.32333	-9.105726516	82.91425539	287.796918	76.11363	56.53304
0.75	69.41258	65.45516	-3.957420674	15.66117839	119.8608571	75.24546	55.66486
1	68.57833	64.59835	-3.979980409	15.84024406	102.2899281	74.38865	54.80805
1.5	67.37862	62.91823	-4.460389708	19.89507635	79.46186223	72.70853	53.12793
2	63.1607	61.28181	-1.878891283	3.530232455	22.05446663	71.07211	51.49151
4	49.48925	55.15081	5.661558034	32.05323937	80.55478347	64.94111	45.36051
6	45.43009	49.63319	4.203099531	17.66604567	169.8953661	59.42349	39.84289
8	43.70438	44.66759	0.963206764	0.927767271	217.8606012	54.45788	34.87729
10	39.929	40.19877	0.269772761	0.072777343	343.5640806	49.98907	30.40848
12	39.58261	36.17705	-3.405564215	11.59786762	356.5250776	45.96734	26.38675
Average	58.46448		SSR	217.6457772	2039.532992		

k_1 (h^{-1})	k_1 (min^{-1})	$t_{1/2}$ (min)	r^2	df	S.E. of y	Critical t	CI
0.052706	0.000878	789.0747	0.893286464	11	4.448143404	2.200985	9.790298

-N3

Time (h)	Peak area	Fitted y	residuals	(residuals)^2	(y-y_{mean})^2	Upper CI	Lower CI
0	68.39687	68.39687	0	0	301.5589405	74.18128	62.61246
0.25	68.24192	66.86428	-1.37764	1.897905205	296.2013963	72.64869	61.07986
0.5	65.70121	65.36602	-0.33519	0.112351109	215.202812	71.15044	59.58161
0.75	64.51682	63.90134	-0.61548	0.378815139	181.8560806	69.68575	58.11693
1	61.87665	62.46948	0.592829	0.351445803	117.619068	68.25389	56.68506
1.5	59.34986	59.70129	0.351429	0.123502365	69.19648563	65.4857	53.91687
2	53.57696	57.05577	3.478805	12.10208634	6.479786619	62.84018	51.27135
4	43.06326	47.59517	4.531906	20.5381684	63.49153394	53.37958	41.81075
6	36.13161	39.70326	3.571648	12.75667176	222.0042635	45.48767	33.91884
8	34.92791	33.11993	-1.80798	3.268778878	259.3229538	38.90435	27.33552
10	28.72591	27.62821	-1.0977	1.204943131	497.5356648	33.41263	21.8438
12	27.86803	23.04709	-4.82094	23.24147615	536.5425205	28.8315	17.26267
Average	51.03142		SSR	75.97614428	2767.011506		

k_1 (h^{-1})	k_1 (min^{-1})	$t_{1/2}$ (min)	r^2	df	S.E. of y	Critical t	CI
0.090649	0.001511	458.7899	0.972542	11	2.628102397	2.200985	5.784414

4. Nonlinear least square fit for CDD degradation in buffer pH 7.4

4.1 At 4 °C

- N1

Time (h)	Peak area	Fitted y	residuals	(residuals)^2	(y-y_{mean})^2	Upper CI	Lower CI
0	57.88861	57.88861	0	0	30.1597391	60.89246	54.88476
0.25	57.24206	57.54243	0.300373	0.09022377	23.47633451	60.54628	54.53859
0.5	56.59551	57.19833	0.602816	0.363386645	17.62898372	60.20217	54.19448
0.75	55.09264	56.85628	1.763636	3.110412848	7.267436486	59.86012	53.85243
1	54.18562	56.51627	2.330652	5.431940573	3.199799477	59.52012	53.51243
1.5	54.96421	55.84235	0.878142	0.771133779	6.591482854	58.8462	52.83851
2	54.00526	55.17647	1.171208	1.371728497	2.587073872	58.18031	52.17262
4	50.68815	52.59139	1.903243	3.622333733	2.919558864	55.59524	49.58755
6	49.41138	50.12743	0.716051	0.51272938	8.912861945	53.13128	47.12358
8	47.71368	47.77891	0.065229	0.004254785	21.93181587	50.78276	44.77506
10	45.29817	45.54042	0.242247	0.058683568	50.39085548	48.54426	42.53657
12	45.67657	43.4068	-2.26977	5.151852223	45.16178246	46.41065	40.40295
Average	52.39682		SSR	20.4886798	220.2277246		

k_1 (h^{-1})	k_1 (min^{-1})	$t_{1/2}$ (min)	r^2	df	S.E. of y	Critical t	CI
0.023992043	0.0004	1733.443	0.906966	11	1.364773701	2.200985	3.003847

-N2

Time (h)	Peak area	Fitted y	residuals	$(residuals)^2$	$(y-y_{mean})^2$	Upper CI	Lower CI
0	55.54993	55.54993	0	0	2.818306485	60.70762	50.39224
0.25	55.24676	55.41123	0.164473624	0.027051573	1.892292555	60.56892	50.25353
0.5	54.94358	55.27287	0.329293568	0.108434254	1.150108786	60.43057	50.11518
0.75	55.34921	55.13486	-0.214346032	0.045944221	2.184665059	60.29256	49.97717
1	54.86853	54.9972	0.128668961	0.016555702	0.994769358	60.15489	49.8395
1.5	54.99445	54.7229	-0.271550713	0.07373979	1.261805698	59.88059	49.5652
2	55.45467	54.44997	-1.004702312	1.009426735	2.507539549	59.60766	49.29227
4	56.04642	53.37179	-2.67463391	7.153666554	4.731805011	58.52948	48.21409
6	56.63817	52.31495	-4.323216083	18.6901973	7.656406598	57.47265	47.15726
8	54.54349	51.27905	-3.264441576	10.65657881	0.452042756	56.43674	46.12135
10	47.11646	50.26366	3.147195233	9.904837836	45.62582011	55.42135	45.10596
12	45.70212	49.26837	3.566248175	12.71812605	66.73303072	54.42606	44.11067
Average	53.87115		SSR	60.40455882	138.0085927		

k_1 (h^{-1})	k_1 (min^{-1})	$t_{1/2}$ (min)	r^2	df	S.E. of y	Critical t	CI
0.01	0.000167	4158.883	0.562313059	11	2.34335732	2.200985	5.157695

-N3

Time (h)	Peak area	Fitted y	residuals	$(residuals)^2$	$(y-y_{mean})^2$	Upper CI	Lower CI
0	55.44595	55.44595	0	0	0.543557837	57.7977	53.0942
0.25	55.82203	55.44595	-0.37607	0.141432406	0.130457313	57.7977	53.0942
0.5	56.1981	55.44595	-0.75215	0.565729622	0.0002216	57.7977	53.0942
0.75	56.33485	55.44595	-0.8889	0.79014321	0.022993552	57.7977	53.0942
1	56.38879	55.44595	-0.94284	0.888947266	0.042261595	57.7977	53.0942
1.5	57.26337	55.44595	-1.81742	3.303015456	1.166737524	57.7977	53.0942
2	56.92162	55.44595	-1.47567	2.177601949	0.54524379	57.7977	53.0942
4	57.54261	55.44595	-2.09666	4.395983156	1.847958165	57.7977	53.0942
6	55.61992	55.44595	-0.17397	0.030265561	0.317299849	57.7977	53.0942
8	55.90579	55.44595	-0.45984	0.211452826	0.076963937	57.7977	53.0942
10	55.22817	55.44595	0.21778	0.047428128	0.912108564	57.7977	53.0942
12	55.52737	55.44595	-0.08142	0.006629216	0.430131024	57.7977	53.0942
Average	56.18321		SSR	12.5586288	6.035934751		

k_1 (h^{-1})	k_1 (min^{-1})	$t_{1/2}$ (min)	r^2	df	S.E. of y	Critical t	CI
0	0	#DIV/0!	-1.08064	11	1.068500598	2.200985	2.351754

4.2 At 25 °C

- N1

Time (h)	Peak area	Fitted y	residuals	$(residuals)^2$	$(y-y_{mean})^2$	Upper CI	Lower CI
0	76.06856	76.06856	0	0	334.148666	89.87435	62.26277
0.25	74.85634	74.80509	-0.05124	0.002625675	291.2998549	88.61089	60.9993
0.5	73.64411	73.56261	-0.0815	0.00664177	251.3900228	87.36841	59.75682
0.75	73.36657	72.34077	-1.0258	1.052267048	242.6661003	86.14656	58.53498
1	57.61312	71.13922	13.5261	182.9553807	0.030872686	84.94501	57.33343
1.5	60.23335	68.79566	8.562312	73.3131783	5.975696364	82.60146	54.98987
2	58.46299	66.52931	8.066318	65.06547808	0.454496762	80.3351	52.72351
4	49.74061	58.18631	8.445699	71.32983597	64.77378481	71.9921	44.38052
6	46.58324	50.88955	4.306311	18.54431416	125.5651632	64.69535	37.08376
8	43.94652	44.50783	0.561311	0.31506963	191.6094423	58.31362	30.70204
10	40.83579	38.9264	-1.90939	3.645772344	287.4054381	52.73219	25.12061
12	38.11472	34.0449	-4.06982	16.56344773	387.0704567	47.85069	20.2391
Average	57.78883		SSR	432.7940114	2182.389995		

k_1 (h^{-1})	k_1 (min^{-1})	$t_{1/2}$ (min)	r^2	df	S.E. of y	Critical t	CI
0.066996237	0.001117	620.7637	0.801688	11	6.272552123	2.200985	13.80579

-N2

Time (h)	Peak area	Fitted y	residuals	$(residuals)^2$	$(y-y_{mean})^2$	Upper CI	Lower CI
0	76.76169	76.76169	0	0	182.2862268	86.55589	66.96749
0.25	74.66356	75.65793	0.994374914	0.988781469	130.0332363	85.45214	65.86373
0.5	72.56543	74.57005	2.004620704	4.018504168	86.58454482	84.36425	64.77585
0.75	74.90422	73.49781	-1.406410836	1.97799144	135.5797474	83.29201	63.70361
1	73.58074	72.44099	-1.139754633	1.299040623	106.5104842	82.23519	62.64678
1.5	72.1998	70.37271	-1.827092574	3.338267275	79.9137961	80.16691	60.5785
2	70.10004	68.36348	-1.736558673	3.015636025	46.7813821	78.15768	58.56928
4	68.11028	60.88409	-7.226190826	52.21783385	23.52183717	70.67829	51.08989
6	43.00872	54.22299	11.21426927	125.7598353	410.1284502	64.01719	44.42879
8	50.53413	48.29066	-2.243474667	5.03317858	161.9566331	58.08486	38.49645
10	46.79959	43.00736	-3.792234193	14.38104018	270.9565649	52.80156	33.21315
12	35.89598	38.30208	2.406102271	5.789328136	748.8086543	48.09628	28.50788
Average	63.26035		SSR	217.8194371	2383.061557		

k_1 (h^{-1})	k_1 (min^{-1})	$t_{1/2}$ (min)	r^2	df	S.E. of y	Critical t	CI
0.057933	0.000966	717.8725	0.908596806	11	4.44991764	2.200985	9.794203

-N3

Time (h)	Peak area	Fitted y	residuals	$(residuals)^2$	$(y-y_{mean})^2$	Upper CI	Lower CI
0	71.22095	71.22095	0	0	163.3198162	75.19629	67.24561
0.25	70.97884	70.2097	-0.76914	0.5915757	157.1902645	74.18504	66.23436
0.5	70.73673	69.21281	-1.52392	2.322334216	151.1779473	73.18815	65.23747
0.75	67.48675	68.23007	0.743323	0.552528878	81.82042199	72.20541	64.25473
1	64.57284	67.26129	2.68845	7.227763629	37.5959565	71.23663	63.28595
1.5	65.1934	65.3648	0.171396	0.029376469	45.59104572	69.34014	61.38945
2	62.77937	63.52177	0.742405	0.551164703	18.81897424	67.49712	59.54643
4	57.96086	56.6549	-1.30596	1.7055294	0.230808981	60.63024	52.67956
6	47.08171	50.53035	3.448644	11.89314815	129.0399631	54.5057	46.55501
8	43.65551	45.06789	1.412378	1.994811147	218.619167	49.04323	41.09255
10	40.84642	40.19593	-0.65049	0.423139151	309.5793037	44.17127	36.22059
12	38.78205	35.85064	-2.93141	8.593158318	386.4855536	39.82598	31.8753
Average	58.44129		SSR	35.88452976	1699.469223		

k_1 (h^{-1})	k_1 (min^{-1})	$t_{1/2}$ (min)	r^2	df	S.E. of y	Critical t	CI
0.057202	0.000953	727.0504	0.978885	11	1.806164438	2.200985	3.975341

4.3 At 37 °C

- N1

Time (h)	Peak area	Fitted y	residuals	$(residuals)^2$	$(y-y_{mean})^2$	Upper CI	Lower CI
0	72.39754	72.39754	0	0	221.1212867	76.46728	68.3278
0.25	69.8189	71.19505	1.376148	1.893782579	151.0811566	75.26478	67.12531
0.5	68.33717	70.01253	1.675358	2.806825591	116.8512896	74.08226	65.94279
0.75	69.30591	68.84965	-0.45626	0.208173092	138.7334745	72.91939	64.77991
1	67.75488	67.70609	-0.04879	0.002380779	104.6015006	71.77582	63.63635
1.5	64.98351	65.47563	0.492117	0.242179072	55.59368817	69.54536	61.40589
2	62.71758	63.31865	0.601066	0.361280002	26.93804629	67.38838	59.24891
4	51.51907	55.37828	3.859205	14.89346501	36.09993926	59.44801	51.30854
6	48.97007	48.43365	-0.53642	0.287742315	73.22776837	52.50339	44.36392
8	45.07691	42.35991	-2.717	7.382082333	155.0145145	46.42965	38.29018
10	39.22955	37.04784	-2.18171	4.759874587	334.8110402	41.11757	32.9781
12	30.21762	32.40191	2.184293	4.771137729	745.823674	36.47165	28.33218
Average	57.52739		SSR	37.60892309	2159.897379		

k_1 (h^{-1})	k_1 (min^{-1})	$t_{1/2}$ (min)	r^2	df	S.E. of y	Critical t	CI
0.066996237	0.001117	620.7637	0.982588	11	1.849051921	2.200985	4.069736

-N2

Time (h)	Peak area	Fitted y	residuals	(residuals)^2	(y-y_{mean})^2	Upper CI	Lower CI
0	80.76463	80.76463	0	0	562.3144314	93.0974	68.43186
0.25	78.24081	78.77345	0.532642365	0.283707889	448.9885534	91.10622	66.44068
0.5	75.63906	76.83137	1.192305382	1.421592124	345.4988738	89.16414	64.49859
0.75	68.09438	74.93716	6.842778767	46.82362125	121.9460821	87.26993	62.60439
1	65.12216	73.08965	7.967492073	63.48092993	65.13619849	85.42242	60.75688
1.5	61.04206	69.53016	8.488101458	72.04786637	15.92488836	81.86293	57.19739
2	56.96461	66.14402	9.179409233	84.26155387	0.007542923	78.47679	53.81125
4	51.08806	54.17014	3.082079581	9.499214544	35.56213956	66.50291	41.83737
6	43.67834	44.36386	0.685520199	0.469937943	178.8403385	56.69663	32.03109
8	39.14163	36.33279	-2.80884395	7.889604333	320.7620106	48.66556	24.00002
10	34.17649	29.75556	-4.420933647	19.54465431	523.2642525	42.08833	17.42279
12	30.66529	24.36899	-6.29630457	39.64345124	696.2299673	36.70176	12.03622
Average	57.05146		SSR	345.3661338	3314.475279		

k_1 (h^{-1})	k_1 (min^{-1})	$t_{1/2}$ (min)	r^2	df	S.E. of y	Critical t	CI
0.099852	0.001664	416.5034	0.895800661	11	5.603295571	2.200985	12.33277

-N3

Time (h)	Peak area	Fitted y	residuals	(residuals)^2	(y-y_{mean})^2	Upper CI	Lower CI
0	68.39687	68.39687	0	0	328.3295378	75.04077	61.75297
0.25	68.09866	66.86849	-1.23017	1.513324076	317.6114166	73.51239	60.22458
0.5	63.42475	65.37426	1.949508	3.800582085	172.8632205	72.01816	58.73035
0.75	61.84484	63.91342	2.068578	4.279016804	133.8148259	70.55732	57.26951
1	58.26297	62.48522	4.222252	17.82741498	63.77565029	69.12913	55.84132
1.5	56.11025	59.72386	3.61361	13.05817403	34.02675695	66.36776	53.07996
2	51.73239	57.08453	5.352138	28.64537688	2.118147924	63.72843	50.44062
4	45.6055	47.64316	2.037664	4.152074383	21.82295118	54.28707	40.99926
6	38.37716	39.76333	1.386173	1.921475164	141.6062912	46.40724	33.11943
8	34.11922	33.18677	-0.93245	0.869466329	261.0739892	39.83067	26.54286
10	29.78281	27.69792	-2.08489	4.346769198	420.0119945	34.34182	21.05402
12	27.56863	23.11689	-4.45174	19.8180256	515.6702573	29.76079	16.47298
Average	50.277		SSR	100.2316995	2412.725039	50.277	

k_1 (h^{-1})	k_1 (min^{-1})	$t_{1/2}$ (min)	r^2	df	S.E. of y	Critical t	CI
0.090397	0.001507	460.0688	0.958457	11	3.018604427	2.200985	6.643904

5. Nonlinear least square fit for CDD degradation in buffer pH 8.0

5.1 At 4 °C

- N1

Time (h)	Peak area	Fitted y	residuals	$(residuals)^2$	$(y-y_{mean})^2$	Upper CI	Lower CI
0	54.45018	54.45018	0	0	10.22471771	56.59004	52.31032
0.25	53.79901	54.26335	0.464347	0.215618456	6.484337575	56.40321	52.12349
0.5	53.14783	54.07717	0.929336	0.863664891	3.592015206	56.21702	51.93731
0.75	53.33483	53.89162	0.556788	0.310012815	4.335811913	56.03148	51.75176
1	52.34708	53.70671	1.359627	1.848585058	1.197954876	55.84656	51.56685
1.5	52.6651	53.33879	0.673686	0.45385248	1.995244532	55.47864	51.19893
2	50.941	52.97339	2.032385	4.130589366	0.097075086	55.11324	50.83353
4	51.05467	51.53664	0.481974	0.232298778	0.039163915	53.6765	49.39679
6	49.63561	50.13887	0.50326	0.253270375	2.614555599	52.27873	47.99901
8	48.39827	48.77901	0.380736	0.144959914	8.147021354	50.91886	46.63915
10	48.82554	47.45602	-1.36952	1.875572884	5.890468553	49.59588	45.31617
12	46.43171	46.16892	-0.26279	0.06905612	23.24067909	48.30878	44.02907
Average	51.25257		SSR	10.39748114	67.8590454		

k_1 (h^{-1})	k_1 (min^{-1})	$t_{1/2}$ (min)	r^2	df	S.E. of y	Critical t	CI
0.013748267	0.000229	3025.023	0.846778	11	0.972227112	2.200985	2.139857

-N2

Time (h)	Peak area	Fitted y	residuals	$(residuals)^2$	$(y-y_{mean})^2$	Upper CI	Lower CI
0	55.63033	55.63033	0	0	3.09471867	58.8058	52.45486
0.25	55.14172	55.34266	0.200943134	0.040378143	1.614351301	58.51813	52.16719
0.5	54.65311	55.05648	0.403373806	0.162710428	0.611463397	58.23195	51.88101
0.75	53.84077	54.77178	0.931014324	0.866787672	0.000922868	57.94725	51.59631
1	52.78251	54.48856	1.706047035	2.910596487	1.185134328	57.66403	51.31309
1.5	52.31023	53.92649	1.616258627	2.612291949	2.436467344	57.10196	50.75102
2	51.31675	53.37022	2.053468149	4.21673144	6.524952974	56.54569	50.19475
4	49.86796	51.20193	1.333968611	1.779472256	16.02552017	54.3774	48.02646
6	47.47056	49.12173	1.651170891	2.726365312	40.96753635	52.2972	45.94626
8	46.25212	47.12605	0.873926053	0.763746746	58.04959909	50.30152	43.95058
10	45.78255	45.21144	-0.571109436	0.326165988	65.42542974	48.38691	42.03597
12	45.92247	43.37462	-2.547849613	6.491537651	63.18149387	46.55009	40.19915
Average	53.87115		SSR	22.89678407	259.1175901		

k_1 (h^{-1})	k_1 (min^{-1})	$t_{1/2}$ (min)	r^2	df	S.E. of y	Critical t	CI
0.020738	0.000346	2005.456	0.911635547	11	1.442749398	2.200985	3.17547

-N3

Time (h)	Peak area	Fitted y	residuals	$(residuals)^2$	$(y-y_{mean})^2$	Upper CI	Lower CI
0	58.286	58.286	0	0	1.52576639	59.82651	56.74549
0.25	58.53846	58.1901	-0.34836	0.121352381	2.213189303	59.73061	56.6496
0.5	58.79092	58.09436	-0.69656	0.485189697	3.028084319	59.63487	56.55386
0.75	57.73053	57.99878	0.268253	0.071959679	0.46205893	59.53929	56.45827
1	58.36883	57.90336	-0.46547	0.216663365	1.737253606	59.44387	56.36285
1.5	59.00808	57.71298	-1.2951	1.677280513	3.831020028	59.25349	56.17247
2	57.27219	57.52323	0.25104	0.063020958	0.049022019	59.06374	55.98272
4	56.53482	56.77044	0.235622	0.055517557	0.266215582	58.31095	55.22993
6	56.59182	56.02751	-0.56431	0.318451396	0.210645047	57.56801	54.487
8	56.36542	55.29429	-1.07113	1.147317386	0.469719472	56.8348	53.75378
10	53.48199	54.57067	1.088682	1.185229084	12.73626801	56.11118	53.03016
12	53.64031	53.85652	0.216213	0.046748204	11.63131131	55.39703	52.31602
Average	57.05078		SSR	5.388730219	38.16055401		

k_1 (h^{-1})	k_1 (min^{-1})	$t_{1/2}$ (min)	r^2	df	S.E. of y	Critical t	CI
0.006587	0.00011	6314.222	0.858788	11	0.699917542	2.200985	1.540508

5.2 At 25 °C

- N1

Time (h)	Peak area	Fitted y	residuals	$(residuals)^2$	$(y-y_{mean})^2$	Upper CI	Lower CI
0	76.39681	76.39681	0	0	346.2570592	84.33574	68.45788
0.25	76.05877	75.349	-0.70977	0.503771431	333.7908446	83.28793	67.41007
0.5	68.33717	74.31556	5.978394	35.74119367	111.2675559	82.2545	66.37663
0.75	67.22247	73.2963	6.07383	36.89141495	88.9936344	81.23523	65.35737
1	70.75501	72.29102	1.536006	2.35931541	168.121921	80.22995	64.35208
1.5	66.08057	70.32162	4.241053	17.9865274	68.75301442	78.26056	62.38269
2	64.16269	68.40588	4.24319	18.00466394	40.6261391	76.34481	60.46695
4	57.53454	61.25078	3.716243	13.81046483	0.064661497	69.18972	53.31185
6	53.82788	54.84409	1.016213	1.032688955	15.6890952	62.78303	46.90516
8	50.12148	49.10753	-1.01395	1.028099242	58.78819852	57.04646	41.1686
10	46.16927	43.97099	-2.19828	4.832418034	135.0140874	51.90993	36.03206
12	42.67682	39.37173	-3.30509	10.92362286	228.3727329	47.31066	31.4328
Average	57.78883		SSR	143.1141807	1595.738944		

k_1 (h^{-1})	k_1 (min^{-1})	$t_{1/2}$ (min)	r^2	df	S.E. of y	Critical t	CI
0.055241076	0.000921	752.8606	0.910315	11	3.606990444	2.200985	7.938932

-N2

Time (h)	Peak area	Fitted y	residuals	(residuals)^2	(y-y_{mean})^2	Upper CI	Lower CI
0	67.00143	67.00143	0	0	268.230968	74.25561	59.74725
0.25	64.04213	65.65427	1.612144834	2.599010967	180.055024	72.90846	58.40009
0.5	68.09438	64.33421	-3.760173939	14.13890805	305.2256497	71.58839	57.08002
0.75	59.95727	63.04068	3.083409072	9.507411505	87.11605785	70.29486	55.7865
1	58.30099	61.77316	3.472170208	12.05596595	58.94121679	69.02734	54.51898
1.5	56.15315	59.31407	3.160915653	9.991387764	30.57513064	66.56825	52.05988
2	53.10234	56.95286	3.850523872	14.82653409	6.143796707	64.20705	49.69868
4	43.83561	48.41134	4.575725448	20.93726338	46.07778119	55.66552	41.15715
6	38.96088	41.15083	2.189946149	4.795864136	136.0207095	48.40501	33.89664
8	35.52686	34.97921	-0.547645379	0.299915461	227.9137225	42.2334	27.72503
10	32.43541	29.73319	-2.702217012	7.301976779	330.8128625	36.98737	22.47901
12	30.07361	25.27395	-4.799664463	23.03677895	422.3050345	32.52813	18.01976
Average	50.62367		SSR	119.491017	2099.417954		

k_1 (h^{-1})	k_1 (min^{-1})	$t_{1/2}$ (min)	r^2	df	S.E. of y	Critical t	CI
0.081245	0.001354	511.8941	0.943083741	11	3.295879204	2.200985	7.254181

-N3

Time (h)	Peak area	Fitted y	residuals	(residuals)^2	(y-y_{mean})^2	Upper CI	Lower CI
0	77.38066	77.38066	0	0	330.470557	87.6381	67.12322
0.25	74.24863	75.99981	1.751183	3.066643556	226.406767	86.25725	65.74238
0.5	68.39687	74.64361	6.246738	39.02173501	84.54911308	84.90104	64.38617
0.75	71.89406	73.3116	1.417544	2.009430183	161.0931889	83.56904	63.05417
1	68.34703	72.00337	3.656339	13.36881415	83.63503361	82.2608	61.74593
1.5	66.90586	69.45652	2.550658	6.505858545	59.35237356	79.71395	59.19908
2	60.05782	66.99975	6.941933	48.19043844	0.732751693	77.25719	56.74232
4	50.52468	58.01148	7.486804	56.05223946	75.2925995	68.26892	47.75405
6	47.34711	50.22903	2.881915	8.30543681	140.5339318	60.48646	39.97159
8	45.36273	43.49061	-1.87212	3.504823057	191.5201583	53.74805	33.23318
10	40.06649	37.65618	-2.41031	5.809577842	366.1605034	47.91362	27.39875
12	39.88979	32.60446	-7.28533	53.07596419	372.9541487	42.8619	22.34703
Average	59.20181		SSR	238.9109612	2092.701127		

k_1 (h^{-1})	k_1 (min^{-1})	$t_{1/2}$ (min)	r^2	df	S.E. of y	Critical t	CI
0.072024	0.0012	577.4304	0.885836	11	4.660383921	2.200985	10.25744

5.3 At 37 °C

- N1

Time (h)	Peak area	Fitted y	residuals	$(residuals)^2$	$(y-y_{mean})^2$	Upper CI	Lower CI
0	68.33717	68.33717	0	0	612.2292041	83.38738	53.28696
0.25	61.45487	66.10346	4.648593	21.60941286	319.0141005	81.15367	51.05325
0.5	55.65153	63.94277	8.291237	68.74461696	145.3863407	78.99298	48.89256
0.75	52.15167	61.8527	9.701028	94.10994155	73.23535606	76.90291	46.80249
1	49.5412	59.83095	10.28975	105.8788636	35.37032773	74.88116	44.78073
1.5	48.72903	55.98353	7.254503	52.62781819	26.36951732	71.03374	40.93332
2	45.28993	52.38353	7.093598	50.31913008	2.876503627	67.43374	37.33332
4	37.90248	40.15434	2.25186	5.070875331	32.39230904	55.20455	25.10413
6	30.77258	30.78012	0.007536	5.67888E-05	164.3863534	45.83033	15.72991
8	26.91555	23.59435	-3.3212	11.03037457	278.1674977	38.64456	8.544138
10	24.6628	18.08613	-6.57667	43.25252885	358.386705	33.13635	3.035924
12	21.71804	13.86384	-7.8542	61.68847147	478.553433	28.91405	-1.18637
Average	43.5939		SSR	514.3320902	2526.367648		

k_1 (h^{-1})	k_1 (min^{-1})	$t_{1/2}$ (min)	r^2	df	S.E. of y	Critical t	CI
0.132930824	0.002216	312.8607	0.796414	11	6.837942874	2.200985	15.05021

-N2

Time (h)	Peak area	Fitted y	residuals	$(residuals)^2$	$(y-y_{mean})^2$	Upper CI	Lower CI
0	68.09438	68.09438	0	0	508.5694381	80.66789	55.52087
0.25	61.91507	66.12345	4.208377737	17.71044318	268.0480869	78.69696	53.54993
0.5	58.58517	64.20956	5.624392384	31.63378969	170.1009154	76.78308	51.63605
0.75	56.27492	62.35107	6.076152769	36.91963247	115.1763427	74.92459	49.77756
1	53.03685	60.54638	7.50952551	56.39297338	56.15934905	73.11989	47.97286
1.5	50.94972	57.09218	6.142455235	37.72975631	29.23374757	69.66569	44.51866
2	47.46583	53.83504	6.369208771	40.56682037	3.697675809	66.40855	41.26152
4	36.70285	42.56168	5.858832763	34.32592134	78.14641034	55.1352	29.98817
6	33.05578	33.64903	0.593250092	0.351945671	155.9280618	46.22254	21.07552
8	29.26188	26.60274	-2.659143627	7.071044832	265.0714766	39.17625	14.02922
10	26.2096	21.03198	-5.177624321	26.80779361	373.7763278	33.60549	8.458461
12	24.9627	16.62776	-8.334936797	69.47117141	423.5444605	29.20128	4.054249
Average	45.5429		SSR	358.9812923	2447.452293		

k_1 (h^{-1})	k_1 (min^{-1})	$t_{1/2}$ (min)	r^2	df	S.E. of y	Critical t	CI
0.117485	0.001958	353.9925	0.853324499	11	5.712675637	2.200985	12.57351

-N3

Time (h)	Peak area	Fitted y	residuals	$(residuals)^2$	$(y-y_{mean})^2$	Upper CI	Lower CI
0	68.39687	68.39687	0	0	413.0945141	79.26058	57.53316
0.25	65.47849	66.68346	1.204966	1.451943778	302.9809043	77.54716	55.81975
0.5	63.4758	65.01297	1.537165	2.362877511	237.2726387	75.87667	54.14926
0.75	57.68236	63.38432	5.701962	32.51237167	92.35626438	74.24803	52.52062
1	54.86122	61.79648	6.935258	48.09780347	46.09156199	72.66018	50.93277
1.5	54.43759	58.73912	4.301535	18.50320212	40.51891127	69.60283	47.87542
2	46.92024	55.83303	8.912793	79.43787722	1.326881289	66.69674	44.96933
4	40.22451	45.57705	5.35254	28.64968423	61.58534893	56.44076	34.71334
6	38.0157	37.20499	-0.81071	0.657249128	101.1320525	48.0687	26.34128
8	32.37779	30.3708	-2.00699	4.028019104	246.3127266	41.2345	19.50709
10	30.92209	24.79198	-6.13011	37.57826655	294.1243293	35.65569	13.92827
12	24.07306	20.23793	-3.83513	14.70819005	575.9560008	31.10164	9.374228
Average	48.07214		SSR	267.9874848	2412.752134		

k_1 (h^{-1})	k_1 (min^{-1})	$t_{1/2}$ (min)	r^2	df	S.E. of y	Critical t	CI
0.101481	0.001691	409.8201	0.888929	11	4.935838188	2.200985	10.86371

6. Nonlinear least square fit for CDD hydrolysis in rat plasma

6.1 At 4 °C

- N1

Time (min)	PAR	Fitted y	residuals	$(residuals)^2$	$(y-y_{mean})^2$	Upper CI	Lower CI
0	0.4983	0.4983	0.0000	0.0000	0.1107	0.6233	0.3734
0.05	0.3516	0.3864	0.0347	0.0012	0.0346	0.5113	0.2614
0.083	0.3133	0.3261	0.0127	0.0002	0.0218	0.4510	0.2011
0.167	0.2520	0.2133	-0.0386	0.0015	0.0074	0.3383	0.0884
0.25	0.0617	0.1396	0.0779	0.0061	0.0108	0.2646	0.0146
0.5	0.1059	0.0391	-0.0668	0.0045	0.0036	0.1641	-0.0859
0.75	0.1046	0.0110	-0.0937	0.0088	0.0037	0.1359	-0.1140
1	0.0962	0.0031	-0.0931	0.0087	0.0048	0.1280	-0.1219
3	0.0206	0.0000	-0.0206	0.0004	0.0210	0.1250	-0.1250
5	0.0136	0.0000	-0.0136	0.0002	0.0231	0.1250	-0.1250
10	0.0046	0.0000	-0.0046	0.0000	0.0259	0.1250	-0.1250
Average	0.1657		SSR	0.0315	0.2675		

k_1 (min^{-1})	$t_{1/2}$ (min)	r^2	df	S.E. of y	Critical t	CI
5.089941431	0.13618	0.88242	10.00	0.056086341	2.228138852	0.124968

-N2

Time (min)	PAR	Fitted y	residuals	$(residuals)^2$	$(y-y_{mean})^2$	Upper CI	Lower CI
0	0.5003	0.5003	0.0000	0.0000	0.1119	0.6509	0.3496
0.05	0.2660	0.4031	0.1371	0.0188	0.0101	0.5537	0.2525
0.083	0.2551	0.3490	0.0939	0.0088	0.0080	0.4997	0.1984
0.167	0.2460	0.2435	-0.0025	0.0000	0.0065	0.3942	0.0929
0.25	0.1990	0.1699	-0.0291	0.0008	0.0011	0.3206	0.0193
0.5	0.1533	0.0577	-0.0956	0.0091	0.0002	0.2084	-0.0929
0.75	0.0902	0.0196	-0.0706	0.0050	0.0057	0.1702	-0.1310
1	0.0611	0.0067	-0.0544	0.0030	0.0109	0.1573	-0.1440
3	0.0123	0.0000	-0.0123	0.0002	0.0235	0.1506	-0.1506
5	0.0000	0.0000	0.0000	0.0000	0.0275	0.1506	-0.1506
10	0.0000	0.0000	0.0000	0.0000	0.0275	0.1506	-0.1506
Average	0.1621		SSR	0.0457	0.2328		

k_1 (min^{-1})	$t_{1/2}$ (min)	r^2	df	S.E. of y	Critical t	CI
4.319087074	0.160485	0.803641	10.00	0.067607491	2.228138852	0.150639

-N3

Time (min)	PAR	Fitted y	residuals	$(residuals)^2$	$(y-y_{mean})^2$	Upper CI	Lower CI
0	0.4995	0.4995	0.0000	0.0000	0.1114	0.5999	0.3990
0.05	0.2961	0.3704	0.0743	0.0055	0.0170	0.4709	0.2699
0.083	0.2427	0.3034	0.0607	0.0037	0.0059	0.4039	0.2030
0.167	0.1993	0.1844	-0.0150	0.0002	0.0011	0.2848	0.0839
0.25	0.1550	0.1120	-0.0430	0.0019	0.0001	0.2125	0.0115
0.5	0.1100	0.0251	-0.0849	0.0072	0.0031	0.1256	-0.0754
0.75	0.0486	0.0056	-0.0430	0.0018	0.0137	0.1061	-0.0949
1	0.0000	0.0013	0.0013	0.0000	0.0275	0.1017	-0.0992
3	0.0000	0.0000	0.0000	0.0000	0.0275	0.1005	-0.1005
5	0.0000	0.0000	0.0000	0.0000	0.0275	0.1005	-0.1005
10	0.0000	0.0000	0.0000	0.0000	0.0275	0.1005	-0.1005
Average	0.1410		SSR	0.0203	0.2622		

k_1 (min^{-1})	$t_{1/2}$ (min)	r^2	df	S.E. of y	Critical t	CI
5.979969435	0.115911	0.922431	10.00	0.045098908	2.228138852	0.100487

6.2 At 25 °C

- N1

Time (h)	PAR	Fitted y	residuals	(residuals)^2	(y-y_{mean})^2	Upper CI	Lower CI
0	0.5061	0.5061	0.0000	0.0000	0.1166	0.5799	0.4323
0.05	0.3894	0.3883	-0.0012	0.0000	0.0505	0.4621	0.3145
0.083	0.2504	0.3254	0.0750	0.0056	0.0074	0.3992	0.2516
0.167	0.2015	0.2092	0.0077	0.0001	0.0014	0.2830	0.1354
0.25	0.1767	0.1345	-0.0422	0.0018	0.0001	0.2083	0.0607
0.5	0.0719	0.0357	-0.0362	0.0013	0.0086	0.1095	-0.0381
0.75	0.0345	0.0095	-0.0250	0.0006	0.0169	0.0833	-0.0643
1	0.0161	0.0025	-0.0135	0.0002	0.0221	0.0763	-0.0713
3	0.0000	0.0000	0.0000	0.0000	0.0271	0.0738	-0.0738
5	0.0000	0.0000	0.0000	0.0000	0.0271	0.0738	-0.0738
Average	0.1647		SSR	0.0096	0.2778		

k_1 (min^{-1})	$t_{1/2}$ (min)	r^2	df	S.E. of y	Critical t	CI
5.301427108	0.130747	0.965519	9.00	0.032626212	2.262157163	0.073806

-N2

Time (h)	PAR	Fitted y	residuals	(residuals)^2	(y-y_{mean})^2	Upper CI	Lower CI
0	0.4965	0.4965	0.0000	0.0000	0.1101	0.5765	0.4166
0.05	0.3322	0.3794	0.0472	0.0022	0.0281	0.4594	0.2995
0.083	0.2628	0.3172	0.0543	0.0029	0.0096	0.3971	0.2372
0.167	0.2021	0.2026	0.0005	0.0000	0.0014	0.2825	0.1226
0.25	0.1769	0.1294	-0.0475	0.0023	0.0001	0.2093	0.0495
0.5	0.0601	0.0337	-0.0264	0.0007	0.0109	0.1136	-0.0462
0.75	0.0583	0.0088	-0.0495	0.0025	0.0113	0.0887	-0.0711
1	0.0202	0.0023	-0.0179	0.0003	0.0209	0.0822	-0.0776
3	0.0182	0.0000	-0.0182	0.0003	0.0214	0.0799	-0.0799
5	0.0000	0.0000	0.0000	0.0000	0.0271	0.0799	-0.0799
Average	0.1627		SSR	0.0112	0.2411		

k_1 (min^{-1})	$t_{1/2}$ (min)	r^2	df	S.E. of y	Critical t	CI
5.379232252	0.128856	0.953395	9.00	0.03533377	2.262157163	0.079931

-N3

Time (min)	PAR	Fitted y	residuals	(residuals)^2	(y-y_{mean})^2	Upper CI	Lower CI
0	0.5004	0.5004	0.0000	0.0000	0.1127	0.5650	0.4359
0.05	0.3138	0.3706	0.0568	0.0032	0.0222	0.4351	0.3060
0.083	0.2893	0.3033	0.0141	0.0002	0.0155	0.3679	0.2388
0.167	0.1750	0.1838	0.0088	0.0001	0.0001	0.2484	0.1193
0.25	0.1500	0.1114	-0.0386	0.0015	0.0002	0.1760	0.0469
0.5	0.0636	0.0248	-0.0388	0.0015	0.0102	0.0894	-0.0398
0.75	0.0307	0.0055	-0.0252	0.0006	0.0180	0.0701	-0.0590
1	0.0155	0.0012	-0.0142	0.0002	0.0223	0.0658	-0.0633
3	0.0000	0.0000	0.0000	0.0000	0.0271	0.0646	-0.0646
5	0.0000	0.0000	0.0000	0.0000	0.0271	0.0646	-0.0646
Average	0.1538		SSR	0.0073	0.2555		

k_1 (min^{-1})	$t_{1/2}$ (min)	r^2	df	S.E. of y	Critical t	CI
6.008764396	0.115356	0.97131	9.00	0.028537672	2.262157163	0.064557

6.3 At 37 °C

- N1

Time (min)	PAR	Fitted y	residuals	(residuals)^2	(y-y_{mean})^2	Upper CI	Lower CI
0	0.5131	0.5131	0.0000	0.0000	0.1184	0.6073	0.4188
0.05	0.2532	0.3472	0.0940	0.0088	0.0071	0.4414	0.2529
0.083	0.2818	0.2676	-0.0142	0.0002	0.0128	0.3619	0.1734
0.167	0.1779	0.1396	-0.0383	0.0015	0.0001	0.2338	0.0453
0.25	0.0929	0.0728	-0.0201	0.0004	0.0058	0.1671	-0.0214
0.5	0.0191	0.0103	-0.0088	0.0001	0.0224	0.1046	-0.0839
0.75	0.0132	0.0015	-0.0118	0.0001	0.0242	0.0957	-0.0928
1	0.0000	0.0002	0.0002	0.0000	0.0285	0.0945	-0.0940
Average	0.1689		SSR	0.0111	0.2194		

k_1 (min^{-1})	$t_{1/2}$ (min)	r^2	df	S.E. of y	Critical t	CI
7.810183459	0.088749	0.9493	7.00	0.039858894	2.364624252	0.094251

-N2

Time (min)	PAR	Fitted y	residuals	$(residuals)^2$	$(y-y_{mean})^2$	Upper CI	Lower CI
0	0.5106	0.5106	0.0000	0.0000	0.1167	0.5843	0.4368
0.05	0.2987	0.3591	0.0604	0.0036	0.0168	0.4328	0.2854
0.083	0.2581	0.2840	0.0260	0.0007	0.0079	0.3577	0.2103
0.167	0.2002	0.1580	-0.0422	0.0018	0.0010	0.2317	0.0842
0.25	0.1096	0.0879	-0.0217	0.0005	0.0035	0.1616	0.0141
0.5	0.0274	0.0151	-0.0122	0.0002	0.0200	0.0889	-0.0586
0.75	0.0115	0.0026	-0.0089	0.0001	0.0248	0.0763	-0.0711
1	0.0000	0.0004	0.0004	0.0000	0.0285	0.0742	-0.0733
Average	0.1770		SSR	0.0068	0.2194		

k_1 (min^{-1})	$t_{1/2}$ (min)	r^2	df	S.E. of y	Critical t	CI
7.038324979	0.098482	0.968972	7.00	0.031181998	2.364624252	0.073734

-N3

Time (min)	PAR	Fitted y	residuals	$(residuals)^2$	$(y-y_{mean})^2$	Upper CI	Lower CI
0	0.5133	0.5133	0.0000	0.0000	0.1186	0.5888	0.4378
0.05	0.2842	0.3444	0.0603	0.0036	0.0133	0.4199	0.2689
0.083	0.2450	0.2640	0.0190	0.0004	0.0058	0.3395	0.1885
0.167	0.1626	0.1358	-0.0268	0.0007	0.0000	0.2113	0.0603
0.25	0.1116	0.0698	-0.0418	0.0017	0.0033	0.1453	-0.0057
0.5	0.0326	0.0095	-0.0231	0.0005	0.0186	0.0850	-0.0660
0.75	0.0133	0.0013	-0.0120	0.0001	0.0242	0.0768	-0.0742
1	0.0000	0.0002	0.0002	0.0000	0.0285	0.0757	-0.0753
Average	0.1703		SSR	0.0071	0.2123		

k_1 (min^{-1})	$t_{1/2}$ (min)	r^2	df	S.E. of y	Critical t	CI
7.979040828	0.086871	0.966386	7.00	0.031930323	2.364624252	0.075503

7. Nonlinear least square fit for CDD hydrolysis in dog plasma

7.1 At 4 °C

- N1

Time (min)	PAR	Fitted y	residuals	$(residuals)^2$	$(y-y_{mean})^2$	Upper CI	Lower CI
0	0.5408	0.5408	0.0000	0.0000	0.0414	0.6469	0.4348
0.083	0.4633	0.5405	0.0772	0.0060	0.0158	0.6466	0.4344
0.25	0.4703	0.5398	0.0695	0.0048	0.0177	0.6458	0.4337
0.5	0.4476	0.5387	0.0911	0.0083	0.0121	0.6448	0.4327
1	0.4755	0.5366	0.0611	0.0037	0.0191	0.6427	0.4305
5	0.4600	0.5200	0.0601	0.0036	0.0150	0.6261	0.4140
15	0.4255	0.4808	0.0553	0.0031	0.0078	0.5869	0.3748
30	0.3820	0.4275	0.0454	0.0021	0.0020	0.5335	0.3214
60	0.3199	0.3379	0.0180	0.0003	0.0003	0.4439	0.2318
90	0.2649	0.2670	0.0022	0.0000	0.0053	0.3731	0.1610
120	0.2200	0.2111	-0.0090	0.0001	0.0138	0.3171	0.1050
150	0.1563	0.1668	0.0105	0.0001	0.0328	0.2729	0.0607
180	0.1489	0.1318	-0.0171	0.0003	0.0355	0.2379	0.0258
210	0.1408	0.1042	-0.0366	0.0013	0.0386	0.2103	-0.0019
240	0.1053	0.0824	-0.0230	0.0005	0.0538	0.1884	-0.0237
Average	0.3347		SSR	0.0342	0.3111		

k_1 (min^{-1})	$t_{1/2}$ (min)	r^2	df	S.E. of y	Critical t	CI
0.007841595	88.39365	0.889928	14.00	0.0494531	2.144786688	0.106066

-N2

Time (min)	PAR	Fitted y	residuals	$(residuals)^2$	$(y-y_{mean})^2$	Upper CI	Lower CI
0	0.5079	0.5079	0.0000	0.0000	0.0291	0.5513	0.4646
0.083	0.4891	0.5076	0.0185	0.0003	0.0230	0.5510	0.4642
0.25	0.4856	0.5070	0.0214	0.0005	0.0220	0.5504	0.4636
0.5	0.4874	0.5060	0.0187	0.0003	0.0225	0.5494	0.4627
1	0.5222	0.5042	-0.0180	0.0003	0.0342	0.5475	0.4608
5	0.4762	0.4893	0.0130	0.0002	0.0193	0.5327	0.4459
15	0.4673	0.4540	-0.0133	0.0002	0.0169	0.4974	0.4106
30	0.4103	0.4058	-0.0045	0.0000	0.0053	0.4492	0.3624
60	0.3610	0.3242	-0.0368	0.0014	0.0006	0.3676	0.2808
90	0.2801	0.2590	-0.0211	0.0004	0.0033	0.3024	0.2156
120	0.2217	0.2069	-0.0148	0.0002	0.0134	0.2503	0.1635
150	0.1611	0.1653	0.0042	0.0000	0.0311	0.2087	0.1219
180	0.0979	0.1320	0.0341	0.0012	0.0573	0.1754	0.0887
210	0.0836	0.1055	0.0218	0.0005	0.0644	0.1489	0.0621
240	0.0699	0.0843	0.0144	0.0002	0.0715	0.1277	0.0409
Average	0.3414		SSR	0.0057	0.4138		

k_1 (min^{-1})	$t_{1/2}$ (min)	r^2	df	S.E. of y	Critical t	CI
0.007484535	92.61059	0.986158	14.00	0.0202271	2.144786688	0.043383

-N3

Time (min)	PAR	Fitted y	residuals	$(residuals)^2$	$(y-y_{mean})^2$	Upper CI	Lower CI
0	0.5264	0.5264	0.0000	0.0000	0.0357	0.5963	0.4564
0.083	0.4732	0.5260	0.0529	0.0028	0.0184	0.5959	0.4561
0.25	0.5047	0.5253	0.0206	0.0004	0.0280	0.5952	0.4554
0.5	0.5004	0.5243	0.0239	0.0006	0.0266	0.5942	0.4544
1	0.5001	0.5222	0.0221	0.0005	0.0265	0.5921	0.4523
5	0.4525	0.5058	0.0533	0.0028	0.0133	0.5757	0.4359
15	0.4168	0.4671	0.0503	0.0025	0.0063	0.5370	0.3972
30	0.3664	0.4145	0.0481	0.0023	0.0008	0.4844	0.3446
60	0.3664	0.3264	-0.0400	0.0016	0.0008	0.3963	0.2565
90	0.2817	0.2570	-0.0246	0.0006	0.0031	0.3269	0.1871
120	0.2223	0.2024	-0.0199	0.0004	0.0132	0.2723	0.1325
150	0.1530	0.1594	0.0064	0.0000	0.0340	0.2293	0.0895
180	0.1134	0.1255	0.0121	0.0001	0.0502	0.1954	0.0556
210	0.0895	0.0988	0.0094	0.0001	0.0614	0.1688	0.0289
240	0.0721	0.0778	0.0057	0.0000	0.0704	0.1477	0.0079
Average	0.3359		SSR	0.0149	0.3887		

k_1 (min^{-1})	$t_{1/2}$ (min)	r^2	df	S.E. of y	Critical t	CI
0.007963895	87.0362	0.961742	14.00	0.0325936	2.144786688	0.069906

7.2 At 25 °C

- N1

Time (min)	PAR	Fitted y	residuals	$(residuals)^2$	$(y-y_{mean})^2$	Upper CI	Lower CI
0	0.5018	0.5018	0.0000	0.0000	0.0664	0.5447	0.4588
0.083	0.4430	0.5004	0.0574	0.0033	0.0396	0.5433	0.4574
0.25	0.4967	0.4976	0.0009	0.0000	0.0638	0.5405	0.4547
0.5	0.4707	0.4935	0.0228	0.0005	0.0513	0.5364	0.4505
1	0.4462	0.4853	0.0390	0.0015	0.0409	0.5282	0.4424
5	0.4119	0.4246	0.0128	0.0002	0.0282	0.4676	0.3817
15	0.3084	0.3041	-0.0042	0.0000	0.0041	0.3471	0.2612
30	0.1835	0.1844	0.0009	0.0000	0.0037	0.2273	0.1414
60	0.0748	0.0677	-0.0070	0.0000	0.0287	0.1107	0.0248
90	0.0299	0.0249	-0.0050	0.0000	0.0459	0.0678	-0.0180
120	0.0110	0.0091	-0.0018	0.0000	0.0544	0.0521	-0.0338
150	0.0000	0.0034	0.0034	0.0000	0.0596	0.0463	-0.0396
180	0.0000	0.0012	0.0012	0.0000	0.0596	0.0442	-0.0417
210	0.0000	0.0005	0.0005	0.0000	0.0596	0.0434	-0.0425
240	0.0000	0.0002	0.0002	0.0000	0.0596	0.0431	-0.0428
Average	0.2252		SSR	0.0056	0.6652		

k_1 (min^{-1})	$t_{1/2}$ (min)	r^2	df	S.E. of y	Critical t	CI
0.033374358	20.76885	0.991567	14.00	0.0200165	2.144786688	0.042931

-N2

Time (min)	PAR	Fitted y	residuals	$(residuals)^2$	$(y-y_{mean})^2$	Upper CI	Lower CI
0	0.4858	0.4858	0.0000	0.0000	0.0584	0.5684	0.4032
0.083	0.5102	0.4847	-0.0254	0.0006	0.0708	0.5673	0.4022
0.25	0.5608	0.4827	-0.0781	0.0061	0.1003	0.5652	0.4001
0.5	0.5553	0.4795	-0.0758	0.0057	0.0969	0.5621	0.3970
1	0.5432	0.4734	-0.0698	0.0049	0.0894	0.5559	0.3908
5	0.4713	0.4267	-0.0446	0.0020	0.0516	0.5093	0.3442
15	0.3443	0.3293	-0.0150	0.0002	0.0100	0.4119	0.2467
30	0.2253	0.2232	-0.0021	0.0000	0.0004	0.3058	0.1406
60	0.0882	0.1025	0.0143	0.0002	0.0243	0.1851	0.0200
90	0.0280	0.0471	0.0192	0.0004	0.0467	0.1297	-0.0355
120	0.0000	0.0216	0.0216	0.0005	0.0596	0.1042	-0.0609
150	0.0000	0.0099	0.0099	0.0001	0.0596	0.0925	-0.0726
180	0.0000	0.0046	0.0046	0.0000	0.0596	0.0871	-0.0780
210	0.0000	0.0021	0.0021	0.0000	0.0596	0.0847	-0.0805
240	0.0000	0.0010	0.0010	0.0000	0.0596	0.0835	-0.0816
Average	0.2542		SSR	0.0207	0.8468		

k_1 (min^{-1})	$t_{1/2}$ (min)	r^2	df	S.E. of y	Critical t	CI
0.025924797	26.73684	0.975495	14.00	0.0384986	2.144786688	0.082571

-N3

Time (min)	PAR	Fitted y	residuals	$(residuals)^2$	$(y-y_{mean})^2$	Upper CI	Lower CI
0	0.5031	0.5031	0.0000	0.0000	0.0671	0.5679	0.4383
0.083	0.5467	0.5018	-0.0449	0.0020	0.0916	0.5666	0.4370
0.25	0.5623	0.4994	-0.0630	0.0040	0.1013	0.5642	0.4346
0.5	0.5351	0.4957	-0.0393	0.0015	0.0847	0.5605	0.4309
1	0.5370	0.4885	-0.0485	0.0023	0.0858	0.5533	0.4237
5	0.4717	0.4344	-0.0373	0.0014	0.0518	0.4992	0.3696
15	0.3487	0.3239	-0.0247	0.0006	0.0109	0.3887	0.2591
30	0.1956	0.2086	0.0129	0.0002	0.0023	0.2734	0.1438
60	0.0663	0.0865	0.0202	0.0004	0.0316	0.1513	0.0217
90	0.0281	0.0359	0.0077	0.0001	0.0467	0.1006	-0.0289
120	0.0000	0.0149	0.0149	0.0002	0.0596	0.0797	-0.0499
150	0.0000	0.0062	0.0062	0.0000	0.0596	0.0710	-0.0586
180	0.0000	0.0026	0.0026	0.0000	0.0596	0.0673	-0.0622
210	0.0000	0.0011	0.0011	0.0000	0.0596	0.0659	-0.0637
240	0.0000	0.0004	0.0004	0.0000	0.0596	0.0652	-0.0644
Average	0.2530		SSR	0.0128	0.8716		

k_1 (min^{-1})	$t_{1/2}$ (min)	r^2	df	S.E. of y	Critical t	CI
0.029347273	23.61879	0.985342	14.00	0.0302086	2.144786688	0.064791

7.3 At 37 °C

- N1

Time (min)	PAR	Fitted y	residuals	$(residuals)^2$	$(y-y_{mean})^2$	Upper CI	Lower CI
0	0.5676	0.5676	0.0000	0.0000	0.0999	0.6654	0.4697
0.083	0.5498	0.5638	0.0140	0.0002	0.0890	0.6616	0.4659
0.25	0.5144	0.5562	0.0419	0.0018	0.0691	0.6540	0.4584
0.5	0.4521	0.5451	0.0930	0.0087	0.0403	0.6429	0.4473
1	0.4102	0.5235	0.1133	0.0128	0.0252	0.6213	0.4256
5	0.3913	0.3788	-0.0125	0.0002	0.0196	0.4766	0.2810
15	0.1923	0.1687	-0.0236	0.0006	0.0035	0.2665	0.0709
30	0.0562	0.0502	-0.0060	0.0000	0.0381	0.1480	-0.0477
60	0.0000	0.0044	0.0044	0.0000	0.0632	0.1023	-0.0934
90	0.0000	0.0004	0.0004	0.0000	0.0632	0.0982	-0.0974
120	0.0000	0.0000	0.0000	0.0000	0.0632	0.0979	-0.0978
150	0.0000	0.0000	0.0000	0.0000	0.0632	0.0978	-0.0978
180	0.0000	0.0000	0.0000	0.0000	0.0632	0.0978	-0.0978
Average	0.2411		SSR	0.0242	0.7008		

k_1 (min^{-1})	$t_{1/2}$ (min)	r^2	df	S.E. of y	Critical t	CI
0.080873855	8.57072	0.965483	12	0.0448988	2.17881283	0.097826

-N2

Time (min)	PAR	Fitted y	residuals	$(residuals)^2$	$(y-y_{mean})^2$	Upper CI	Lower CI
0	0.6014	0.6014	0.0000	0.0000	0.1225	0.6944	0.5085
0.083	0.5521	0.5962	0.0441	0.0019	0.0904	0.6892	0.5033
0.25	0.5300	0.5860	0.0560	0.0031	0.0776	0.6789	0.4930
0.5	0.4991	0.5709	0.0718	0.0052	0.0613	0.6639	0.4779
1	0.4543	0.5419	0.0876	0.0077	0.0412	0.6349	0.4490
5	0.3344	0.3573	0.0228	0.0005	0.0069	0.4502	0.2643
15	0.1817	0.1261	-0.0556	0.0031	0.0049	0.2191	0.0331
30	0.0441	0.0264	-0.0177	0.0003	0.0430	0.1194	-0.0665
60	0.0000	0.0012	0.0012	0.0000	0.0632	0.0941	-0.0918
90	0.0000	0.0001	0.0001	0.0000	0.0632	0.0930	-0.0929
120	0.0000	0.0000	0.0000	0.0000	0.0632	0.0930	-0.0930
150	0.0000	0.0000	0.0000	0.0000	0.0632	0.0930	-0.0930
180	0.0000	0.0000	0.0000	0.0000	0.0632	0.0930	-0.0930
Average	0.2459		SSR	0.0218	0.7638		

k_1 (min^{-1})	$t_{1/2}$ (min)	r^2	df	S.E. of y	Critical t	CI
0.104152005	6.65515	0.971399	12	0.0426673	2.17881283	0.092964

-N3

Time (min)	PAR	Fitted y	residuals	$(residuals)^2$	$(y-y_{mean})^2$	Upper CI	Lower CI
0	0.6090	0.6090	0.0000	0.0000	0.1278	0.6586	0.5594
0.083	0.5991	0.6047	0.0056	0.0000	0.1209	0.6544	0.5551
0.25	0.5701	0.5963	0.0262	0.0007	0.1015	0.6459	0.5467
0.5	0.5387	0.5839	0.0452	0.0020	0.0825	0.6335	0.5343
1	0.5199	0.5598	0.0400	0.0016	0.0721	0.6095	0.5102
5	0.4388	0.3999	-0.0389	0.0015	0.0351	0.4495	0.3502
15	0.1680	0.1724	0.0044	0.0000	0.0070	0.2220	0.1228
30	0.0312	0.0488	0.0176	0.0003	0.0485	0.0984	-0.0008
60	0.0000	0.0039	0.0039	0.0000	0.0632	0.0535	-0.0457
90	0.0000	0.0003	0.0003	0.0000	0.0632	0.0499	-0.0493
120	0.0000	0.0000	0.0000	0.0000	0.0632	0.0496	-0.0496
150	0.0000	0.0000	0.0000	0.0000	0.0632	0.0496	-0.0496
180	0.0000	0.0000	0.0000	0.0000	0.0632	0.0496	-0.0496
Average	0.2673		SSR	0.0062	0.9115		

k_1 (min^{-1})	$t_{1/2}$ (min)	r^2	df	S.E. of y	Critical t	CI
0.084138155	8.238203	0.993175	12	0.0227687	2.17881283	0.049609

8. Nonlinear least square fit for CDD hydrolysis in human plasma

8.1 At 4 °C

- N1

Time (min)	PAR	Fitted y	residuals	$(residuals)^2$	$(y-y_{mean})^2$	Upper CI	Lower CI
0	0.5092	0.5092	0.0000	0.0000	0.0464	0.5909	0.4275
0.083	0.4507	0.5082	0.0574	0.0033	0.0246	0.5899	0.4265
0.25	0.5064	0.5062	-0.0002	0.0000	0.0452	0.5879	0.4245
0.5	0.4529	0.5032	0.0503	0.0025	0.0253	0.5849	0.4215
0.75	0.4571	0.5002	0.0431	0.0019	0.0266	0.5819	0.4186
1	0.4576	0.4973	0.0397	0.0016	0.0268	0.5790	0.4156
5	0.3795	0.4525	0.0729	0.0053	0.0073	0.5342	0.3708
15	0.3133	0.3573	0.0440	0.0019	0.0004	0.4390	0.2756
30	0.2433	0.2507	0.0074	0.0001	0.0026	0.3324	0.1690
45	0.1750	0.1759	0.0009	0.0000	0.0141	0.2576	0.0942
60	0.1412	0.1234	-0.0177	0.0003	0.0233	0.2051	0.0418
90	0.0911	0.0608	-0.0303	0.0009	0.0411	0.1425	-0.0209
120	0.0653	0.0299	-0.0354	0.0013	0.0522	0.1116	-0.0518
150	0.0448	0.0147	-0.0301	0.0009	0.0620	0.0964	-0.0670
180	0.0258	0.0073	-0.0185	0.0003	0.0719	0.0889	-0.0744
Average	0.2875		SSR	0.0203	0.4699		

k_1 (min^{-1})	$t_{1/2}$ (min)	r^2	df	S.E. of y	Critical t	CI
0.0236	29.3500	0.9568	14.0000	0.0381	2.1448	0.0817

-N2

Time (min)	PAR	Fitted y	residuals	$(residuals)^2$	$(y-y_{mean})^2$	Upper CI	Lower CI
0	0.4993	0.4993	0.0000	0.0000	0.0422	0.5489	0.4498
0.083	0.5130	0.4983	-0.0147	0.0002	0.0480	0.5478	0.4487
0.25	0.4974	0.4962	-0.0012	0.0000	0.0414	0.5457	0.4466
0.5	0.4797	0.4931	0.0133	0.0002	0.0345	0.5426	0.4435
0.75	0.4479	0.4899	0.0420	0.0018	0.0237	0.5395	0.4404
1	0.4352	0.4869	0.0517	0.0027	0.0200	0.5364	0.4373
5	0.4194	0.4401	0.0207	0.0004	0.0157	0.4896	0.3905
15	0.3085	0.3418	0.0333	0.0011	0.0002	0.3914	0.2923
30	0.2288	0.2340	0.0052	0.0000	0.0042	0.2835	0.1844
45	0.1679	0.1602	-0.0078	0.0001	0.0159	0.2097	0.1106
60	0.1242	0.1096	-0.0146	0.0002	0.0288	0.1592	0.0601
90	0.0665	0.0514	-0.0151	0.0002	0.0517	0.1009	0.0018
120	0.0404	0.0241	-0.0163	0.0003	0.0643	0.0736	-0.0255
150	0.0185	0.0113	-0.0072	0.0001	0.0758	0.0608	-0.0383
180	0.0212	0.0053	-0.0159	0.0003	0.0744	0.0548	-0.0443
Average	0.2845		SSR	0.0075	0.5409		

k_1 (min^{-1})	$t_{1/2}$ (min)	r^2	df	S.E. of y	Critical t	CI
0.0253	27.4325	0.9862	14.0000	0.0231	2.1448	0.0496

-N3

Time (min)	PAR	Fitted y	residuals	$(residuals)^2$	$(y-y_{mean})^2$	Upper CI	Lower CI
0	0.5526	0.5526	0.0000	0.0000	0.0669	0.6322	0.4730
0.083	0.5015	0.5516	0.0501	0.0025	0.0431	0.6312	0.4720
0.25	0.4956	0.5495	0.0538	0.0029	0.0407	0.6291	0.4699
0.5	0.4893	0.5464	0.0571	0.0033	0.0382	0.6260	0.4668
0.75	0.4800	0.5433	0.0633	0.0040	0.0346	0.6229	0.4637
1	0.4708	0.5402	0.0694	0.0048	0.0313	0.6198	0.4606
5	0.4703	0.4933	0.0230	0.0005	0.0311	0.5729	0.4137
15	0.3724	0.3931	0.0207	0.0004	0.0062	0.4727	0.3135
30	0.2836	0.2797	-0.0039	0.0000	0.0001	0.3593	0.2001
45	0.1975	0.1990	0.0015	0.0000	0.0093	0.2786	0.1194
60	0.1483	0.1416	-0.0068	0.0000	0.0212	0.2212	0.0620
90	0.0857	0.0717	-0.0140	0.0002	0.0434	0.1513	-0.0079
120	0.0539	0.0363	-0.0177	0.0003	0.0576	0.1159	-0.0433
150	0.0171	0.0184	0.0012	0.0000	0.0766	0.0980	-0.0612
180	0.0254	0.0093	-0.0161	0.0003	0.0721	0.0889	-0.0703
Average	0.3096		SSR	0.0193	0.5723		

k_1 (min^{-1})	$t_{1/2}$ (min)	r^2	df	S.E. of y	Critical t	CI
0.0227	30.5386	0.9663	14.0000	0.0371	2.1448	0.0796

8.2 At 25 °C

- N1

Time (min)	PAR	Fitted y	residuals	$(residuals)^2$	$(y-y_{mean})^2$	Upper CI	Lower CI
0	0.5028	0.5028	0.0000	0.0000	0.0479	0.5485	0.4570
0.083	0.4911	0.4996	0.0085	0.0001	0.0429	0.5453	0.4538
0.25	0.4741	0.4932	0.0191	0.0004	0.0361	0.5390	0.4475
0.5	0.4690	0.4839	0.0149	0.0002	0.0342	0.5297	0.4382
0.75	0.4360	0.4748	0.0387	0.0015	0.0231	0.5205	0.4290
1	0.4158	0.4658	0.0500	0.0025	0.0174	0.5115	0.4201
5	0.3447	0.3432	-0.0015	0.0000	0.0037	0.3889	0.2975
15	0.1689	0.1599	-0.0090	0.0001	0.0132	0.2057	0.1142
30	0.0575	0.0509	-0.0066	0.0000	0.0513	0.0966	0.0051
45	0.0237	0.0162	-0.0075	0.0001	0.0677	0.0619	-0.0296
60	0.0143	0.0051	-0.0092	0.0001	0.0727	0.0509	-0.0406
90	0.0175	0.0005	-0.0170	0.0003	0.0710	0.0463	-0.0452
120	0.0087	0.0001	-0.0087	0.0001	0.0758	0.0458	-0.0457
Average	0.2634		SSR	0.0053	0.5571		

k_1 (min^{-1})	$t_{1/2}$ (min)	r^2	df	S.E. of y	Critical t	CI
0.0764	9.0778	0.9905	12.0000	0.0210	2.1788	0.0457

-N2

Time (min)	PAR	Fitted y	residuals	$(residuals)^2$	$(y-y_{mean})^2$	Upper CI	Lower CI
0	0.6197	0.6197	0.0000	0.0000	0.1127	0.7503	0.4890
0.083	0.5552	0.6137	0.0584	0.0034	0.0736	0.7443	0.4830
0.25	0.5429	0.6018	0.0589	0.0035	0.0670	0.7325	0.4712
0.5	0.5379	0.5845	0.0466	0.0022	0.0645	0.7151	0.4539
0.75	0.4626	0.5677	0.1051	0.0110	0.0319	0.6983	0.4370
1	0.4486	0.5513	0.1027	0.0106	0.0271	0.6820	0.4207
5	0.3179	0.3455	0.0276	0.0008	0.0011	0.4761	0.2149
15	0.1939	0.1074	-0.0865	0.0075	0.0081	0.2381	-0.0232
30	0.0726	0.0186	-0.0539	0.0029	0.0447	0.1493	-0.1120
45	0.0338	0.0032	-0.0306	0.0009	0.0626	0.1339	-0.1274
60	0.0206	0.0006	-0.0200	0.0004	0.0694	0.1312	-0.1301
90	0.0000	0.0000	0.0000	0.0000	0.0807	0.1307	-0.1306
120	0.0000	0.0000	0.0000	0.0000	0.0807	0.1306	-0.1306
Average	0.2927		SSR	0.0431	0.7240		

k_1 (min^{-1})	$t_{1/2}$ (min)	r^2	df	S.E. of y	Critical t	CI
0.1168	5.9329	0.9404	12.0000	0.0600	2.1788	0.1306

-N3

Time (min)	PAR	Fitted y	residuals	$(residuals)^2$	$(y-y_{mean})^2$	Upper CI	Lower CI
0	0.5614	0.5614	0.0000	0.0000	0.0770	0.5903	0.5325
0.083	0.5311	0.5578	0.0268	0.0007	0.0610	0.5867	0.5289
0.25	0.5270	0.5507	0.0237	0.0006	0.0591	0.5796	0.5218
0.5	0.5269	0.5402	0.0134	0.0002	0.0590	0.5691	0.5113
0.75	0.5462	0.5299	-0.0162	0.0003	0.0687	0.5589	0.5010
1	0.5049	0.5199	0.0149	0.0002	0.0488	0.5488	0.4909
5	0.3735	0.3823	0.0087	0.0001	0.0080	0.4112	0.3533
15	0.1826	0.1772	-0.0054	0.0000	0.0103	0.2061	0.1483
30	0.0593	0.0559	-0.0033	0.0000	0.0505	0.0849	0.0270
45	0.0242	0.0177	-0.0065	0.0000	0.0675	0.0466	-0.0112
60	0.0090	0.0056	-0.0035	0.0000	0.0756	0.0345	-0.0233
90	0.0000	0.0006	0.0006	0.0000	0.0807	0.0295	-0.0284
120	0.0000	0.0001	0.0001	0.0000	0.0807	0.0290	-0.0289
Average	0.2875		SSR	0.0203	0.4699		

k_1 (min^{-1})	$t_{1/2}$ (min)	r^2	df	S.E. of y	Critical t	CI
0.0769	9.0174	0.9972	12.0000	0.0133	2.1788	0.0289

8.3 At 37 °C

- N1

Time (min)	PAR	Fitted y	residuals	$(residuals)^2$	$(y-y_{mean})^2$	Upper CI	Lower CI
0	0.5274	0.5274	0.0000	0.0000	0.0778	0.5503	0.5046
0.083	0.5074	0.5200	0.0126	0.0002	0.0670	0.5429	0.4972
0.25	0.5010	0.5055	0.0046	0.0000	0.0637	0.5284	0.4827
0.5	0.4946	0.4845	-0.0101	0.0001	0.0605	0.5073	0.4616
0.75	0.4827	0.4643	-0.0184	0.0003	0.0548	0.4872	0.4415
1	0.4669	0.4450	-0.0219	0.0005	0.0477	0.4679	0.4222
5	0.2166	0.2255	0.0090	0.0001	0.0010	0.2484	0.2027
15	0.0299	0.0412	0.0114	0.0001	0.0478	0.0641	0.0184
30	0.0000	0.0032	0.0032	0.0000	0.0618	0.0261	-0.0196
45	0.0000	0.0003	0.0003	0.0000	0.0618	0.0231	-0.0226
60	0.0000	0.0000	0.0000	0.0000	0.0618	0.0229	-0.0228
90	0.0000	0.0000	0.0000	0.0000	0.0618	0.0228	-0.0228
120	0.0000	0.0000	0.0000	0.0000	0.0618	0.0228	-0.0228
Average	0.2482		SSR	0.0013	0.7293		

k_1 (min^{-1})	$t_{1/2}$ (min)	r^2	df	S.E. of y	Critical t	CI
0.1699	4.0793	0.9982	12.0000	0.0105	2.1788	0.0228

-N2

Time (min)	PAR	Fitted y	residuals	$(residuals)^2$	$(y-y_{mean})^2$	Upper CI	Lower CI
0	0.5127	0.5127	0.0000	0.0000	0.0698	0.5378	0.4875
0.083	0.4860	0.5062	0.0202	0.0004	0.0564	0.5314	0.4810
0.25	0.4798	0.4935	0.0137	0.0002	0.0535	0.5187	0.4683
0.5	0.4874	0.4750	-0.0123	0.0002	0.0571	0.5002	0.4499
0.75	0.4492	0.4573	0.0081	0.0001	0.0403	0.4825	0.4321
1	0.4493	0.4402	-0.0092	0.0001	0.0403	0.4654	0.4150
5	0.2531	0.2393	-0.0138	0.0002	0.0000	0.2645	0.2141
15	0.0300	0.0521	0.0221	0.0005	0.0478	0.0773	0.0269
30	0.0000	0.0053	0.0053	0.0000	0.0618	0.0305	-0.0199
45	0.0000	0.0005	0.0005	0.0000	0.0618	0.0257	-0.0246
60	0.0000	0.0001	0.0001	0.0000	0.0618	0.0252	-0.0251
90	0.0000	0.0000	0.0000	0.0000	0.0618	0.0252	-0.0252
120	0.0000	0.0000	0.0000	0.0000	0.0618	0.0252	-0.0252
Average	0.2421		SSR	0.0016	0.6739		

k_1 (min^{-1})	$t_{1/2}$ (min)	r^2	df	S.E. of y	Critical t	CI
0.1524	4.5482	0.9976	12.0000	0.0116	2.1788	0.0252

-N3

Time (min)	PAR	Fitted y	residuals	$(residuals)^2$	$(y-y_{mean})^2$	Upper CI	Lower CI
0	0.5101	0.5101	0.0000	0.0000	0.0684	0.5541	0.4660
0.083	0.5132	0.5051	-0.0081	0.0001	0.0701	0.5491	0.4611
0.25	0.5075	0.4953	-0.0122	0.0001	0.0671	0.5394	0.4513
0.5	0.4843	0.4810	-0.0033	0.0000	0.0556	0.5250	0.4370
0.75	0.4768	0.4671	-0.0097	0.0001	0.0521	0.5111	0.4231
1	0.4604	0.4536	-0.0068	0.0000	0.0449	0.4976	0.4096
5	0.3275	0.2837	-0.0438	0.0019	0.0062	0.3277	0.2397
15	0.0390	0.0878	0.0488	0.0024	0.0439	0.1318	0.0437
30	0.0000	0.0151	0.0151	0.0002	0.0618	0.0591	-0.0289
45	0.0000	0.0026	0.0026	0.0000	0.0618	0.0466	-0.0414
60	0.0000	0.0004	0.0004	0.0000	0.0618	0.0445	-0.0436
90	0.0000	0.0000	0.0000	0.0000	0.0618	0.0440	-0.0440
120	0.0000	0.0000	0.0000	0.0000	0.0618	0.0440	-0.0440
Average	0.2553		SSR	0.0049	0.7171		

k_1 (min^{-1})	$t_{1/2}$ (min)	r^2	df	S.E. of y	Critical t	CI
0.1173	5.9081	0.9932	12.0000	0.0202	2.1788	0.0440

9. Nonlinear least square fit for MSCUR metabolism in rat plasma

9.1 At 4 °C

- N1

Time (min)	PAR	Fitted y	residuals	$(residuals)^2$	$(y-y_{mean})^2$	Upper CI	Lower CI
0	0.0000	-0.0351	-0.0351	0.0012	0.0020	0.0583	-0.1285
0.05	0.0412	0.0317	-0.0095	0.0001	0.0000	0.1251	-0.0617
0.083	0.0868	0.0641	-0.0227	0.0005	0.0017	0.1575	-0.0293
0.167	0.0796	0.1142	0.0346	0.0012	0.0012	0.2076	0.0207
0.25	0.0382	0.1341	0.0959	0.0092	0.0000	0.2275	0.0407
0.5	0.0674	0.1160	0.0486	0.0024	0.0005	0.2094	0.0225
0.75	0.0621	0.0735	0.0113	0.0001	0.0003	0.1669	-0.0200
1	0.0667	0.0415	-0.0253	0.0006	0.0005	0.1349	-0.0520
3	0.0000	0.0002	0.0002	0.0000	0.0020	0.0936	-0.0933
5	0.0000	0.0000	0.0000	0.0000	0.0020	0.0934	-0.0934
10	0.0000	0.0000	0.0000	0.0000	0.0020	0.0934	-0.0934
Average	0.0402		SSR	0.0154	0.0124		

k_1 (min^{-1})	k_2 (min^{-1})	t_{max} (min)	r^2	df	S.E. of y	Critical t	CI
2.8807	4.3684	0.2119	-0.2400	9.0000	0.0413	2.2622	0.0934

- N2

Time (min)	PAR	Fitted y	residuals	$(residuals)^2$	$(y-y_{mean})^2$	Upper CI	Lower CI
0	0.0000	-0.0191	-0.0191	0.0004	0.0020	0.0340	-0.0721
0.05	0.0684	0.0517	-0.0168	0.0003	0.0005	0.1047	-0.0014
0.083	0.0857	0.0842	-0.0015	0.0000	0.0016	0.1372	0.0311
0.167	0.0973	0.1296	0.0323	0.0010	0.0027	0.1826	0.0765
0.25	0.0913	0.1421	0.0508	0.0026	0.0021	0.1952	0.0890
0.5	0.0838	0.1067	0.0230	0.0005	0.0015	0.1598	0.0536
0.75	0.0637	0.0600	-0.0037	0.0000	0.0003	0.1130	0.0069
1	0.0423	0.0302	-0.0120	0.0001	0.0000	0.0833	-0.0228
3	0.0000	0.0001	0.0001	0.0000	0.0020	0.0531	-0.0530
5	0.0000	0.0000	0.0000	0.0000	0.0020	0.0531	-0.0531
10	0.0000	0.0000	0.0000	0.0000	0.0020	0.0531	-0.0531
Average	0.0484		SSR	0.0050	0.0170		

k_1 (min^{-1})	k_2 (min^{-1})	t_{max} (min)	r^2	df	S.E. of y	Critical t	CI
3.2650	4.9301	0.2166	0.7092	9.0000	0.0235	2.2622	0.0531

- N3

Time (min)	PAR	Fitted y	residuals	$(residuals)^2$	$(y-y_{mean})^2$	Upper CI	Lower CI
0	0.0000	-0.0119	-0.0119	0.0001	0.0020	0.0347	-0.0585
0.05	0.1026	0.0878	-0.0148	0.0002	0.0033	0.1344	0.0411
0.083	0.1094	0.1216	0.0122	0.0001	0.0041	0.1683	0.0750
0.167	0.1063	0.1439	0.0375	0.0014	0.0037	0.1905	0.0973
0.25	0.0922	0.1258	0.0336	0.0011	0.0022	0.1724	0.0792
0.5	0.0726	0.0502	-0.0224	0.0005	0.0008	0.0968	0.0036
0.75	0.0312	0.0154	-0.0158	0.0002	0.0002	0.0621	-0.0312
1	0.0000	0.0044	0.0044	0.0000	0.0020	0.0510	-0.0423
3	0.0000	0.0000	0.0000	0.0000	0.0020	0.0466	-0.0466
5	0.0000	0.0000	0.0000	0.0000	0.0020	0.0466	-0.0466
10	0.0000	0.0000	0.0000	0.0000	0.0020	0.0466	-0.0466
Average	0.0468		SSR	0.0038	0.0245		

k_1 (min^{-1})	k_2 (min^{-1})	t_{max} (min)	r^2	df	S.E. of y	Critical t	CI
5.3548	8.0615	0.1435	0.8442	9.0000	0.0206	2.2622	0.0466

9.2 At 25 °C

- N1

Time (h)	PAR	Fitted y	residuals	$(residuals)^2$	$(y-y_{mean})^2$	Upper CI	Lower CI
0	0.0000	-0.0520	-0.0520	0.0027	0.0014	0.0249	-0.1290
0.05	0.0423	0.0736	0.0313	0.0010	0.0000	0.1506	-0.0033
0.083	0.0782	0.1127	0.0345	0.0012	0.0017	0.1897	0.0357
0.167	0.0871	0.1324	0.0453	0.0020	0.0025	0.2094	0.0554
0.25	0.0651	0.1085	0.0435	0.0019	0.0008	0.1855	0.0316
0.5	0.0330	0.0342	0.0012	0.0000	0.0000	0.1112	-0.0428
0.75	0.0151	0.0083	-0.0068	0.0000	0.0005	0.0853	-0.0687
1	0.0086	0.0019	-0.0067	0.0000	0.0008	0.0788	-0.0751
3	0.0000	0.0000	0.0000	0.0000	0.0014	0.0770	-0.0770
5	0.0000	0.0000	0.0000	0.0000	0.0014	0.0770	-0.0770
Average	0.0329		SSR	0.0089	0.0105		

k_1 (min^{-1})	k_2 (min^{-1})	t_{max} (min)	r^2	df	S.E. of y	Critical t	CI
6.1930	9.4995	0.1389	0.1474	8.0000	0.0334	2.3060	0.0770

- N2

Time (h)	PAR	Fitted y	residuals	$(residuals)^2$	$(y-y_{mean})^2$	Upper CI	Lower CI
0	0.0000	-0.0259	-0.0259	0.0007	0.0014	0.0385	-0.0904
0.05	0.1135	0.1148	0.0013	0.0000	0.0058	0.1792	0.0503
0.083	0.0741	0.1380	0.0639	0.0041	0.0014	0.2024	0.0736
0.167	0.0865	0.1126	0.0261	0.0007	0.0024	0.1771	0.0482
0.25	0.0690	0.0681	-0.0008	0.0000	0.0010	0.1325	0.0037
0.5	0.0318	0.0093	-0.0224	0.0005	0.0000	0.0737	-0.0551
0.75	0.0165	0.0010	-0.0155	0.0002	0.0004	0.0655	-0.0634
1	0.0081	0.0001	-0.0080	0.0001	0.0008	0.0645	-0.0643
3	0.0000	0.0000	0.0000	0.0000	0.0014	0.0644	-0.0644
5	0.0000	0.0000	0.0000	0.0000	0.0014	0.0644	-0.0644
Average	0.0400		SSR	0.0062	0.0161		

k_1 (min^{-1})	k_2 (min^{-1})	t_{max} (min)	r^2	df	S.E. of y	Critical t	CI
9.0821	13.7118	0.1123	0.6116	8.0000	0.0279	2.3060	0.0644

- N3

Time (h)	PAR	Fitted y	residuals	(residuals)^2	(y-y_{mean})^2	Upper CI	Lower CI
0	0.0000	-0.0254	-0.0254	0.0006	0.0014	0.0389	-0.0897
0.05	0.1147	0.1211	0.0064	0.0000	0.0060	0.1855	0.0568
0.083	0.0769	0.1402	0.0633	0.0040	0.0016	0.2045	0.0759
0.167	0.0793	0.1052	0.0259	0.0007	0.0018	0.1695	0.0409
0.25	0.0682	0.0588	-0.0095	0.0001	0.0010	0.1231	-0.0055
0.5	0.0303	0.0064	-0.0238	0.0006	0.0000	0.0708	-0.0579
0.75	0.0141	0.0006	-0.0135	0.0002	0.0005	0.0649	-0.0637
1	0.0052	0.0001	-0.0051	0.0000	0.0010	0.0644	-0.0643
3	0.0000	0.0000	0.0000	0.0000	0.0014	0.0643	-0.0643
5	0.0000	0.0000	0.0000	0.0000	0.0014	0.0643	-0.0643
Average	0.0389		SSR	0.0062	0.0133		

k_1 (min^{-1})	k_2 (min^{-1})	t_{max} (min)	r^2	df	S.E. of y	Critical t	CI
9.8671	14.9336	0.1020	0.5324	8.0000	0.0279	2.3060	0.0643

9.3 At 37 °C

- N1

Time (min)	PAR	Fitted y	residuals	(residuals)^2	(y-y_{mean})^2	Upper CI	Lower CI
0	0.0000	-0.0270	-0.0270	0.0007	0.0021	0.0258	-0.0798
0.05	0.0886	0.1210	0.0325	0.0011	0.0018	0.1738	0.0682
0.083	0.1163	0.1424	0.0261	0.0007	0.0049	0.1952	0.0896
0.167	0.0954	0.1106	0.0151	0.0002	0.0024	0.1634	0.0578
0.25	0.0552	0.0638	0.0086	0.0001	0.0001	0.1166	0.0110
0.5	0.0126	0.0077	-0.0049	0.0000	0.0011	0.0605	-0.0451
0.75	0.0000	0.0008	0.0008	0.0000	0.0021	0.0536	-0.0520
1	0.0000	0.0001	0.0001	0.0000	0.0021	0.0529	-0.0527
Average	0.0460		SSR	0.0028	0.0168		

k_1 (min^{-1})	k_2 (min^{-1})	t_{max} (min)	r^2	df	S.E. of y	Critical t	CI
9.5083	14.5222	0.0924	0.8333	6.0000	0.0216	2.4469	0.0528

- N2

Time (min)	PAR	Fitted y	residuals	$(residuals)^2$	$(y-y_{mean})^2$	Upper CI	Lower CI
0	0.0000	-0.0277	-0.0277	0.0008	0.0021	0.0352	-0.0907
0.05	0.1003	0.1221	0.0218	0.0005	0.0029	0.1850	0.0591
0.083	0.0957	0.1419	0.0461	0.0021	0.0025	0.2048	0.0789
0.167	0.0840	0.1069	0.0229	0.0005	0.0014	0.1698	0.0439
0.25	0.0636	0.0599	-0.0037	0.0000	0.0003	0.1228	-0.0031
0.5	0.0143	0.0066	-0.0077	0.0001	0.0010	0.0696	-0.0563
0.75	0.0000	0.0006	0.0006	0.0000	0.0021	0.0635	-0.0623
1	0.0000	0.0001	0.0001	0.0000	0.0021	0.0630	-0.0629
Average	0.0447		SSR	0.0040	0.0145		

k_1 (min^{-1})	k_2 (min^{-1})	t_{max} (min)	r^2	df	S.E. of y	Critical t	CI
9.8148	14.9691	0.0952	0.7267	6.0000	0.0257	2.4469	0.0629

- N3

Time (min)	PAR	Fitted y	residuals	$(residuals)^2$	$(y-y_{mean})^2$	Upper CI	Lower CI
0	0.0000	-0.0222	-0.0222	0.0005	0.0021	0.0311	-0.0755
0.05	0.1099	0.1272	0.0173	0.0003	0.0041	0.1805	0.0739
0.083	0.1049	0.1444	0.0394	0.0016	0.0035	0.1977	0.0911
0.167	0.0855	0.1049	0.0193	0.0004	0.0016	0.1581	0.0516
0.25	0.0640	0.0570	-0.0070	0.0000	0.0003	0.1103	0.0037
0.5	0.0146	0.0058	-0.0088	0.0001	0.0010	0.0591	-0.0475
0.75	0.0000	0.0005	0.0005	0.0000	0.0021	0.0538	-0.0528
1	0.0000	0.0000	0.0000	0.0000	0.0021	0.0533	-0.0533
Average	0.0474		SSR	0.0028	0.0168		

k_1 (min^{-1})	k_2 (min^{-1})	t_{max} (min)	r^2	df	S.E. of y	Critical t	CI
10.1017	15.4044	0.0886	0.8303	6.0000	0.0218	2.4469	0.0533

10. Nonlinear least square fit for MSCUR metabolism in dog plasma

10.1 At 4 °C

- N1

Time (min)	PAR	Fitted y	residuals	$(residuals)^2$	$(y-y_{mean})^2$	Upper CI	Lower CI
0	0.0000	0.0000	0.0000	0.0000	0.0161	0.0258	-0.0258
0.083	0.0000	0.0003	0.0003	0.0000	0.0161	0.0261	-0.0255
0.25	0.0000	0.0009	0.0009	0.0000	0.0161	0.0267	-0.0249
0.5	0.0000	0.0018	0.0018	0.0000	0.0161	0.0276	-0.0240
1	0.0000	0.0036	0.0036	0.0000	0.0161	0.0294	-0.0222
5	0.0407	0.0176	-0.0231	0.0005	0.0074	0.0434	-0.0082
15	0.0622	0.0500	-0.0122	0.0001	0.0042	0.0758	0.0243
30	0.1067	0.0922	-0.0145	0.0002	0.0004	0.1180	0.0665
60	0.1550	0.1568	0.0018	0.0000	0.0008	0.1825	0.1310
90	0.1945	0.2000	0.0055	0.0000	0.0046	0.2258	0.1742
120	0.2252	0.2269	0.0017	0.0000	0.0097	0.2527	0.2011
150	0.2214	0.2414	0.0200	0.0004	0.0089	0.2672	0.2157
180	0.2479	0.2467	-0.0011	0.0000	0.0146	0.2725	0.2210
210	0.2669	0.2453	-0.0216	0.0005	0.0196	0.2710	0.2195
240	0.2329	0.2389	0.0060	0.0000	0.0112	0.2647	0.2132
Average	0.1169		SSR	0.0018	0.1620		

k_1 (min^{-1})	k_2 (min^{-1})	t_{max} (min)	r^2	df	S.E. of y	Critical t	CI
0.0067	0.0042	171.6576	0.9886	13.0000	0.0119	2.1604	0.0258

- N2

Time (min)	PAR	Fitted y	residuals	$(residuals)^2$	$(y-y_{mean})^2$	Upper CI	Lower CI
0	0.0000	0.0000	0.0000	0.0000	0.0161	0.0236	-0.0236
0.083	0.0000	0.0004	0.0004	0.0000	0.0161	0.0239	-0.0232
0.25	0.0052	0.0011	-0.0041	0.0000	0.0148	0.0247	-0.0225
0.5	0.0075	0.0022	-0.0053	0.0000	0.0142	0.0258	-0.0214
1	0.0062	0.0044	-0.0018	0.0000	0.0146	0.0279	-0.0192
5	0.0459	0.0213	-0.0246	0.0006	0.0066	0.0449	-0.0023
15	0.0676	0.0601	-0.0075	0.0001	0.0035	0.0836	0.0365
30	0.1090	0.1095	0.0005	0.0000	0.0003	0.1331	0.0859
60	0.1801	0.1822	0.0021	0.0000	0.0028	0.2058	0.1586
90	0.2179	0.2277	0.0098	0.0001	0.0083	0.2513	0.2041
120	0.2609	0.2534	-0.0075	0.0001	0.0180	0.2770	0.2299
150	0.2698	0.2649	-0.0049	0.0000	0.0204	0.2884	0.2413
180	0.2652	0.2662	0.0011	0.0000	0.0191	0.2898	0.2427
210	0.2403	0.2606	0.0203	0.0004	0.0129	0.2842	0.2370
240	0.2660	0.2503	-0.0157	0.0002	0.0193	0.2739	0.2267
Average	0.1294		SSR	0.0015	0.1871		

k_1 (min^{-1})	k_2 (min^{-1})	t_{max} (min)	r^2	df	S.E. of y	Critical t	CI
0.0087	0.0038	183.9597	0.9917	13.0000	0.0109	2.1604	0.0236

- N3

Time (min)	PAR	Fitted y	residuals	$(residuals)^2$	$(y-y_{mean})^2$	Upper CI	Lower CI
0	0.0000	0.0000	0.0000	0.0000	0.0161	0.0485	-0.0485
0.083	0.0000	0.0004	0.0004	0.0000	0.0161	0.0489	-0.0481
0.25	0.0063	0.0012	-0.0052	0.0000	0.0145	0.0497	-0.0473
0.5	0.0064	0.0023	-0.0040	0.0000	0.0145	0.0508	-0.0462
1	0.0092	0.0046	-0.0046	0.0000	0.0138	0.0531	-0.0439
5	0.0644	0.0225	-0.0419	0.0018	0.0039	0.0710	-0.0260
15	0.0913	0.0633	-0.0280	0.0008	0.0013	0.1118	0.0148
30	0.1645	0.1148	-0.0497	0.0025	0.0014	0.1633	0.0663
60	0.1645	0.1892	0.0247	0.0006	0.0014	0.2377	0.1407
90	0.2118	0.2341	0.0223	0.0005	0.0072	0.2826	0.1856
120	0.2479	0.2580	0.0101	0.0001	0.0146	0.3065	0.2095
150	0.2619	0.2669	0.0050	0.0000	0.0182	0.3154	0.2184
180	0.2767	0.2655	-0.0112	0.0001	0.0224	0.3140	0.2170
210	0.2543	0.2572	0.0029	0.0000	0.0162	0.3057	0.2087
240	0.2550	0.2444	-0.0105	0.0001	0.0164	0.2929	0.1959
Average	0.1343		SSR	0.0066	0.1783		

k_1 (min^{-1})	k_2 (min^{-1})	t_{max} (min)	r^2	df	S.E. of y	Critical t	CI
0.0088	0.0042	169.2892	0.9632	13.0000	0.0224	2.1604	0.0485

10.2 At 25 °C

- N1

Time (min)	PAR	Fitted y	residuals	$(residuals)^2$	$(y-y_{mean})^2$	Upper CI	Lower CI
0	0.0000	0.0000	0.0000	0.0000	0.0082	0.0159	-0.0159
0.083	0.0039	0.0014	-0.0026	0.0000	0.0075	0.0173	-0.0145
0.25	0.0079	0.0042	-0.0037	0.0000	0.0068	0.0200	-0.0117
0.5	0.0173	0.0083	-0.0090	0.0001	0.0054	0.0242	-0.0076
1	0.0206	0.0164	-0.0042	0.0000	0.0049	0.0322	0.0005
5	0.0634	0.0743	0.0110	0.0001	0.0007	0.0902	0.0585
15	0.1676	0.1754	0.0078	0.0001	0.0059	0.1912	0.1595
30	0.2481	0.2459	-0.0021	0.0000	0.0248	0.2618	0.2301
60	0.2625	0.2463	-0.0162	0.0003	0.0296	0.2621	0.2304
90	0.1910	0.1894	-0.0016	0.0000	0.0101	0.2053	0.1735
120	0.1316	0.1323	0.0007	0.0000	0.0017	0.1482	0.1165
150	0.0835	0.0885	0.0050	0.0000	0.0000	0.1043	0.0726
180	0.0528	0.0578	0.0050	0.0000	0.0014	0.0736	0.0419
210	0.0327	0.0373	0.0046	0.0000	0.0033	0.0531	0.0214
240	0.0162	0.0239	0.0077	0.0001	0.0055	0.0397	0.0080
Average	0.0866		SSR	0.0007	0.1160		

k_1 (min^{-1})	k_2 (min^{-1})	t_{max} (min)	r^2	df	S.E. of y	Critical t	CI
0.0334	0.0151	43.3370	0.9940	13.0000	0.0073	2.1604	0.0159

- N2

Time (min)	PAR	Fitted y	residuals	$(residuals)^2$	$(y-y_{mean})^2$	Upper CI	Lower CI
0	0.0000	0.0000	0.0000	0.0000	0.0082	0.0318	-0.0318
0.083	0.0098	0.0017	-0.0081	0.0001	0.0065	0.0335	-0.0301
0.25	0.0116	0.0052	-0.0064	0.0000	0.0062	0.0370	-0.0266
0.5	0.0138	0.0103	-0.0035	0.0000	0.0059	0.0421	-0.0215
1	0.0194	0.0204	0.0009	0.0000	0.0050	0.0522	-0.0115
5	0.0769	0.0909	0.0140	0.0002	0.0002	0.1228	0.0591
15	0.1960	0.2071	0.0111	0.0001	0.0111	0.2389	0.1753
30	0.2877	0.2775	-0.0102	0.0001	0.0389	0.3093	0.2457
60	0.2910	0.2611	-0.0298	0.0009	0.0402	0.2930	0.2293
90	0.2091	0.1950	-0.0141	0.0002	0.0141	0.2268	0.1632
120	0.1376	0.1357	-0.0019	0.0000	0.0022	0.1675	0.1039
150	0.0806	0.0920	0.0114	0.0001	0.0001	0.1238	0.0602
180	0.0471	0.0617	0.0146	0.0002	0.0019	0.0936	0.0299
210	0.0204	0.0413	0.0209	0.0004	0.0049	0.0731	0.0095
240	0.0075	0.0275	0.0200	0.0004	0.0069	0.0593	-0.0043
Average	0.0939		SSR	0.0028	0.1523		

k_1 (min^{-1})	k_2 (min^{-1})	t_{max} (min)	r^2	df	S.E. of y	Critical t	CI
0.0431	0.0135	52.4741	0.9815	13.0000	0.0147	2.1604	0.0318

- N3

Time (min)	PAR	Fitted y	residuals	$(residuals)^2$	$(y-y_{mean})^2$	Upper CI	Lower CI
0	0.0000	0.0000	0.0000	0.0000	0.0082	0.0241	-0.0241
0.083	0.0109	0.0017	-0.0092	0.0001	0.0063	0.0258	-0.0224
0.25	0.0000	0.0050	0.0050	0.0000	0.0082	0.0291	-0.0191
0.5	0.0254	0.0100	-0.0154	0.0002	0.0042	0.0341	-0.0141
1	0.0224	0.0197	-0.0028	0.0000	0.0046	0.0438	-0.0044
5	0.0862	0.0882	0.0020	0.0000	0.0000	0.1123	0.0641
15	0.1966	0.2020	0.0054	0.0000	0.0113	0.2261	0.1779
30	0.2690	0.2721	0.0031	0.0000	0.0319	0.2962	0.2481
60	0.2758	0.2557	-0.0201	0.0004	0.0343	0.2798	0.2316
90	0.2032	0.1882	-0.0150	0.0002	0.0127	0.2122	0.1641
120	0.1265	0.1278	0.0013	0.0000	0.0013	0.1519	0.1037
150	0.0756	0.0840	0.0084	0.0001	0.0002	0.1081	0.0599
180	0.0392	0.0545	0.0153	0.0002	0.0026	0.0786	0.0304
210	0.0221	0.0351	0.0129	0.0002	0.0047	0.0592	0.0110
240	0.0117	0.0225	0.0109	0.0001	0.0062	0.0466	-0.0016
Average	0.2252		SSR	0.0056	0.6652		

k_1 (min^{-1})	k_2 (min^{-1})	t_{max} (min)	r^2	df	S.E. of y	Critical t	CI
0.0402	0.0149	46.9822	0.9882	13.0000	0.0111	2.1604	0.0241

10.3 At 37 °C

- N1

Time (min)	PAR	Fitted y	residuals	$(residuals)^2$	$(y-y_{mean})^2$	Upper CI	Lower CI
0	0.0000	0.0000	0.0000	0.0000	0.0039	0.0264	-0.0264
0.083	0.0140	0.0040	-0.0100	0.0001	0.0024	0.0303	-0.0224
0.25	0.0143	0.0119	-0.0025	0.0000	0.0024	0.0382	-0.0145
0.5	0.0280	0.0234	-0.0046	0.0000	0.0012	0.0498	-0.0030
1	0.0415	0.0453	0.0038	0.0000	0.0005	0.0717	0.0190
5	0.1550	0.1758	0.0207	0.0004	0.0085	0.2021	0.1494
15	0.2970	0.2823	-0.0146	0.0002	0.0548	0.3087	0.2560
30	0.2428	0.2273	-0.0154	0.0002	0.0324	0.2537	0.2010
60	0.0615	0.0807	0.0191	0.0004	0.0000	0.1070	0.0543
90	0.0118	0.0237	0.0119	0.0001	0.0026	0.0501	-0.0026
120	0.0000	0.0067	0.0067	0.0000	0.0039	0.0330	-0.0197
150	0.0000	0.0019	0.0019	0.0000	0.0039	0.0282	-0.0245
180	0.0000	0.0005	0.0005	0.0000	0.0039	0.0269	-0.0258
Average	0.0666		SSR	0.0016	0.1205		

k_1 (min^{-1})	k_2 (min^{-1})	t_{max} (min)	r^2	df	S.E. of y	Critical t	CI
0.0851	0.0428	16.7148	0.9869	11.0000	0.0120	2.2010	0.0264

- N2

Time (min)	PAR	Fitted y	residuals	$(residuals)^2$	$(y-y_{mean})^2$	Upper CI	Lower CI
0	0.0000	0.0000	0.0000	0.0000	0.0039	0.0226	-0.0226
0.083	0.0042	0.0037	-0.0006	0.0000	0.0034	0.0263	-0.0190
0.25	0.0184	0.0110	-0.0074	0.0001	0.0020	0.0336	-0.0117
0.5	0.0214	0.0216	0.0002	0.0000	0.0017	0.0442	-0.0011
1	0.0406	0.0418	0.0013	0.0000	0.0005	0.0645	0.0192
5	0.1428	0.1635	0.0207	0.0004	0.0064	0.1861	0.1409
15	0.2782	0.2657	-0.0125	0.0002	0.0464	0.2883	0.2430
30	0.2249	0.2138	-0.0111	0.0001	0.0263	0.2364	0.1911
60	0.0536	0.0715	0.0179	0.0003	0.0001	0.0941	0.0488
90	0.0112	0.0187	0.0075	0.0001	0.0027	0.0413	-0.0040
120	0.0000	0.0045	0.0045	0.0000	0.0039	0.0271	-0.0181
150	0.0000	0.0010	0.0010	0.0000	0.0039	0.0237	-0.0216
180	0.0000	0.0002	0.0002	0.0000	0.0039	0.0229	-0.0224
Average	0.0612		SSR	0.0012	0.1052		

k_1 (min^{-1})	k_2 (min^{-1})	t_{max} (min)	r^2	df	S.E. of y	Critical t	CI
0.0740	0.0496	13.5986	0.9889	11.0000	0.0103	2.2010	0.0226

- N3

Time (min)	PAR	Fitted y	residuals	$(residuals)^2$	$(y-y_{mean})^2$	Upper CI	Lower CI
0	0.0000	0.0000	0.0000	0.0000	0.0039	0.0168	-0.0168
0.083	0.0106	0.0040	-0.0066	0.0000	0.0027	0.0208	-0.0128
0.25	0.0158	0.0118	-0.0040	0.0000	0.0022	0.0286	-0.0050
0.5	0.0234	0.0232	-0.0003	0.0000	0.0016	0.0400	0.0064
1	0.0410	0.0449	0.0038	0.0000	0.0005	0.0617	0.0281
5	0.1574	0.1718	0.0144	0.0002	0.0089	0.1886	0.1550
15	0.2823	0.2655	-0.0168	0.0003	0.0482	0.2823	0.2487
30	0.1898	0.1981	0.0083	0.0001	0.0161	0.2149	0.1813
60	0.0563	0.0569	0.0006	0.0000	0.0000	0.0737	0.0401
90	0.0132	0.0127	-0.0004	0.0000	0.0025	0.0295	-0.0041
120	0.0000	0.0026	0.0026	0.0000	0.0039	0.0194	-0.0142
150	0.0000	0.0005	0.0005	0.0000	0.0039	0.0173	-0.0163
180	0.0000	0.0001	0.0001	0.0000	0.0039	0.0169	-0.0167
Average	0.0608		SSR	0.0006	0.0985		

k_1 (min^{-1})	k_2 (min^{-1})	t_{max} (min)	r^2	df	S.E. of y	Critical t	CI
0.0787	0.0548	14.6087	0.9935	11.0000	0.0076	2.2010	0.0168

11. Nonlinear least square fit for MSCUR metabolism in human plasma

11.1 At 4 °C

- N1

Time (min)	PAR	Fitted y	residuals	$(residuals)^2$	$(y-y_{mean})^2$	Upper CI	Lower CI
0	0.0000	0.0000	0.0000	0.0000	0.0086	0.0553	-0.0553
0.083	0.0121	0.0009	-0.0112	0.0001	0.0065	0.0562	-0.0544
0.25	0.0145	0.0027	-0.0118	0.0001	0.0061	0.0580	-0.0526
0.5	0.0245	0.0054	-0.0191	0.0004	0.0046	0.0607	-0.0499
0.75	0.0288	0.0081	-0.0207	0.0004	0.0041	0.0634	-0.0472
1	0.0359	0.0107	-0.0252	0.0006	0.0032	0.0660	-0.0446
5	0.1090	0.0497	-0.0593	0.0035	0.0003	0.1051	-0.0056
15	0.1634	0.1234	-0.0400	0.0016	0.0050	0.1787	0.0681
30	0.1692	0.1858	0.0165	0.0003	0.0059	0.2411	0.1305
45	0.1926	0.2098	0.0172	0.0003	0.0100	0.2651	0.1545
60	0.1882	0.2107	0.0225	0.0005	0.0091	0.2660	0.1554
90	0.1705	0.1796	0.0091	0.0001	0.0061	0.2349	0.1243
120	0.1453	0.1363	-0.0090	0.0001	0.0028	0.1916	0.0810
150	0.1144	0.0971	-0.0173	0.0003	0.0005	0.1525	0.0418
180	0.0799	0.0666	-0.0133	0.0002	0.0002	0.1219	0.0113
Average	0.0966		SSR	0.0085	0.0728		

k_1 (min^{-1})	k_2 (min^{-1})	t_{max} (min)	r^2	df	S.E. of y	Critical t	CI
0.0215	0.0165	50.3667	0.8830	13.0000	0.0256	2.1604	0.0553

- N2

Time (min)	PAR	Fitted y	residuals	$(residuals)^2$	$(y-y_{mean})^2$	Upper CI	Lower CI
0	0.0000	0.0000	0.0000	0.0000	0.0086	0.0364	-0.0364
0.083	0.0000	0.0013	0.0013	0.0000	0.0086	0.0376	-0.0351
0.25	0.0070	0.0037	-0.0033	0.0000	0.0073	0.0401	-0.0326
0.5	0.0142	0.0074	-0.0068	0.0000	0.0061	0.0438	-0.0290
0.75	0.0036	0.0111	0.0074	0.0001	0.0079	0.0475	-0.0253
1	0.0515	0.0147	-0.0368	0.0014	0.0017	0.0511	-0.0217
5	0.0990	0.0663	-0.0327	0.0011	0.0000	0.1027	0.0299
15	0.1659	0.1544	-0.0115	0.0001	0.0054	0.1908	0.1181
30	0.2047	0.2117	0.0070	0.0000	0.0126	0.2481	0.1753
45	0.2034	0.2180	0.0147	0.0002	0.0123	0.2544	0.1816
60	0.1846	0.1999	0.0153	0.0002	0.0085	0.2363	0.1635
90	0.1415	0.1425	0.0010	0.0000	0.0024	0.1789	0.1061
120	0.1114	0.0909	-0.0204	0.0004	0.0004	0.1273	0.0545
150	0.0601	0.0547	-0.0053	0.0000	0.0011	0.0911	0.0184
180	0.0400	0.0318	-0.0082	0.0001	0.0028	0.0682	-0.0046
Average	0.0858		SSR	0.0037	0.0855		

k_1 (min^{-1})	k_2 (min^{-1})	t_{max} (min)	r^2	df	S.E. of y	Critical t	CI
0.0301	0.0206	43.7788	0.9569	13.0000	0.0168	2.1604	0.0364

- N3

Time (min)	PAR	Fitted y	residuals	$(residuals)^2$	$(y-y_{mean})^2$	Upper CI	Lower CI
0	0.0000	0.0000	0.0000	0.0000	0.0086	0.0423	-0.0423
0.083	0.0063	0.0012	-0.0051	0.0000	0.0075	0.0435	-0.0411
0.25	0.0149	0.0036	-0.0114	0.0001	0.0060	0.0459	-0.0387
0.5	0.0244	0.0071	-0.0173	0.0003	0.0047	0.0494	-0.0352
0.75	0.0258	0.0106	-0.0152	0.0002	0.0045	0.0529	-0.0317
1	0.0272	0.0141	-0.0132	0.0002	0.0043	0.0563	-0.0282
5	0.0908	0.0641	-0.0267	0.0007	0.0000	0.1064	0.0219
15	0.1884	0.1529	-0.0355	0.0013	0.0092	0.1952	0.1107
30	0.2124	0.2169	0.0045	0.0000	0.0144	0.2592	0.1746
45	0.2088	0.2308	0.0220	0.0005	0.0135	0.2731	0.1886
60	0.1942	0.2185	0.0243	0.0006	0.0103	0.2608	0.1763
90	0.1583	0.1656	0.0073	0.0001	0.0043	0.2079	0.1233
120	0.1246	0.1119	-0.0128	0.0002	0.0010	0.1541	0.0696
150	0.0937	0.0710	-0.0226	0.0005	0.0000	0.1133	0.0288
180	0.0614	0.0434	-0.0180	0.0003	0.0010	0.0857	0.0011
Average	0.0954		SSR	0.0050	0.0891		

k_1 (min^{-1})	k_2 (min^{-1})	t_{max} (min)	r^2	df	S.E. of y	Critical t	CI
0.0260	0.0199	46.9701	0.9441	13.0000	0.0196	2.1604	0.0423

11.2 At 25 °C

- N1

Time (min)	PAR	Fitted y	residuals	$(residuals)^2$	$(y-y_{mean})^2$	Upper CI	Lower CI
0	0.0000	0.0000	0.0000	0.0000	0.0026	0.0166	-0.0166
0.083	0.0108	0.0041	-0.0066	0.0000	0.0016	0.0208	-0.0125
0.25	0.0185	0.0122	-0.0062	0.0000	0.0010	0.0289	-0.0044
0.5	0.0413	0.0239	-0.0174	0.0003	0.0001	0.0405	0.0073
0.75	0.0416	0.0350	-0.0066	0.0000	0.0001	0.0516	0.0184
1	0.0528	0.0456	-0.0071	0.0001	0.0000	0.0623	0.0290
5	0.1532	0.1574	0.0042	0.0000	0.0105	0.1740	0.1408
15	0.1826	0.1869	0.0043	0.0000	0.0174	0.2035	0.1703
30	0.0937	0.0934	-0.0004	0.0000	0.0019	0.1100	0.0767
45	0.0391	0.0351	-0.0040	0.0000	0.0001	0.0517	0.0185
60	0.0198	0.0118	-0.0080	0.0001	0.0009	0.0284	-0.0049
90	0.0065	0.0011	-0.0054	0.0000	0.0019	0.0178	-0.0155
120	0.0017	0.0001	-0.0016	0.0000	0.0024	0.0167	-0.0165
Average	0.0509		SSR	0.0006	0.0406		

k_1 (min^{-1})	k_2 (min^{-1})	t_{max} (min)	r^2	df	S.E. of y	Critical t	CI
0.0996	0.0861	12.3279	0.9845	11.0000	0.0076	2.2010	0.0166

- N2

Time (min)	PAR	Fitted y	residuals	$(residuals)^2$	$(y-y_{mean})^2$	Upper CI	Lower CI
0	0.0000	0.0000	0.0000	0.0000	0.0026	0.0252	-0.0252
0.083	0.0125	0.0036	-0.0089	0.0001	0.0015	0.0288	-0.0216
0.25	0.0202	0.0106	-0.0096	0.0001	0.0009	0.0358	-0.0146
0.5	0.0388	0.0207	-0.0180	0.0003	0.0001	0.0460	-0.0045
0.75	0.0589	0.0305	-0.0285	0.0008	0.0001	0.0557	0.0053
1	0.0417	0.0398	-0.0019	0.0000	0.0001	0.0650	0.0146
5	0.1305	0.1417	0.0112	0.0001	0.0064	0.1669	0.1165
15	0.1831	0.1832	0.0001	0.0000	0.0176	0.2084	0.1580
30	0.1071	0.1051	-0.0019	0.0000	0.0032	0.1303	0.0799
45	0.0467	0.0460	-0.0007	0.0000	0.0000	0.0712	0.0208
60	0.0191	0.0182	-0.0009	0.0000	0.0010	0.0434	-0.0070
90	0.0032	0.0025	-0.0007	0.0000	0.0022	0.0277	-0.0227
120	0.0000	0.0003	0.0003	0.0000	0.0026	0.0255	-0.0249
Average	0.0509		SSR	0.0014	0.0382		

k_1 (min^{-1})	k_2 (min^{-1})	t_{max} (min)	r^2	df	S.E. of y	Critical t	CI
0.0699	0.1000	9.2430	0.9622	11.0000	0.0115	2.2010	0.0252

- N3

Time (min)	PAR	Fitted y	residuals	$(residuals)^2$	$(y-y_{mean})^2$	Upper CI	Lower CI
0	0.0000	0.0000	0.0000	0.0000	0.0026	0.0274	-0.0274
0.083	0.0129	0.0034	-0.0095	0.0001	0.0014	0.0308	-0.0241
0.25	0.0217	0.0099	-0.0117	0.0001	0.0008	0.0374	-0.0175
0.5	0.0313	0.0195	-0.0118	0.0001	0.0004	0.0469	-0.0079
0.75	0.0442	0.0287	-0.0155	0.0002	0.0000	0.0561	0.0013
1	0.0522	0.0375	-0.0147	0.0002	0.0000	0.0649	0.0101
5	0.1113	0.1366	0.0253	0.0006	0.0037	0.1640	0.1092
15	0.1985	0.1859	-0.0125	0.0002	0.0219	0.2134	0.1585
30	0.1152	0.1140	-0.0012	0.0000	0.0042	0.1414	0.0866
45	0.0455	0.0526	0.0071	0.0001	0.0000	0.0800	0.0252
60	0.0167	0.0217	0.0050	0.0000	0.0011	0.0491	-0.0058
90	0.0000	0.0031	0.0031	0.0000	0.0026	0.0306	-0.0243
120	0.0000	0.0004	0.0004	0.0000	0.0026	0.0278	-0.0270
Average	0.0500		SSR	0.0017	0.0413		

k_1 (min^{-1})	k_2 (min^{-1})	t_{max} (min)	r^2	df	S.E. of y	Critical t	CI
0.0723	0.0861	12.2882	0.9586	11.0000	0.0125	2.2010	0.0274

11.3 At 37 °C

- N1

Time (min)	PAR	Fitted y	residuals	$(residuals)^2$	$(y-y_{mean})^2$	Upper CI	Lower CI
0	0.0000	0.0000	0.0000	0.0000	0.0013	0.0071	-0.0071
0.083	0.0158	0.0084	-0.0074	0.0001	0.0004	0.0155	0.0013
0.25	0.0242	0.0243	0.0001	0.0000	0.0001	0.0315	0.0172
0.5	0.0437	0.0462	0.0025	0.0000	0.0001	0.0533	0.0390
0.75	0.0642	0.0657	0.0015	0.0000	0.0008	0.0728	0.0585
1	0.0798	0.0831	0.0032	0.0000	0.0019	0.0902	0.0759
5	0.1813	0.1785	-0.0028	0.0000	0.0211	0.1857	0.1714
15	0.0640	0.0654	0.0014	0.0000	0.0008	0.0725	0.0582
30	0.0000	0.0057	0.0057	0.0000	0.0013	0.0128	-0.0015
45	0.0000	0.0004	0.0004	0.0000	0.0013	0.0075	-0.0068
60	0.0000	0.0000	0.0000	0.0000	0.0013	0.0072	-0.0071
90	0.0000	0.0000	0.0000	0.0000	0.0013	0.0071	-0.0071
120	0.0000	0.0000	0.0000	0.0000	0.0013	0.0071	-0.0071
Average	0.0364		SSR	0.0001	0.0330		

k_1 (min^{-1})	k_2 (min^{-1})	t_{max} (min)	r^2	df	S.E. of y	Critical t	CI
0.1945	0.2281	5.0610	0.9965	11.0000	0.0032	2.2010	0.0071

- N2

Time (min)	PAR	Fitted y	residuals	$(residuals)^2$	$(y-y_{mean})^2$	Upper CI	Lower CI
0	0.0000	0.0000	0.0000	0.0000	0.0013	0.0111	-0.0111
0.083	0.0158	0.0076	-0.0082	0.0001	0.0004	0.0187	-0.0035
0.25	0.0300	0.0221	-0.0079	0.0001	0.0000	0.0332	0.0110
0.5	0.0462	0.0421	-0.0041	0.0000	0.0001	0.0532	0.0310
0.75	0.0569	0.0601	0.0033	0.0000	0.0004	0.0712	0.0490
1	0.0685	0.0763	0.0078	0.0001	0.0011	0.0874	0.0652
5	0.1749	0.1727	-0.0022	0.0000	0.0193	0.1838	0.1616
15	0.0722	0.0720	-0.0002	0.0000	0.0013	0.0831	0.0609
30	0.0000	0.0076	0.0076	0.0001	0.0013	0.0187	-0.0035
45	0.0000	0.0006	0.0006	0.0000	0.0013	0.0117	-0.0105
60	0.0000	0.0000	0.0000	0.0000	0.0013	0.0111	-0.0110
90	0.0000	0.0000	0.0000	0.0000	0.0013	0.0111	-0.0111
120	0.0000	0.0000	0.0000	0.0000	0.0013	0.0111	-0.0111
Average	0.0357		SSR	0.0003	0.0304		

k_1 (min^{-1})	k_2 (min^{-1})	t_{max} (min)	r^2	df	S.E. of y	Critical t	CI
0.1814	0.2153	5.4938	0.9908	11.0000	0.0050	2.2010	0.0111

- N3

Time (min)	PAR	Fitted y	residuals	$(residuals)^2$	$(y-y_{mean})^2$	Upper CI	Lower CI
0	0.0000	0.0000	0.0000	0.0000	0.0013	0.0131	-0.0131
0.083	0.0141	0.0074	-0.0067	0.0000	0.0005	0.0205	-0.0057
0.25	0.0258	0.0214	-0.0044	0.0000	0.0001	0.0345	0.0083
0.5	0.0484	0.0408	-0.0076	0.0001	0.0002	0.0539	0.0277
0.75	0.0616	0.0583	-0.0033	0.0000	0.0006	0.0714	0.0452
1	0.0797	0.0740	-0.0057	0.0000	0.0019	0.0871	0.0609
5	0.1596	0.1689	0.0093	0.0001	0.0153	0.1820	0.1558
15	0.0807	0.0721	-0.0086	0.0001	0.0020	0.0852	0.0590
30	0.0000	0.0079	0.0079	0.0001	0.0013	0.0210	-0.0052
45	0.0000	0.0007	0.0007	0.0000	0.0013	0.0138	-0.0124
60	0.0000	0.0001	0.0001	0.0000	0.0013	0.0132	-0.0131
90	0.0000	0.0000	0.0000	0.0000	0.0013	0.0131	-0.0131
120	0.0000	0.0000	0.0000	0.0000	0.0013	0.0131	-0.0131
Average	0.0361		SSR	0.0004	0.0284		

k_1 (min^{-1})	k_2 (min^{-1})	t_{max} (min)	r^2	df	S.E. of y	Critical t	CI
0.1765	0.2162	6.1824	0.9863	11.0000	0.0060	2.2010	0.0131

APPENDIX F

Certificate of dog plasma

Certificate of Analysis

Product:	Innovative Grade™ US Origin Beagle Plasma		
Anticoagulant:	Na Heparin		
Lot:	20351		
Quantity:	2	Age:	Not Applicable
Volume:	100ml	Gender:	Not Applicable
Storage:	-20°	Race:	Not Applicable
Notes:			
Description:	Innovative Grade™ US Origin Beagle Plasma is drawn from healthy normal beagles. The beagles are of US Origin only. The blood is collected from beagles of mixed sex and vary in age. The blood is then processed into plasma. The plasma remains frozen and is shipped on dry ice for maximum stability.		
Expiration:	Innovative Grade™ material is stable for at least 3 years from the date of draw when stored at a minimum of -20° c. Storing at -80° will retain stability even longer		
Handling:	This material is sold for in-vitro use only in manufacturing and research. This material is not suitable for human use. It is the responsibility of the user to undertake sufficient verification and testing to determine the suitability of each product's application. The statements herein are offered for informational purposes only and are intended to be used solely for your consideration, investigation and verification.		

Contact Information:
Phone: 248.896.0145 | Fax: 248.896.0149
Email: sales@innov-reseach.com
46430 Peary Court, Novi, MI 48377
www.innov-research.com

Innovative™ RESEARCH
"Results Driven Research"

APPENDIX G

Certificate of human plasma

Certificate of Analysis

Product:	Pooled Normal Human Plasma		
Anticoagulant:	Na Heparin		
Lot:	17793		
Quantity:	2	Age:	Not Applicable
Volume:	100ml	Gender:	Not Applicable
Storage:	-20°	Race:	Not Applicable
Notes:			
Description:	Human Plasma is collected at an FDA Licensed commercial donor center / facility within the United States. Each unit is tested and found negative for: HBsAg, HCV, HIV-1, HIV-2, HIV-1Ag or HIV 1-NAT, ALT, and syphilis by FDA-Approved Methods.		
Expiration:	Based upon evaluation of the stability of "signal chemistries" (critical parameters of the sera from the biochemical profile) serum and plasma is stable for 3 years from date of manufacture when stored in unopened containers at temperatures of (– 20) deg C or below.		
Handling:	This material is sold for in-vitro use only in manufacturing and research. This material is not suitable for human use. It is the responsibility of the user to undertake sufficient verification and testing to determine the suitability of each product's application. The statements herein are offered for informational purposes only and are intended to be used solely for your consideration, investigation and verification.		

Contact Information:
Phone: 248.896.0145 | Fax: 248.896.0149
Email: sales@innov-reseach.com
46430 Peary Court, Novi, MI 48377
www.innov-research.com

Innovative™ RESEARCH
"Results Driven Research"

APPENDIX H

Permission to reuse materials

JOHN WILEY AND SONS LICENSE TERMS AND CONDITIONS

Dec 18, 2018

This Agreement between Chulalongkorn University ("You") and John Wiley and Sons ("John Wiley and Sons") consists of your license details and the terms and conditions provided by John Wiley and Sons and Copyright Clearance Center.

License Number	4452551477009
License date	Oct 19, 2018
Licensed Content Publisher	John Wiley and Sons
Licensed Content Publication	Wiley Books
Licensed Content Title	Carboxylesterases: Overview, Structure, Function, and Polymorphism
Licensed Content Author	Masakiyo Hosokawa, Tetsuo Satoh
Licensed Content Date	Mar 28, 2011
Licensed Content Pages	14
Type of use	Dissertation/Thesis
Requestor type	University/Academic
Format	Print and electronic
Portion	Figure/table
Number of figures/tables	2
Original Wiley figure/table number(s)	Figure 4.1 and 4.3
Will you be translating?	No
Title of your thesis / dissertation	A study on the in vitro stability and metabolism of curcumin diethyl disuccinate in plasma
Expected completion date	Nov 2018
Expected size (number of pages)	100
Requestor Location	Chulalongkorn University 254 Phyathai Rd., Wangmai Patumwan, Bangkok 10330 Thailand Attn: Chulalongkorn University
Publisher Tax ID	EU826007151
Total	0.00 USD

SPRINGER NATURE LICENSE
TERMS AND CONDITIONS

Dec 18, 2018

This Agreement between Chulalongkorn University ("You") and Springer Nature ("Springer Nature") consists of your license details and the terms and conditions provided by Springer Nature and Copyright Clearance Center.

License Number	4459300207560
License date	Oct 31, 2018
Licensed Content Publisher	Springer Nature
Licensed Content Publication	Nature Structural & Molecular Biology
Licensed Content Title	Structure and evolution of the serum paraoxonase family of detoxifying and anti-atherosclerotic enzymes
Licensed Content Author	Michal Harel, Amir Aharoni, Leonid Gaidukov, Boris Brumshtein, Olga Khersonsky et al.
Licensed Content Date	Apr 18, 2004
Licensed Content Volume	11
Licensed Content Issue	5
Type of Use	Thesis/Dissertation
Requestor type	academic/university or research institute
Format	print and electronic
Portion	figures/tables/illustrations
Number of figures/tables/illustrations	1
High-res required	no
Will you be translating?	no
Circulation/distribution	20,001 to 50,000
Author of this Springer Nature content	no
Title	A study on the in vitro stability and metabolism of curcumin diethyl disuccinate in plasma
Institution name	n/a
Expected presentation date	Nov 2018
Portions	Figure 4b
Requestor Location	Chulalongkorn University 254 Phyathai Rd., Wangmai Patumwan, Bangkok 10330 Thailand Attn: Chulalongkorn University
Billing Type	Invoice
Billing Address	Chulalongkorn University 254 Phyathai Rd., Wangmai Patumwan, Thailand 10330 Attn: Chulalongkorn University
Total	0.00 USD

VITA

NAME	Pahweenvaj Ratnatilaka Na Bhuket
DATE OF BIRTH	21 September 1990
PLACE OF BIRTH	Bangkok, Thailand
INSTITUTIONS ATTENDED	2008 - 2013 Bachelor of Science in Pharmacy (Second class honors) Faculty of Pharmaceutical Sciences, Chulalongkorn University, Thailand
HOME ADDRESS	57 Soi Ngamwongwan 27, Ngamwongwan Road, Bangkhen, Mueang, Nonthaburi, 11000
PUBLICATION	1. Wichitnithad W, Kiatkumjorn T, Jithavech P, Thanawattanawanich P, Ratnatilaka na Bhuket P, Rojsitthisak P. A simple and sensitive HPLC-fluorescence method for the determination of moxifloxacin in human plasma and its application in a pharmacokinetic study. Pharmazie. 2018, 11: 625-629 doi: 10.1691/ph.2018.8148 2. Ratnatilaka Na Bhuket P, Luckanagul JA, Rojsitthisak P and Wang Q. Chemical Modification of Enveloped Viruses for Biomedical Applications. Integr. Biol. 2018 DOI: 10.1039/C8IB00118A (Highlighted on the journal cover) 3. Sorasitthiyanukarn FN, Muangnoi C, Ratnatilaka Na Bhuket P, Rojsitthisak P and Rojsitthisak P. Chitosan/alginate nanoparticles as a promising approach for oral delivery of curcumin diglutaric acid for cancer treatment. Mater. Sci. Eng. C. 2018, 93: 178-190 https://doi.org/10.1016/j.msec.2018.07.069 4. Muangnoi C, Jithavech P, Ratnatilaka Na Bhuket P, Supasena W, Wichitnithad W, Towiwat P, Niwattisaiwong N, Haworth IS and Rojsitthisak P. A curcumin-diglutaric acid

conjugated prodrug with improved water solubility and antinociceptive properties compared to curcumin. Biosci. Biotechnol. Biochem. 2018, 82(8): 1301-1308 DOI: 10.1080/09168451.2018.1462694

5. Luckanagul JA, Pitakchatwong C, Ratnatilaka Na Bhuket P, Muangnoi C, Rojsitthisak P, Chirachanchai S, Wang Q, and Rojsitthisak P. Chitosan-based polymer hybrids for thermo-responsive nanogel delivery of curcumin. Carbohydr. Polym. 2017, 181: 1119-1127. https://doi.org/10.1016/j.carbpol.2017.11.027

6. Yusakul G, Nuntawong P, Sakamoto S, Ratnatilaka Na Bhuket P, Kohno T, Kikkawa N; Rojsitthisak P, Shimizu K, Tanaka H, and Morimoto S. Bacterial expressions of single-chain variable fragment (scFv) antibody against ganoderic acid A, a cost-effective approach for its quantitative analysis using the scFv based enzyme-linked immunosorbent assay. Biol. Pharm. Bull. 2017; 40(10): 1767-1774. http://doi.org/10.1248/bpb.b17-00531

7. Ratnatilaka Na Bhuket P, El-Magboub A, Haworth IS and Rojsitthisak P. Enhancement of Curcumin Bioavailability Via the Prodrug Approach: Challenges and Prospects. Eur. J. Drug Metab. Pharmacokinet. 2017; 42: 341-353. DOI: 10.1007/s13318-016-0377-7.

8. Ratnatilaka Na Bhuket P, Niwattisaiwong N, Limpikirati P, Khemawoot P, Ongpipattanakul B and Rojsitthisak P. Simultaneous determination of curcumin diethyl disuccinate and its active metabolite curcumin in rat plasma by LC–MS/MS: Application of esterase inhibitors in the stabilization of an ester-containing prodrug. J. Chromatogr. B. 2016; 1033–1034: 301-310. DOI: 10.1016/j.jchromb.2016.08.039.

9. Ratnatilaka Na Bhuket P, Teerawonganan P, Yoosakul E, Supasena W, Watananikorn C, Chuasuwan B, et al. Validation of liquid chromatography–tandem mass spectrometric method for simultaneous determination of lopinavir and ritonavir in human plasma, and its application in a bioequivalence study in Thai volunteers. J. Health Res. 2015; 29(6): 417-24. DOI: 10.14456/jhr.2015.34.
10. Vattanarongkup J, Yoosakul E, Manamuti C, Teerawonganan P, Seeduang C, Ratnatilaka Na Bhuket P, Rojanawiwat A, Karachot B, Chuasuwan B and Techatanawat I. Bioequivalence study of Ribavirin 400 mg tablets in healthy Thai male volunteers under fed conditions. Mahidol Univ. J. Pharm. Sci. 2015; 42(3), 118-125. DOI: 10.14456/mujps.2015.15.
11. Teerawonganan P, Yoosakul E, Ratnatilaka Na Bhuket P, Chuasuwan B, Techatanawat I, Narakorn P, Rojanawiwat A, and Eksaengsri A. Bioequivalence study of torsemide 10 mg tablets in healthy Thai volunteers. Mahidol Univ. J. Pharm. Sci. 2015; 42(1), 8-13. DOI: 10.14456/mujps.2015.4.
12. Techatanawat I, Ratnatilaka Na Bhuket P, Teerawonganan P, Yoosakul E, Khaowroongrueng V, Paisarnsinsook W, et al. Bioequivalence study of duloxetine hydrochloride 60 mg EC capsules in the fasting and fed states in healthy Thai male volunteers. J. Health Res. 2015; 29(3): 165-169. DOI: 10.14456/jhr.2015.2.
13. Teerawonganan P, Yoosakul E, Ratnatilaka Na Bhuket P, Chuasuwan B, Techatanawat I, Narakorn P, Rojanawiwat A, and Eksaengsri A. Bioequivalence study of levocetirizine dihydrochloride 5 mg tablets in healthy Thai male volunteers. IJPS. 2015; 11(1): 79-88.
14. Chuasuwan B, Ratnatilaka Na Bhuket P, Supasena W,

Manamuti C, Techatanawat I, Narakorn P, Rojanawiwat A, and Eksaengsri A. Bioequivalence study of sildenafil 20 mg tablets in healthy Thai male volunteers. Mahidol Univ. J. Pharm. Sci. 2014; 41(2), 1-6.

AWARD RECEIVED

2017 The 90th Anniversary of Chulalongkorn University Ratchadaphiseksomphot Endowment Fund for thesis research.

2015-2017 Scholarship from the Graduate School, Chulalongkorn University to commemorate the 72th anniversary of his Majesty King Bhumibol Adulyadej.

2011 Daewoong Foundation activity titled Global Scholarship 2011, Daewoong Pharmaceutical (Thailand) Co., Ltd.